TRANSPORTATION RESEARCH

RECORD

No. 1302

Highway and Facility Design

Roadside Safety Features 1991

A peer-reviewed publication of the Transportation Research Board

TRANSPORTATION RESEARCH BOARD
NATIONAL RESEARCH COUNCIL
WASHINGTON, D.C. 1991

Transportation Research Record 1302
Price: $13.00

Subscriber Category
IIA highway and facility design

TRB Publications Staff
Director of Publications: Nancy A. Ackerman
Senior Editor: Naomi C. Kassabian
Associate Editor: Alison G. Tobias
Assistant Editors: Luanne Crayton, Kathleen Solomon, Norman Solomon
Graphics Coordinator: Diane L. Ross
Production Coordinator: Karen S. Waugh
Office Manager: Phyllis D. Barber
Production Assistant: Betty L. Hawkins

Printed in the United States of America

Library of Congress Cataloging-in-Publication Data
National Research Council. Transportation Research Board.

Roadside safety features 1991.
p. cm.—(Transportation research record, ISSN 0361-1981 ; no. 1302)
"A peer-reviewed publication of the Transportation Research Board."
ISBN 0-309-05109-6
1. Roads—Guard fences—Testing. 2. Roads—Safety measures. I. National Research Council (U.S.). Transportation Research Board. II. Series: Transportation research record ; 1302.
TE7.H5 no. 1302
[TE228]
388 s—dc20
[625.7'95] 91-27407
CIP

Sponsorship of Transportation Research Record 1302

GROUP 2—DESIGN AND CONSTRUCTON OF TRANSPORTATION FACILITIES
Chairman: Raymond A. Forsyth, Sacramento, California

General Design Section
Chairman: Jarvis D. Michie, Dynatech Engineering Inc.

Committee on Roadside Safety Features
Chairman: William W. Hunter, University of North Carolina
Robert F. Baker, Maurice E. Bronstad, James E. Bryden, Ronald M. Canner, Jr., John F. Carney III, Duane O. Christensen, Julie Anna Cirillo, Arthur M. Dinitz, John C. Durkos, Michael D. Freitas, James H. Hatton, Jr., T. Heijer, John A. Hinch, Ivor B. Laker, Mark A. Marek, William G. Marley, Jr., John W. Melvin, David Pope, Edward Robert Post, Robert Quincy, James F. Roberts, Hayes E. Ross, Jr., Rudolph Kenneth Shearin, Jr., Roger L. Stoughton, Flory J. Tamanini, Harry W. Taylor, Thomas Turbell

GROUP 3—OPERATION, SAFETY, AND MAINTENANCE OF TRANSPORTATION FACILITIES
Chairman: H. Douglas Robertson, University of North Carolina–Charlotte

Users and Vehicles Section
Chairman: Charles V. Zegeer, University of North Carolina

Committee on Traffic Records and Accident Analysis
Chairman: James O'Day, Salem, South Carolina
Secretary: C. Arthur Geurts, CAG Associates
David J. Bozak, Thomas E. Bryer, Kenneth L. Campbell, Myung-Soon Chang, Benjamin V. Chatfield, John T. Dempster, Jr., Mark Lee Edwards, Nicholas J. Garber, D. D. Hinton, Alan F. Hoskin, Paul P. Jovanis, Martin E. Lipinski, Philip P. Madonia, Joseph C. Marsh IV, Judson S. Matthias, Craig Miller, Clarence W. Mosher, Olga Pendleton, Carol Lederhaus Popkin, Rick Reischl, Robert R. Roberts, Howard S. Stein, John G. Viner, Melvyn S. Wasserman

Frank R. McCullagh and Richard F. Pain, Transportation Research Board staff

Sponsorship is indicated by a footnote at the end of each paper. The organizational units, officers, and members are as of December 31, 1990.

Transportation Research Record 1302

Contents

Foreword

This Record contains five papers on roadside safety features. Two of these deal with barrier system performance, one with guidelines, one with accident data base investigation, and the final one with laboratory testing of flexible delineators.

Glauz et al. crash tested a retrofit Thrie beam bridge rail and transition, and report that the crash test satisfied the requirements for structural adequacy, occupant risk, and vehicle trajectory in *NCHRP Report 230*, as well as the evaluation criteria in the AASHTO *Guide Specifications for Bridge Railings*. Beason et al. discuss the development of a single-slope concrete median barrier as either a permanent or a temporary barrier. The primary advantage of the barrier is that the pavement can be overlaid without changing performance, and it has been crash tested in both permanent and temporary configurations. Pigman and Agent discuss the development of guidelines representative of Kentucky conditions for the use of the AASHTO *Roadside Design Guide* for barrier selection and installation. Troxel et al. present the results of an investigation of the 1980–1985 Fatal Accident Reporting System and the 1982–1985 National Accident Sampling System data base of side impact collisions with roadside obstacles. These accidents usually involve trees, utility poles and luminaires, typically occur late at night or early in the morning, and usually involve young drivers. Development of effective countermeasures requires an appreciation of their unique characteristics. Zwahlen et al. subjected four types of flexible delineator posts to the accelerated mechanical fatigue evaluation test and determined an evaluation procedure.

Crash Tests of a Retrofit Thrie Beam Bridge Rail and Transition

DORAN L. GLAUZ, ROGER L. STOUGHTON, AND J. JAY FOLSOM

Two crash tests each were performed on a Thrie beam bridge rail and on the adjoining transition section to the approach guardrail. The bridge rail was designed (a) as a retrofit to replace the rail portion of an inadequate bridge rail supported on W6X15.5 steel posts at 6 ft 3-in. spacing, or (b) as a completely new barrier installed using resin capsule anchors to attach the posts to the edge of an existing bridge deck. The transition uses the same rail element, a 10-gauge Thrie beam, supported on standard wood posts. The tests performed approximated those required for a PL-1 bridge rail outlined in the 1989 American Association of State Highway and Transportation Officials *Guide Specifications for Bridge Railings*. The bridge rail was struck by a 5,400-lb pickup truck at 44.9 mph at an angle of 21 degrees and a 1,830-lb car at 48.7 mph at an angle of 18¼ degrees. The transition was hit by a 5,400-lb pickup truck at a speed of 44.7 mph at an angle of 18 degrees and a 1,930-lb car at 49.1 mph at an angle of 20¾ degrees. The crash tests satisfied the requirements for structural adequacy, occupant risk, and vehicle trajectory in *National Cooperative Highway Research Program Report 230* as well as the evaluation criteria in the American Association of State Highway and Transportation Officials guide specification.

There are many old bridge rails in service that do not meet modern standards of crashworthiness. These are mostly on narrow bridges on rural low-volume roads that have low speed limits. One common type in California, with more than 1,000 now in service, is a W-section metal beam and steel post bridge rail (Figure 1). This railing was crash tested in 1959 with a 4,000-lb vehicle/55 mph/30 degrees test condition (*1*). The concrete deck failed at the post connection, the rail pocketed and deflected 50 in., and the car was trapped and stood up almost on end. If there had been no earth support beyond the simulated deck, the vehicle would have continued through the rail and off the deck.

On federally funded local projects to upgrade old bridges, the Federal Highway Administration (FHWA) has required that bridge rails be replaced or retrofitted with designs that have been crash tested successfully under *National Cooperative Highway Research Program Report 230* (*2*) and the American Association of State Highway and Transportation Officials (AASHTO) *Guide Specifications for Bridge Railings* (*3*). The recently published AASHTO guide specifications for the first time provide for crash testing of "Performance Level One (PL1)" rails. PL1 rails are intended for local roads.

The Caltrans designers wanted a retrofit bridge rail design that would meet PL1 crash test requirements, that would eliminate deficiencies in the old design, and that would be simple and inexpensive to install.

California Department of Transportation, P.O. Box 19128, 5900 Folsom Boulevard, Sacramento, California 95819.

SCOPE OF RESEARCH

Two crash tests were performed on a Thrie beam bridge rail and on a transition to that rail. The tests followed the AASHTO *Guide Specifications for Bridge Railings* (*3*) for a performance level one bridge rail. The tests were conducted and evaluated using the criteria in *National Cooperative Highway Research Program Report 230* (*2*) and the AASHTO guide specifications (*3*). Intended impact conditions are shown in Table 1.

BRIDGE RAIL AND TRANSITION DESIGN

The Thrie beam bridge rail consisted of a 10-gauge Thrie beam rail blocked out and mounted with a top-of-rail height of 32 in. on W 6 × 15.5 steel posts (Figure 2). The designers favored a strong conservative rail and replaced the old 12-gauge W-section rail with a 10-gauge Thrie beam. This would limit rail deflection in impacts and keep vehicles from traveling many inches over the edge of the deck. The use of the Thrie beam raised the top of the rail height from 27 in. to 32 in. A rail height of 27 in. was set many years ago for passenger cars. In recent years, increased numbers of vans, pickup trucks, and other passenger vehicles with centers of gravity that are 6 or more in. higher than passenger cars travel the highways. The Thrie beam, with a height of 20 in., should accommodate a wider range of vehicle heights better than the old 12¼-in. W-section rail. Steel blockouts were used to (a) extend the

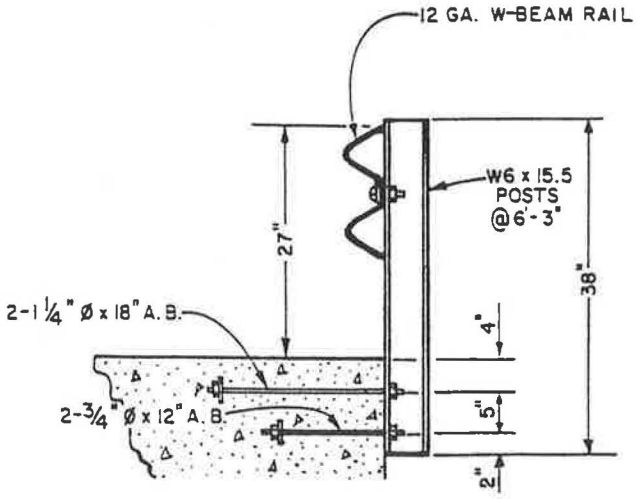

FIGURE 1 Metal bridge rail, 1959.

TABLE 1 TEST VEHICLES: IMPACT CONDITIONS

Test #	Target Weight (lbs)	Target Speed (mph)	Target Angle (deg)	Make	Model	Year	Weight (lbs)	Seat Belt?
473	5400	45	20	Chevrolet	Pick up	1983	5400	no
474	1800	50	20	Chevrolet	Spectrum	1986	1770	no
475	5400	45	20	Chevrolet	Pick up	1983	5400	yes
476	1800	50	20	Chevrolet	Spectrum	1987	1930	no

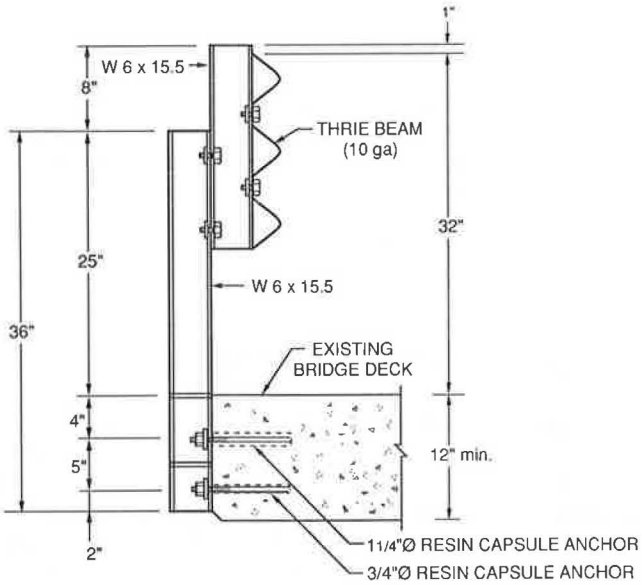

FIGURE 2 Thrie beam bridge rail cross section.

effective height of the post so that the Thrie beam could be used on the existing short posts, and (b) set the rail away from the posts to minimize the potential of snagging vehicles on the posts during impacts. Stiffener plates were welded to the posts at deck level to ensure good bending strength. (Alternate post designs will be tested statically in a follow-on project to try to eliminate the stiffeners.) Many existing bridge rails have inadequate post anchor bolts. Chipping out the deck so that new anchor bolts could be embedded would be costly. Therefore, resin anchor capsules with A307 threaded rod were installed in drilled holes in the simulated deck for the test barrier. If these proved strong enough, the concrete edge of the deck would not need to be replaced in retrofit jobs. A standard backup plate was mounted between the rail and steel block at posts in which there was no splice. The rail elements were mounted to the blocks with two ⅝-in. button head bolts. The blocks were mounted to the posts with two ⅝-in. hex head bolts.

The bridge approach transition is a 10-gauge Thrie beam, 12 ft 6 in. long supported on three 6-ft-long 6 × 8-in. Douglas fir posts and blocks and one bridge rail post (Figure 3). The posts nearest to the bridge rail are spaced at 3 ft 1½ in. and the third post is 6 ft 3 in. from the second. The approach transition is then connected to a standard metal beam guardrail using a standard W-beam to the Thrie beam transition piece. The guardrail is terminated with a breakaway cable terminal (Figure 4). The total minimum length of the transition, guardrail, and terminal is 50 ft. The terminal end is laid out on a 37.5-ft parabola with a 4-ft offset.

The tested bridge rail was 74 ft 9 in. long supported by 13 posts at 6 ft 3 in. on center. The third space (between Posts 3 and 4) was 6 ft to avoid existing anchor bolts used in the previous tests. The posts were mounted to the side of a simulated bridge deck using resin capsule anchors. Holes for the anchors were drilled with diamond core drills. Transition and terminal posts were set in strong soil.

Test Vehicles

All vehicles used in these tests were in good condition and free of any major body damage or missing parts. They had front-mounted engines and automatic transmissions. The vehicle models and weights are shown in Table 1. The trucks were ballasted to 5,400 lb with 50-lb steel plates mounted on the truck bed using 1-in.-diameter bolts. The small cars had front wheel drive. The vehicles were self powered in all tests.

Test Dummy

For each test an anthropomorphic dummy, 50th percentile American male, 165 lb, was placed in the driver's seat. It was

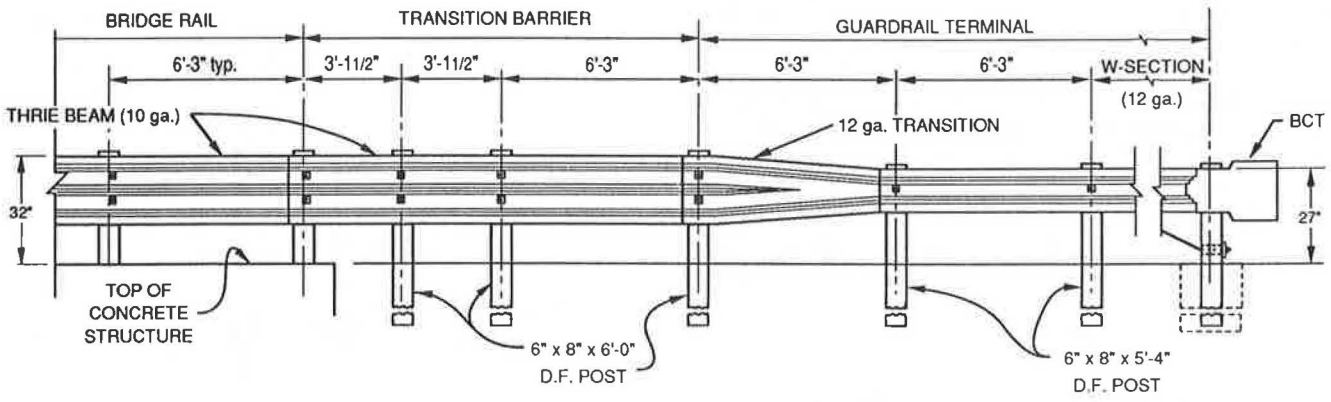

FIGURE 3 Bridge rail and transition elevation.

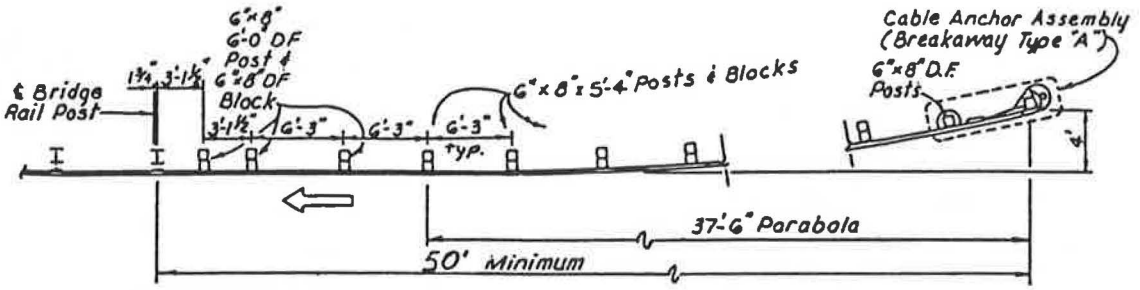

FIGURE 4 Approach guardrail layout (no scale).

unrestrained except in test 475. A set of three mutually perpendicular accelerometers was installed in the dummy's head.

Test Instrumentation

Test vehicles were instrumented with two sets of three accelerometers (independently recorded) and rate gyros near the center of gravity of the vehicle. Potentiometers were attached to the top of posts in the impact area. They measured the dynamic deflection of the posts during impact. Several high-speed cameras were used to record the impact.

TEST RESULTS

Test 473

Test Description

The right front bumper of the test vehicle struck the bridge rail near the midpoint between Posts 4 and 5 at a speed of 44.9 mph at an impact angle of 21 degrees. Vehicle contact with the Thrie beam began 2.7 ft downstream from Post 4 and continued for a length of about 16 ft (Figure 5). The vehicle was smoothly redirected, without exhibiting any tendency for the front wheel to snag on a post or wedge under the rail, and lost contact with the barrier at an exit angle of 6¼ degrees. The maximum roll was 10 degrees. The vehicle stopped on a safety berm about 140 ft downstream from impact and 37 ft in front of the face of the rail. It was lightly damaged (Figure 6).

Bridge Rail Damage

Post and rail damage were limited to the impact area. The permanent lateral deflection of the rail measured at the posts ranged from ⅛- to 9/16-in. deflection in a smooth long curve between Posts 2 and 9 (Figure 7). The displacements of each of the posts is shown in Table 2. The maximum dynamic lateral movement was 10.9 in.

On Posts 4, 5 ,6, and 7, the washers at the top mounting studs that attached the posts to the deck were pulled into the holes in the posts as the post flange was pushed around the nuts. The web was buckled at the bottom of Posts 4, 5, 6, and 7 (Figure 8). At Posts 5 and 6, the flange fractured at the upper mounting stud holes.

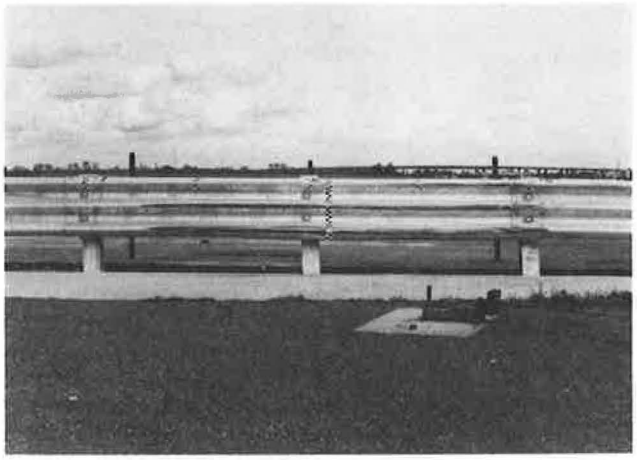

FIGURE 5 Vehicle contact marks, Test 473.

FIGURE 6 Vehicle after Test 473.

Dummy Response

During the collision, the unrestrained dummy was thrown to the right. Its shoulder hit the right door, and bent the top of the door outward. The dummy's final position was lying on its back across the passenger floor area with its legs wedged under the steering wheel.

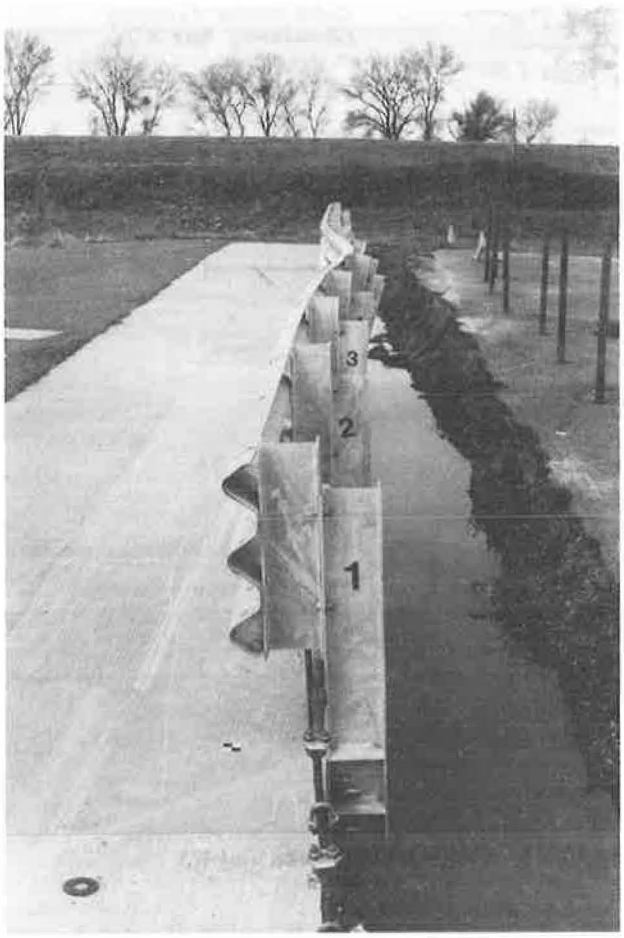

FIGURE 7 Rail damage: bent rail, bent posts, Test 473.

TABLE 2 POST DEFLECTIONS (in.)

Post	Test 473	Test 474
3	1/8	
4	3-9/16	1/16
5	9-1/16	7/16
6	8-5/16	1-7/16
7	2-1/2	1-5/16
8	1/8	5/16
9	1/4	0

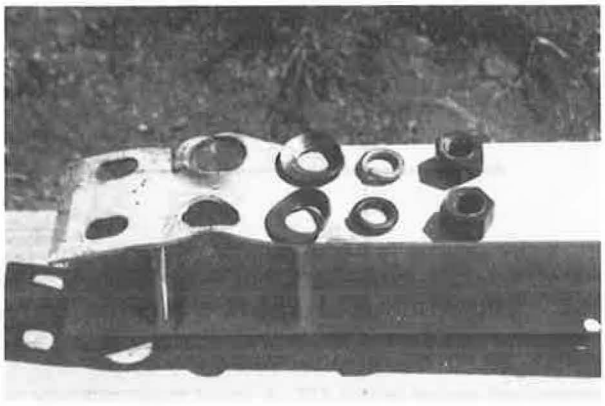

(a)

(b)

FIGURE 8 Post 6 was severely bent after Test 473.

Test 474

Test Description

The right front bumper of the test vehicle struck the bridge rail upstream from Post 6 at a speed of 48.7 mph at an angle of 18 degrees. Vehicle contact with the Thrie beam began 1.0 ft upstream from Post 6 and continued for a length of 7.0 ft (Figure 9). The vehicle was smoothly redirected, without exhibiting any tendency to snag on a post or wedge under the rail, and lost contact with the barrier at an angle of 5 degrees. The exit speed of the vehicle was about 39 mph. The maximum roll was about −1.3 degrees. The remote brakes were activated approximately 0.4 sec before impact. The final location of the vehicle was about 127 ft downstream from impact and 10 ft in front of the rail (Figure 10). The right front cover of the vehicle was moderately damaged (Figure 11).

Bridge Rail Damage

The post and rail damage were limited to the impact area. The permanent lateral displacement of the rail measured at

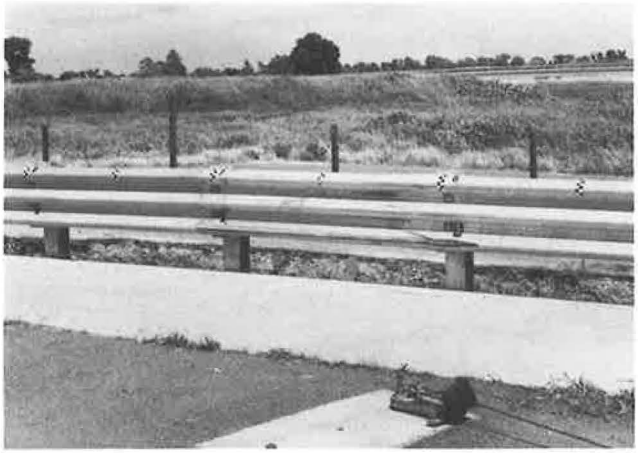

FIGURE 9 Vehicle contact marks, Test 474.

FIGURE 11 Damage to front of vehicle, Test 474.

the posts ranged from 1/16 to 1 7/16 in. (Figure 10). The displacements of each of the posts is shown in Table 2. The maximum dynamic barrier deflection was 3.8 in.

Dummy Response

During the collision, the unrestrained dummy was thrown to the right side of the vehicle. Its shoulder hit the inside of the right door, bending it outwards. Its head was outside the vehicle, sliding along the top of the rail while the vehicle was in contact with the rail. The dummy's head hit the block at Post 8, tearing the skin of the head. The dummy's final position was lying on its side with its upper body across the passenger side of the vehicle and its feet wedged underneath the driver's seat.

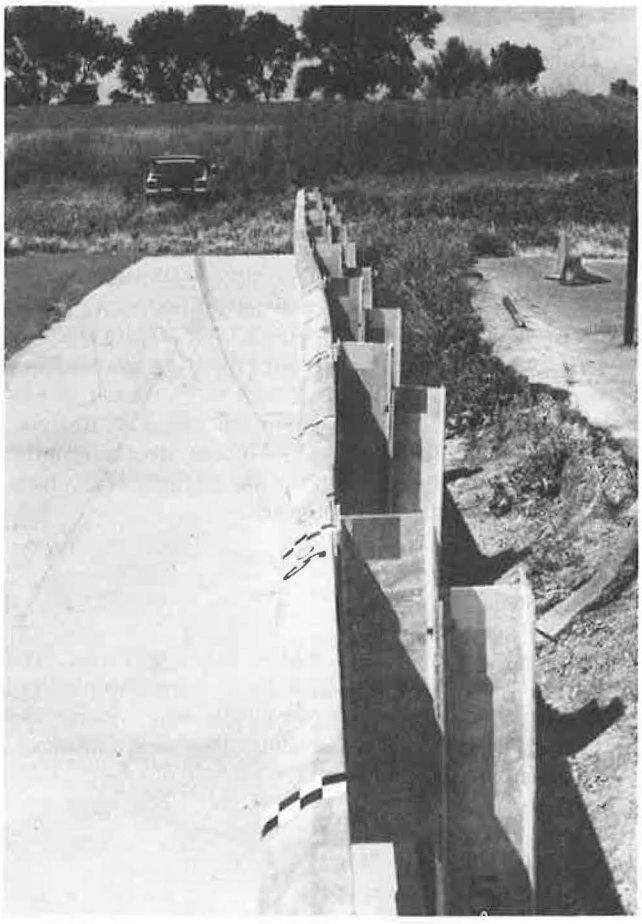

FIGURE 10 Rail damage: bent rail, bent posts, Test 474.

Test 475

Test Description

The right front bumper of the test vehicle struck the bridge approach transition near the midpoint between Posts 2 and 3 of the transition at a speed of 44.1 mph at an impact angle of 18 degrees. Vehicle contact with the transition began 3.1 ft downstream from Post 3 and continued for a distance of about 10 ft (Figure 12). The vehicle was smoothly redirected without exhibiting any tendency to snag or pocket and lost contact with the barrier at an exit angle of 4¼ degrees. The maximum roll was −2¾ degrees. The final location of the pickup truck was 140 ft downstream from impact and 37 ft in front of the bridge rail face (Figure 13). The vehicle was lightly damaged (Figure 14).

FIGURE 12 Vehicle contact marks, Test 475.

FIGURE 13 Rail damage: displaced posts, bent rail, broken post, Test 475.

FIGURE 14 Vehicle after Test 475.

Barrier Damage

Post and rail damage was limited to the impact area. Damage consisted of a slight bend in the transition rail, displacement of posts, and one broken post (Figure 15). Post 3 was broken about 15 in. below ground level at a knot.

The permanent lateral deflection, measured at the posts, ranged from 1/16 to 4⅜ in. The displacements of each of the posts is shown in Table 3. The maximum displacement was 5⅛ in. between Posts 2 and 3. The maximum dynamic lateral movement was 9.6 in. at Post 3. The total length of vehicle contact was about 15 ft. The approach transition was permanently bent and the Thrie beam–W-beam transition was damaged; both were replaced.

Dummy Response

During impact, the unrestrained dummy was thrown to the right side of the vehicle. The dummy's final position was lying on its side with its upper body across the passenger side and its legs wedged under the steering wheel.

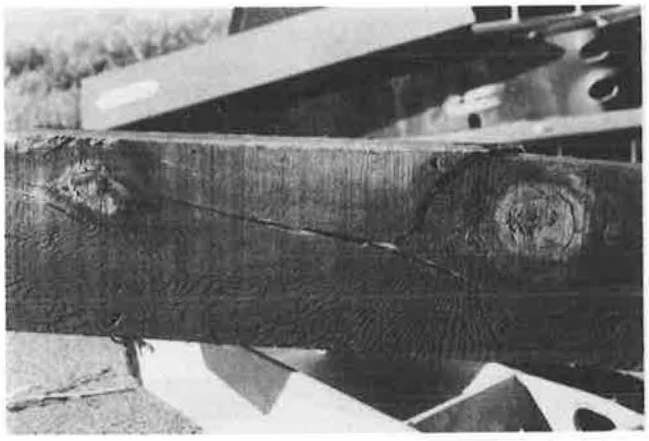

FIGURE 15 Rail damage, Test 475.

TABLE 3 POST DEFLECTIONS (in.)

Post	Test 475	Test 476
1	2 7/8	-3/8
2	4 3/8	13/16
3	3 3/4	1/2
4	1 1/16	1/16
5	3/8	-1/4
6	1/16	1/16

Test 476

Test Description

The right front bumper of the test vehicle struck the bridge approach transition near the midpoint between Posts 2 and 3 of the transition at a speed of 49.4 mph at an angle of 20¾ degrees. Vehicle contact with the rail began 3.3 ft downstream of Post 3 and continued for a length of 7.4 ft (Figure 16). The car was smoothly redirected without exhibiting any tendency to snag or pocket and lost contact with the barrier at an exit angle of 4¾ degrees. The maximum roll was +2¾ degrees. The final location of the car was 118 ft downstream from the impact point and 58.5 ft in front of the barrier. The vehicle was moderately damaged (Figure 17).

Barrier Damage

Post and rail damage was limited to the impact area. The barrier damage consisted of a slight bend of the transition rail and displacement of posts. Displacements were nominal and are tabulated in Table 3. The maximum dynamic lateral movement was 6.3 in. at Post 2.

Dummy Response

During collision, the unrestrained dummy was forcefully thrown to the right side of the vehicle and pushed the door outward.

FIGURE 16 Vehicle contact marks, Test 476.

FIGURE 17 Vehicle after Test 476.

The dummy's final position was lying on its side with its upper body across the passenger side with its legs wedged under the steering wheel.

Static Post Tests

A series of static tests on W6 × 15.5 steel posts were conducted. There were five tests, each on a different bridge rail post design. Post designs for Tests *A* through *E* are shown in Figure 18.

The purpose of the tests was to evaluate the effect of eliminating the web stiffeners at the base of the post and alternate post-strengthening schemes. Test *A* used a post as crash tested, Test *B* used the preferred alternate strengthening scheme, and Test *C* used an unstrengthened post. Tests *D* and *E* were additional alternate strengthening schemes. The test device consisted of a load frame anchored to the simulated bridge deck, a 75-ton hydraulic jack, a load cell, two linearly variable differential transformers (LVDTs), and a bearing plate. Load was applied 26 in. above the deck surface; the LVDTs measured displacement 4½ in. above the deck (Figure 19).

The test results are summarized in Table 4. Typically the web at the base of the post would buckle upon failure (Figure 20*a*, *b*, and *c*). In Tests *A* and *B* the web stiffeners and sandwich plates added sufficient strength so that the top anchor bolts pulled out. Total deformation of test Post *A* was less than two of the posts in Crash Test 473 (Figure 21).

DISCUSSION

Structural Adequacy

In Tests 473 and 475, a 5,400-lb pickup truck tested the structural adequacy of the bridge rail and the transition. The barriers were not penetrated or vaulted and there were no detached barrier elements; thus the design is adequate for the tested conditions. The bending of the bridge rail post with the partial pull through of the nuts and washers at the flange (Figure 8) indicate that the system is being significantly stressed by the impact. There was not much reserve strength to handle more severe impacts. The 10-gauge rail was effective in distributing impact loads among several posts. Vehicle contact in Test 473 was between Posts 4 and 7, and there was bending of Posts 3 through 9.

The transition tested appears to be of about the same stiffness as the bridge rail, evidenced by the dynamic deflections. The smaller magnitude of the residual deflection in the transition illustrates the greater resilience of the soil-wood post support as compared with the steel post. It is noteworthy that the transition performed well even though one post broke below grade. (The post fractured because of a flaw in the structure of the wood, a large knot through the 8-in. faces, that was near the allowable limit for that type of defect.)

Occupant Risk

Tests 474 and 476, small car, were to evaluate occupant risk factors. Occupant risk factors were also calculated for the other tests. The occupant impact velocities and ridedown accelerations were below those required by the AASHTO *Guide Specifications for Bridge Railings* (*3*) (Table 5). The vehicles in all tests remained upright and exhibited no tendency to roll over—all roll angles were less than 10 degrees. There was no evidence of the vehicles snagging or pocketing on the bridge rail or transition. Tire marks were observed on the ground about 3 in. from the face of posts and there was no evidence of any vehicle contact with posts.

The effective coefficient of friction (μ) for each test was calculated. It ranged from 0.07 to 0.22, within the good range per the AASHTO *Guide Specifications for Bridge Railings* (*3*).

Vehicle Trajectory

The post impact trajectory of the vehicles followed the same general pattern in each test; the vehicle moved away from the barrier in a straight line or slight curve (Figure 22). The exit angle for each test was low (4 to 6¼ degrees), well below 60 percent of the impact angle.

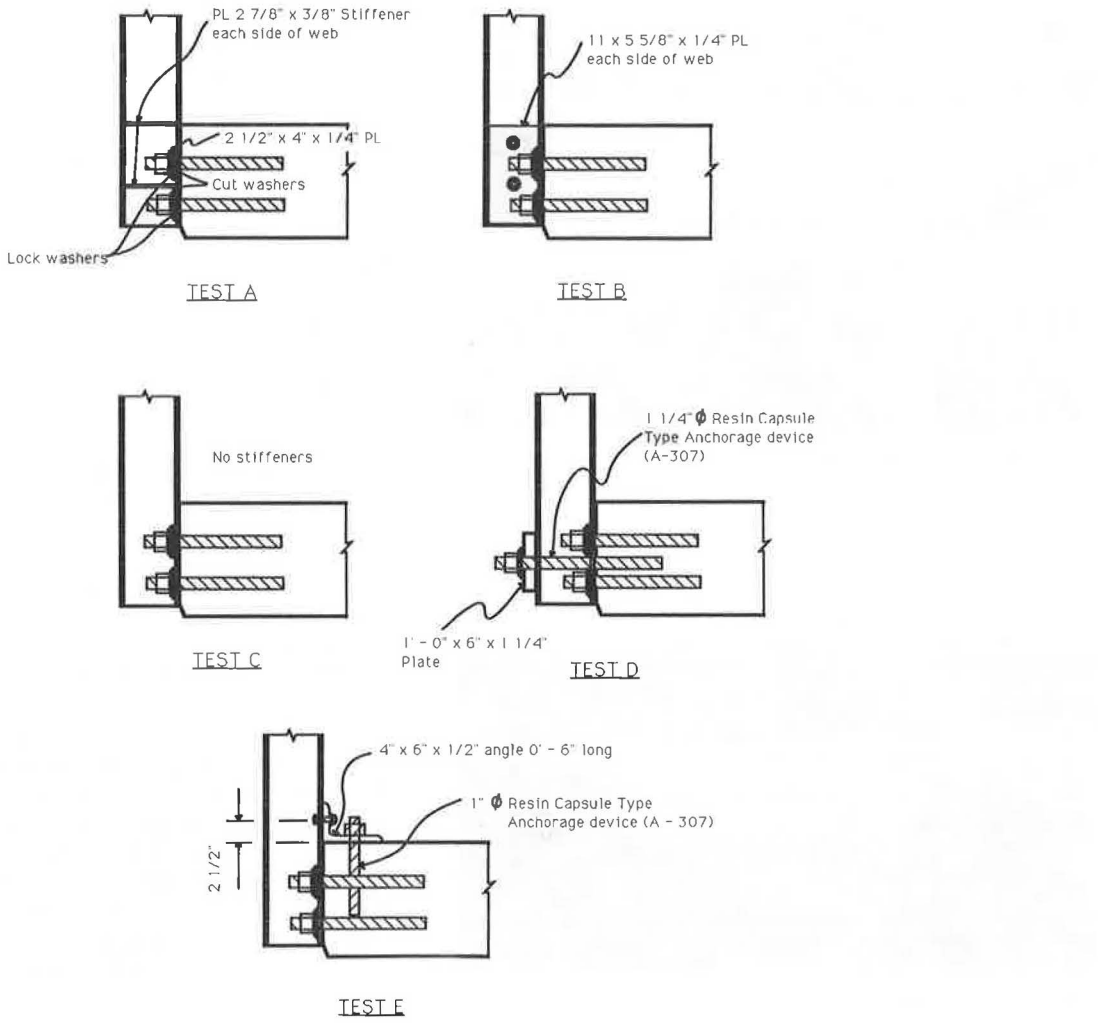

FIGURE 18 Static tested post designs.

The Guide Specification evaluation criterion "*h*" indicates that the vehicle should be no more than 20 ft from the face of the barrier after having traveled 100 ft. Measurements were not taken after each test to determine if this criterion was met or not. If it is assumed that the vehicle path was straight after impact—generally not the case—the criterion can be derived that "*h*" was not met. There was not enough information available to determine this.

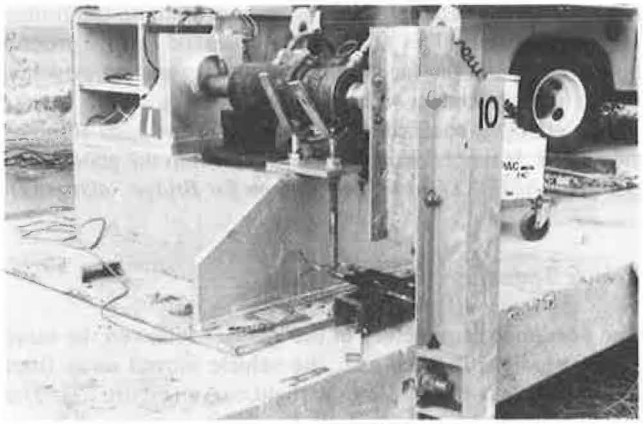

FIGURE 19 Static test setup.

TABLE 4 STATIC LOADS ON W 6 × 15.5 POSTS

Test	Maximum Load(KIP)	Failure Mode
A	7.7	Anchor bolts pulled out and concrete spalled
B	7.7	Anchor bolts pulled out and concrete spalled
C	6.6	Web Buckled
D	7.7	Web Buckled
E	8.7	Concrete supporting bracket spalled

Rail Installation and Maintenance

There were no problems encountered during the installation of the bridge rail, although it is possible that there could be problems on an actual bridge. Large resin capsule anchors, ¼ in. and 1 in., require a considerable force to set the threaded rod to the proper depth before the resin sets. The shape of

(a)

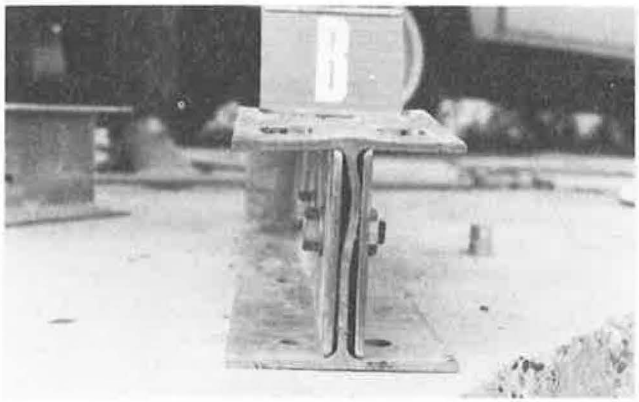

(b)

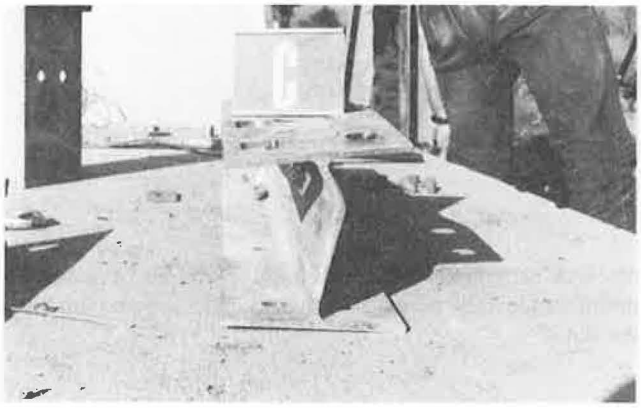

(c)

FIGURE 20 Bottom end of three posts after static tests.

the trench behind the simulated bridge deck facilitated applying that force; on an actual deck some other provision must be made to support workers. Installation of the posts and rail elements was similarly eased by being able to stand behind the rail on the ground. Rail installation was slightly more difficult than a structural tube rail because of the large number of fasteners at the rail splices.

After Test 473, the seven bent posts and three rail elements were replaced. Removal of Posts 5 and 6 was quite difficult; the holes and the post flanges were pushed around the washers

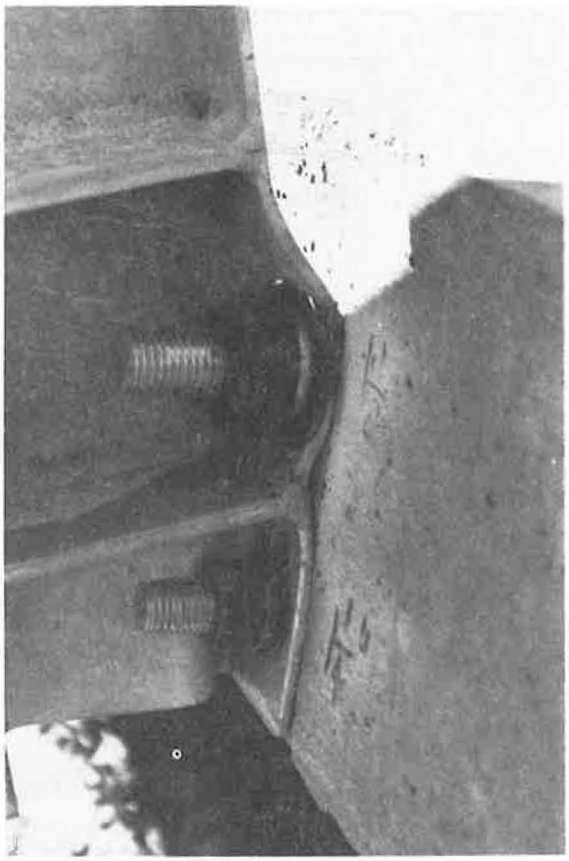

FIGURE 21 Buckled web contacted lower fastening nut on Post 6.

TABLE 5 VEHICLE KINEMATICS

Test #	Occ. Impact Velocity (fps) Long.	Lat	Ride down Acceleration (g) Long.	Lat.	Coeff. of Friction μ
473	7.7	n/a	n/a	n/a	0.07
474	13.2	-17.3	-0.6	-6.0	0.05
475	6.8	-17.5	-0.4	-10.3	0.12
476	11.6	-20.9	-1.4	-11.4	0.22

and nuts, making access to the top fasteners quite difficult. Also, the collapse of the web at the bottom of the post restricted the movement of one of the nuts (Figure 21). A cutting torch would be required to remove such a damaged post from a bridge deck with access only from the deck. The bridge approach transition was constructed and repaired by a guard rail maintenance crew by hand methods. No problems were encountered during installation or repair.

CONCLUSIONS

The following conclusions were drawn:

1. The Thrie beam bridge rail and transition design presented in this paper can successfully contain a 5,400-lb. ballasted pickup truck striking at a 20 degree angle at 45 mph.

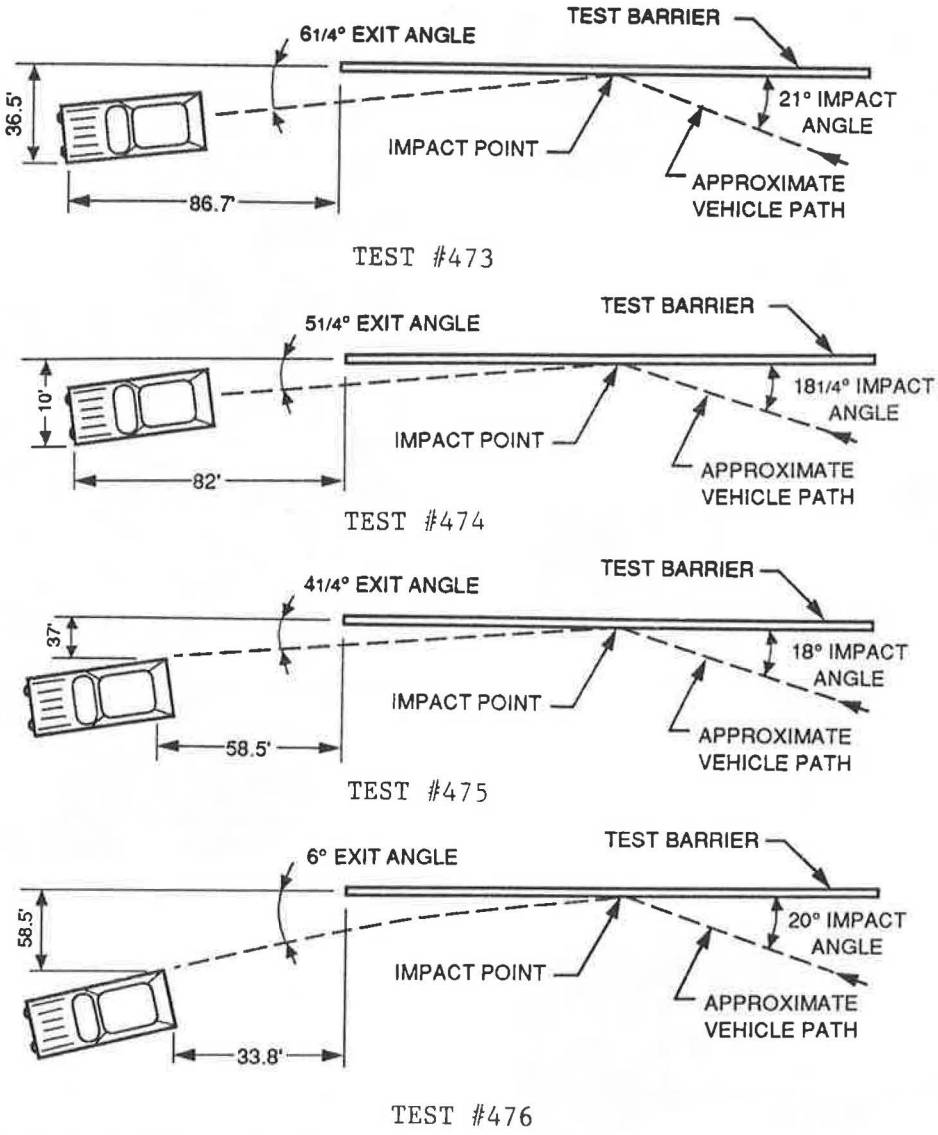

FIGURE 22 Vehicle trajectories.

2. The bridge rail and transition can smoothly redirect a small car and a pickup truck without any signs of undesirable behavior and without exceeding occupant risk evaluation guidelines.

3. Resin capsule anchors are adequate to withstand the impact loading on a W6×15.5 steel post when installed in reinforced concrete.

4. The Thrie beam bridge rail and transition designs essentially met the requirements for Performance Level 1 crash testing in the AASHTO *Guide Specifications for Bridge Railings* (*3*) and would be suitable for use as new or retrofit barriers on narrow, low-speed, low-volume local roads.

5. Some sort of post strengthening should be included on a Thrie beam bridge rail. Welded web stiffeners were crash tested; bolted-in sandwich plates would probably perform similarly at a lower cost.

ACKNOWLEDGMENTS

The work reported in this paper is the result of a research project federally funded through the highway planning and research program. The California Department of Transportation conducted the crash tests and collected and analyzed the data.

REFERENCES

1. J. L. Beaton and R. N. Field. *Dynamic Full-Scale Tests of Bridge Rails*, Materials and Research Department, California Division of Highways, Sacramento, Dec. 1960.

2. Recommended Procedures for the Safety Performance Evaluation of Highway Appurtenances. *National Cooperative Highway Research Program Report 230*, TRB, National Research Council, Washington, D.C., March 1981.

3. *Guide Specifications for Bridge Railings*. American Association of State Highway and Transportation Officials, 1989.

Publication of this paper sponsored by Committee on Roadside Safety Features.

Single-Slope Concrete Median Barrier

W. LYNN BEASON, H. E. ROSS, JR., H. S. PERERA, AND MARK MAREK

A single-slope concrete median barrier has been developed for use as either a permanent concrete median barrier or as a temporary barrier. It is designed to meet accepted criteria for the performance of longitudinal barriers and to be used in applications in which the New Jersey concrete median barrier would normally be employed. The primary advantage of the new barrier is that the pavement adjacent to it can be overlaid several times without changing the performance of the barrier. This should help to reduce the maintenance costs associated with its use. The performance of the new barrier is documented with the presentation of results from four full-scale crash tests. These tests were conducted with the new single-slope concrete median barrier deployed in both permanent and temporary configurations.

Over the past several years, the New Jersey concrete median barrier (CMB) has gained widespread acceptance. Further, other types of longitudinal barriers employing the New Jersey shape, including bridge rails and portable barriers, have become very popular. Full-scale crash tests have shown that the New Jersey longitudinal barrier is capable of meeting the requirements specified in *National Cooperative Highway Research Program Report 230* (*1*), including both strength and stability requirements.

Although the use of the New Jersey CMB has been successful, there are disadvantages associated with its use. One of the biggest of these is that the profile of the New Jersey shape varies with height above grade. This means that if the roadway is resurfaced, both the height of the barrier and the shape of the barrier face will be changed. As the thickness of the overlay is increased, the performance of the New Jersey CMB will become unsatisfactory, if only because of the reduction of the overall height of the barrier. Therefore, New Jersey CMBs must be reset as the pavement height is increased in the overlaying process. The resetting process is both expensive and time consuming.

The purpose of the research presented in this paper was to develop a new CMB shape, the performance of which would not be impaired by the application of several inches of pavement overlays. Further, a major effort was made to develop the geometry of the new CMB so that its effect on vehicles striking it is equivalent to the effect of the New Jersey CMB under similar circumstances as determined through the use of computer simulations (*2*).

The new barrier has a single-slope face. This shape was suggested by engineers with the Texas State Department of Highways and Public Transportation (SDHPT) (*2*). Because the barrier face has a single, constant slope, the shape of the barrier face is not affected by overlaying the adjacent pavement. Rather, the additional pavement overlay serves to anchor the barrier more securely at its base, thus increasing its resistance to lateral impact forces. The new single-slope CMB can be used in both temporary and permanent applications. The performance of the single-slope CMB was examined in a series of four full-scale crash tests. The first test was conducted to verify that the performance of the barrier is acceptable in a temporary application. The second and third tests were conducted to establish the performance of the barrier in a permanent application. The fourth test was conducted to establish the performance of the single-slope CMB in an alternate temporary configuration.

The remainder of this paper is divided into three major sections. In the next section, a brief description of the newly developed single-slope CMB is presented. This is followed by a section on the full-scale testing of the single-slope CMB. The final section presents conclusions and recommendations for the use of the single-slope CMB.

DEVELOPMENT OF THE SINGLE-SLOPE CMB

The objective of the research presented in this paper was to develop a single-slope CMB. The design of the single-slope CMB is based on the results of a series of computer simulations and engineering judgments, as discussed in the following paragraphs.

The initial geometric constraints were that the single-slope CMB should be 42 in. (106.7 cm) tall, with a flat top that is a minimum of 8 in. (20.3 cm) wide. In addition, it was required that the impact face of the single-slope CMB incorporate a constant slope.

It is known that a rigid barrier with a vertical face results in the minimum vehicle instability during impact. Vertical face rigid barriers have undergone extensive testing with a variety of different vehicles ranging from compact automobiles to tractor-trailers (*3,4*). Computer simulations and practical experience suggest that as the angle of the barrier face (measured with respect to the vertical) is increased, vehicles striking it will be subjected to increasing instabilities. If the angle of the barrier face becomes large enough, the vehicle instabilities will lead to ramping or vehicle roll-over, or both.

Vehicles are clearly more stable during impacts with vertical, rigid barriers, but it is possible that a vehicle striking a tall, vertical barrier will be subjected to accelerations that are large enough to cause the heads of the occupants to be propelled through the vehicle side windows and against the barrier. This behavior has been observed in crash tests that incorporated anthropomorphic dummies. The angle of the barrier face was set so that an impacting vehicle will roll away from the barrier to prevent this phenomenon.

Texas Transportation Institute, The Texas A&M University System, College Station, Texas 77843.

Although the design of the single-slope barrier was not based solely on the results of computer simulations, such results were used to study the effect of the barrier slope on the vehicle redirection characteristics. The computer program used to evaluate the performance of the single-slope CMB was Highway-Vehicle-Object-Simulation-Model (HVOSM) (*5*). The version of HVOSM used in this study was the RD2 version, which incorporates modifications developed by researchers at the Texas Transportation Institute (TTI). The TTI modifications permit the structure of the vehicle to interact with a multi-faced rigid barrier. Studies of rigid New Jersey CMBs made with this modified version of HVOSM have been reasonably successful (*6,7*). Therefore, the RD2 version of HVOSM was used to study the effects of various barrier face angles on the performance of the single-slope CMB.

The performance of rigid longitudinal barriers is evaluated by the stability of the vehicle after impact and the severity of the occupant impact forces. The roll angle of the vehicle is an important measure of vehicle stability and occupant impact velocity is controlled to limit occupant impact forces. Large barrier face angles (measured from the vertical) increase the propensity for the vehicle to become unstable, whereas small angles increase occupant impact velocities. The objective of the computer simulation study was to provide critical input into the selection of a barrier face angle that results in vehicle roll angles and occupant impact velocities that are similar to those associated with the New Jersey CMB.

The HVOSM program was first used to simulate various barrier impacts involving a 4,500-lb (2,043-kg) automobile with a speed of 60 mph (96 km/hr) and an impact angle of 25 degrees. The performance of a New Jersey CMB and a set of rigid single-slope CMBs with various barrier face angles was examined. The 42-in. (106.7-cm) high single-slope barriers, examined with the computer simulations, contained horizontal offsets of 0 in. (0 cm), 4 in. (10.2 cm), 8 in. (20.3 cm), and 12 in. (30.5). These geometries resulted in single-slope barriers with angles of 0, 5.4, 10.8, and 14 degrees measured from the vertical. Maximum roll angles and occupant impact velocities determined using the HVOSM program are presented in Table 1 for these conditions.

The HVOSM program was next used to simulate barrier impacts involving an 1,800–lb (817–kg) automobile with a speed of 60 mph (96 km/hr) and an impact angle of 20 degrees. The maximum roll angles and the occupant impact velocities determined using the HVOSM program for this latter vehicle type are presented in Table 2.

The primary use of the data presented in Tables 1 and 2 was to provide a mechanism for relative comparisons of the performance of the different barriers. Computer simulations are not yet sophisticated enough so that a barrier design can be based solely on computer simulation data. Further, it would be naive to believe that the computer simulation results should agree precisely with full-scale crash test results.

Examinations of the simulation data contained in Tables 1 and 2 show that a single-slope CMB with a barrier face angle of 10.8 degrees results in an overall barrier-vehicle interaction that is reasonably similar to that achieved with the New Jersey CMB. Based on these data, engineering judgment, and the initial geometric constraints, it was determined that the single-slope CMB should have a base width of 24 in. (61 cm), a top width of 8 in. (20.3 cm), and a height of 42 in. (106.7 cm), as shown in Figure 1. This conclusion was reinforced by simplified approximate analyses and the collective judgment of the TTI research staff.

A comparison of the cross-section properties of the single-slope CMB and the New Jersey CMB is presented in Figure 2. The single-slope CMB is approximately 30 percent taller than the New Jersey CMB. The weight of the single-slope CMB is about 675 lb/ft (1,000 kg/m). This estimated weight is approximately 40 percent more than the New Jersey CMB. The weight increase is a result of the increased barrier height. The resistance to overturning provided by the dead weight of the single-slope CMB is approximately 20 percent more than that shown for the New Jersey CMB. Finally, the center of gravity of the single-slope CMB, which is approximately 18 in. (45.7 cm), is much closer to the center of gravity of typical automobiles than the center of gravity of the New Jersey CMB, which is approximately 11.5 in. (29.2 cm). All of these geometric factors combine to suggest that the single-slope CMB should display a better impact performance than the New Jersey CMB, particularly in the temporary configuration.

Construction details of the single-slope CMB are presented in Figure 3. It is recommended that the single-slope CMB be fabricated in 30 ft (9.1 m) lengths. Two steel pipes are embedded in the barrier segments approximately at the quarter points to facilitate handling of the barrier. The procedure for lifting the barrier involves the insertion of steel lifting bars through the steel pipes. Chains are then draped around the lifting bars

TABLE 1 COMPUTER SIMULATION RESULTS FOR LARGE AUTOMOBILE

Barrier Type	Maximum Roll Angle	Occupant Impact Velocity ft/s (m/s)	
	degrees	Longitudinal	Lateral
New Jersey CMB	20	16.3 (5.0)	20.6 (6.3)
Vertical Single-Slope CMB	26	18.5 (5.6)	21.3 (6.5)
5.4 Degree Single-Slope CMB	26	17.4 (5.3)	22.7 (6.9)
10.8 Degree Single-Slope CMB	24	15.9 (4.8)	21.3 (6.5)
14 Degree Single-Slope CMB	38	13.7 (4.2)	20.1 (6.1)

TABLE 2 COMPUTER SIMULATION RESULTS FOR SUBCOMPACT AUTOMOBILE

Barrier Type	Maximum Roll Angle degrees	Occupant Impact Velocity ft/s (m/s)	
		Longitudinal	Lateral
New Jersey CMB	20	11.9 (3.6)	21.4 (6.5)
Vertical Single-Slope CMB	11	13.9 (4.2)	20.2 (6.2)
5.4 Degree Single-Slope CMB	16	15.8 (4.8)	22.4 (6.8)
10.8 Degree Single-Slope CMB	13	12.2 (3.7)	20.7 (6.3)
14 Degree Single-Slope CMB	31	11.8 (3.6)	20.5 (6.2)

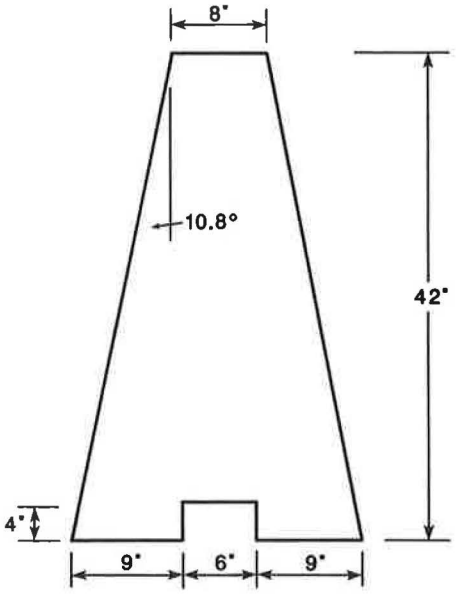

FIGURE 1 Typical cross section of single-slope CMB.

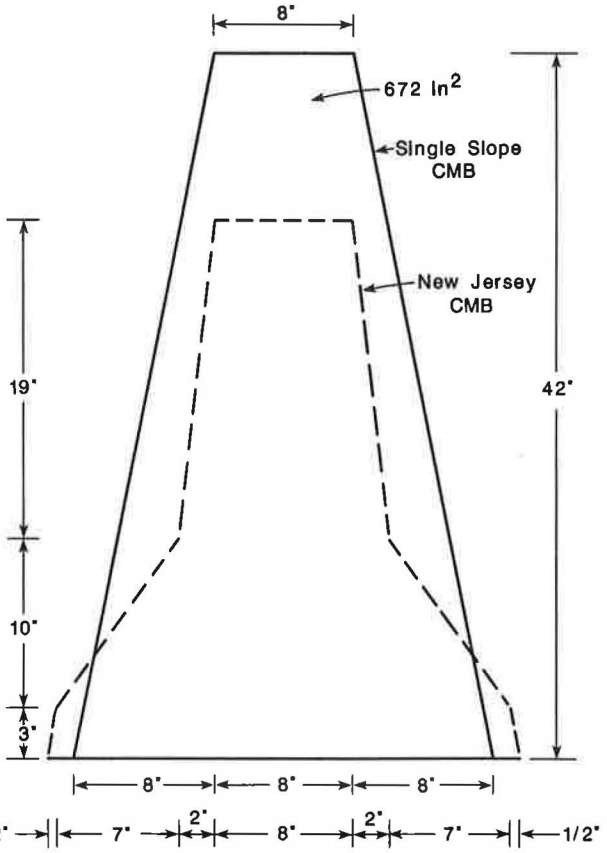

FIGURE 2 Comparison of single-slope CMB and New Jersey CMB.

and the barrier is moved with either two pieces of light lifting equipment or a single piece of heavy lifting equipment. In the current project the barrier segments were moved with two forklift machines with approximately the same ease as moving similar 30 ft (9.1 m) segments of the New Jersey CMB.

The ends of the single-slope CMB segments are equipped with provisions for two different types of connections. The first involves the use of external steel angles that are attached to the barrier segment ends with specially fabricated bolts, as shown in Figures 3 and 4. This angle-splice connection is for use with temporary connections and is not required when the barrier is installed in the permanent configuration.

The second connection detail involves a slot that is cast into both ends of the barrier segments, as shown in Figure 3. A permanent connection is made by inserting a reinforcing bar grid into the slots of both ends of mating barrier segments and filling the slots and the space between the barrier ends with grout. The permanent installation is completed by locking the barrier segment into place with a minimum of 1 in. (2.54 cm) of asphalt overlay placed next to both faces of the barrier.

An alternative temporary connection can be accomplished by inserting the reinforcing bar grid into the slots without using the grout. Although this temporary connection is not as strong as the angle-splice connection, it is adequate for temporary applications.

FULL-SCALE CRASH TESTS

Four full-scale crash tests were conducted to evaluate the performance of the single-slope CMB for structural adequacy, occupant risk, and vehicle exit trajectory. The first test involved a 4,500-lb (2,043-kg) full-size automobile that struck the single-slope CMB in the angle-splice temporary configuration. The second and third tests involved a 4,500-lb (2,043-kg) full-size automobile and an 1,800-lb (817-kg) subcompact

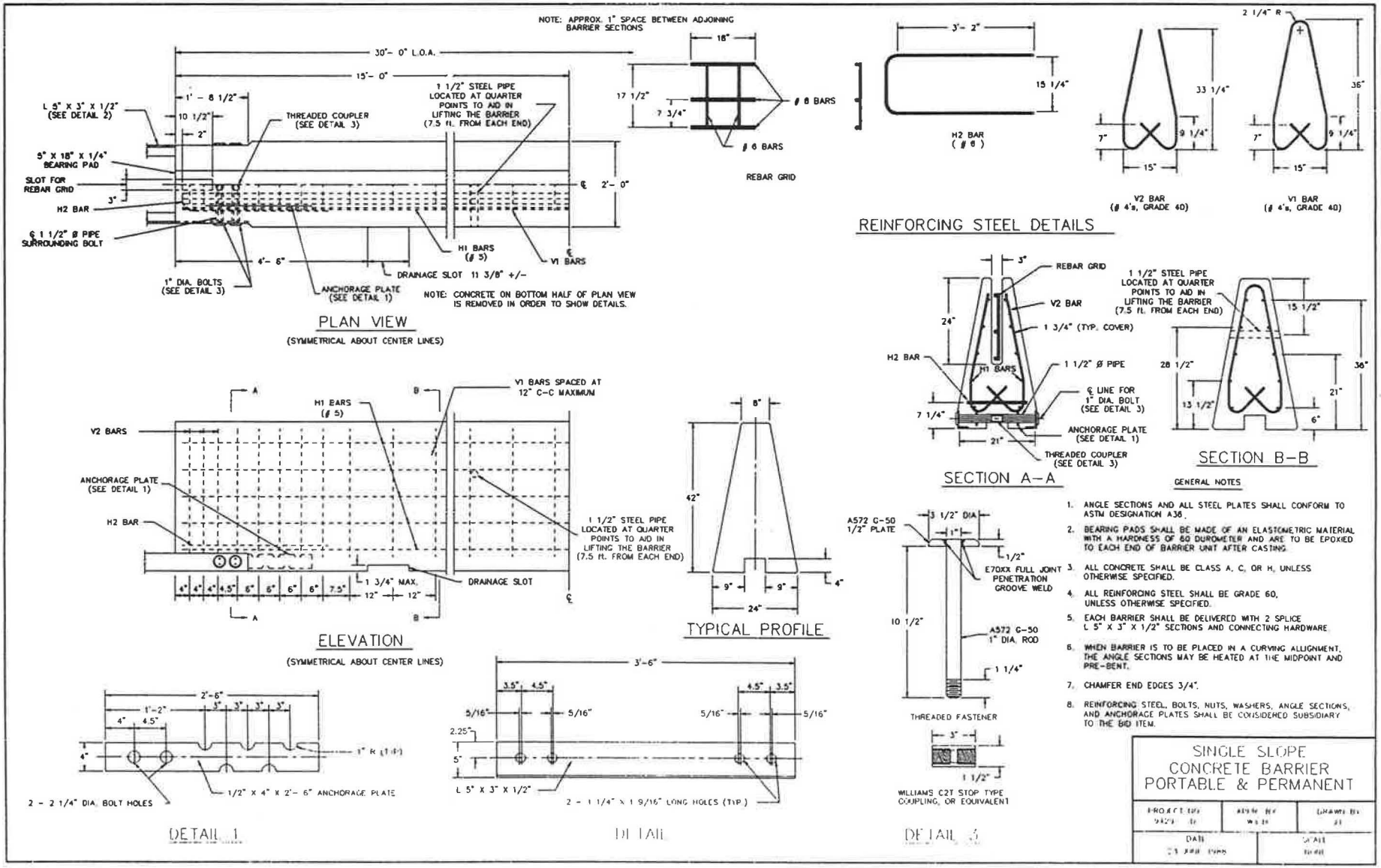

FIGURE 3 Construction details for single-slope CMB.

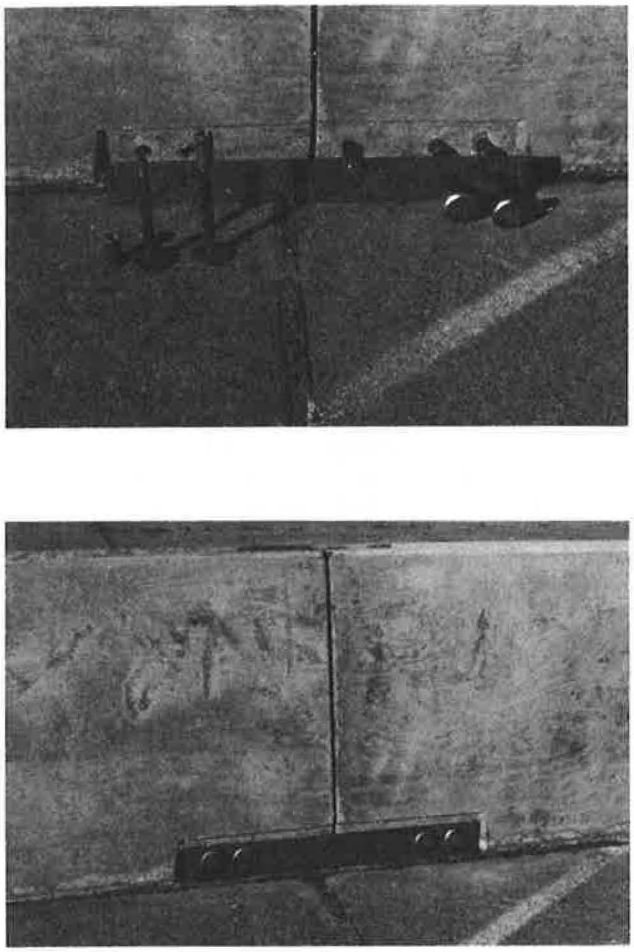

FIGURE 4 Temporary angle-splice connection.

automobile, respectively. The vehicles in the second and third tests struck the single-slope CMB deployed in the permanent configuration. The fourth test involved a 4,500-lb (2,043-kg) full-size automobile that struck the single-slope CMB in the alternate temporary configuration.

A total of six 30-ft (9.1-m) single-slope barrier segments were fabricated for testing. The first three full-scale crash tests were conducted using four 30-ft (9.1-m) single-slope CMB segments connected together to form a 120-ft (36.4-m) longitudinal barrier. The fourth full-scale crash test was conducted using all six of the 30-ft (9.1-m) CMB segments for an overall length of 180 ft (54.6 m).

In all of the full-scale crash tests, the vehicle struck the longitudinal barrier at a point approximately 5 ft (1.5 m) upstream of the middle barrier segment joint. This impact point was chosen to provide the most critical impact situation for both strength and snagging.

Test results show that the single-slope CMB, in all configurations, contained and smoothly redirected the test vehicles with minimal lateral movement in the temporary configurations and no lateral movement in the permanent configuration. There were no intrusions into occupant compartments and there were minimal deformations of the occupant compartments. The vehicles remained upright and relatively stable during the collisions. The vehicle trajectories at loss of contact indicated minimal intrusions into the adjacent traffic lanes. Test statistics for the four crash tests are summarized in Table 3. Complete photographic and acceleration data are presented elsewhere (*2*). Brief descriptions of each test are provided in the following paragraphs.

Test 1

Test 1 involved testing the single-slope barrier deployed in a temporary configuration. In this test, the barrier segments

TABLE 3 SUMMARY OF CRASH TEST RESULTS

Test No.	1	2	3	4
Vehicle Weight, lb (kg)	4500(2043)	1800(817)	4500(2043)	4500(2043)
Impact Speed, mi/h (km/hr)	60.3(97.0)	60.7(97.70)	63.1(101.5)	62.0(99.8)
Exit Angle, degrees	0.5	4.3	8.5	3.5
Impact Angle, degrees	15.2	19.9	26.5	15.1
Displacement, in (cm)	7.0(17.8)	0.0(0.0)	0.0(0.0)	6.0(15.2)
Maximum Roll angle, degrees	12	6.3	32.5	17
Occupant Impact Velocity ft/s (m/s) Longitudinal Lateral	 14.4(4.4) 17.6(5.4)	 15.7(4.8) 27.7(8.4)	 22.1(6.7) 28.9(8.8)	 16.3(5.0) 18.4(5.6)
Occupant Ridedown Acceleration g's Longitudinal Lateral	 -2.5 -7.7	 -2.3 -9.2	 -4.2 -10.7	 -3.2 -6.2
Vehicle Damage Classification TAD CDC	 11LFQ4 11FLEK2& 11LFEW3	 11LFQ5 11LFEW3	 11LFQ5 11LFAW3	 11FLQ4 11FLEK2& 11LFEW1

were joined together with the angle-splice temporary barrier connections. Because the angle-splice connections are reasonably stiff, it was determined that four barrier segments would adequately represent a continuous barrier installation. The barrier segments were positioned on an existing concrete surface at the TTI test track with no positive attachment to the roadway surface.

A 1980 Cadillac Sedan DeVille was directed into the single-slope CMB. The test inertia mass of the vehicle was 4,500 lb (2,043 kg). The speed of the vehicle at impact was 60.3 mph (97.0 km/hr) and the angle of impact was 15.2 degrees. These impact conditions are recommended in *National Cooperative Highway Research Program Report 230* (*1*) for temporary barriers. The vehicle struck approximately 55 ft (16.8 m) from the upstream end of the barrier. The maximum roll angle of the vehicle was about 12 degrees. The barrier received minimal cosmetic damage, as shown in Figure 5. The maximum lateral movement of the barrier was 7 in. (17.8 cm). The vehicle sustained moderate damage to the left side, as shown in Figure 6.

National Cooperative Highway Research Program Report 230 (*1*) contains occupant impact velocity and occupant ridedown acceleration performance limits for tests involving 1,800-lb (817-kg) vehicles striking with angles of 15 degrees and velocities of 60 mph (96 km/hr). These limits do not apply to the current test; the values are presented for information only. The longitudinal and lateral occupant impact velocities were determined to be 14.4 ft/s (4.4 m/s) and 17.6 ft/s (5.4 m/s), respectively. The highest 0.010-sec occupant ridedown accelerations were determined to be −2.5 g (longitudinal) and −6.8 g (lateral). A detailed summary of these and other pertinent crash test data is presented in Figure 7.

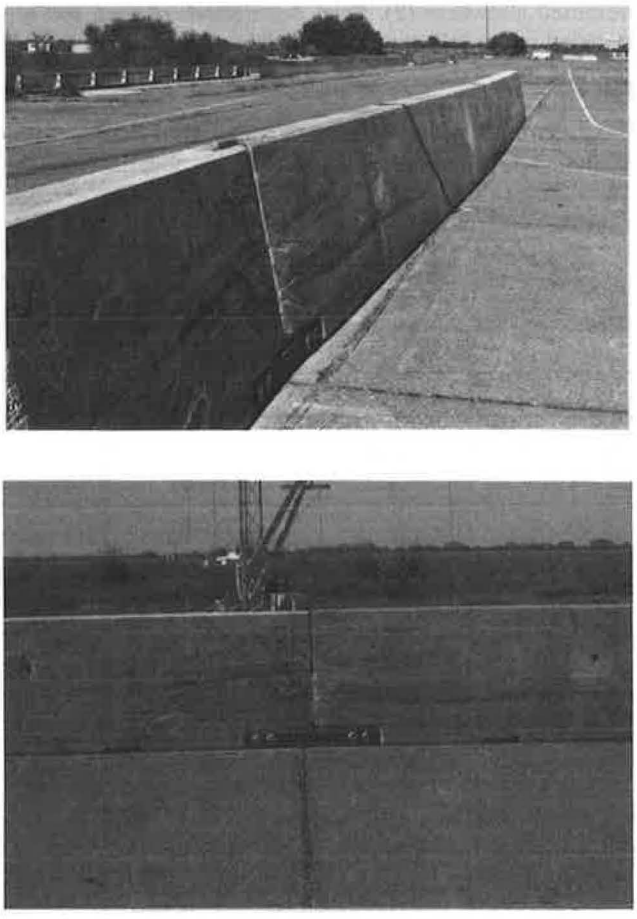

FIGURE 5 Single-slope barrier after Test 1.

Test 2

Test 2 involved testing the single-slope CMB deployed in a permanent configuration. In this test, the barrier segments were positioned on a subbase consisting of 2 in. (5.1 cm) of hot mix asphalt on top of 4 in. (10.2 cm) of compacted crushed limestone. The subbase area was approximately 125 ft (37.9 m) long and 8 ft (2.4 m) wide. Because the subbase provides continuous support for the barrier segments, it was judged that the performance of the barrier should be relatively independent of the barrier length. Therefore, it was determined

FIGURE 6 Vehicle after Test 1.

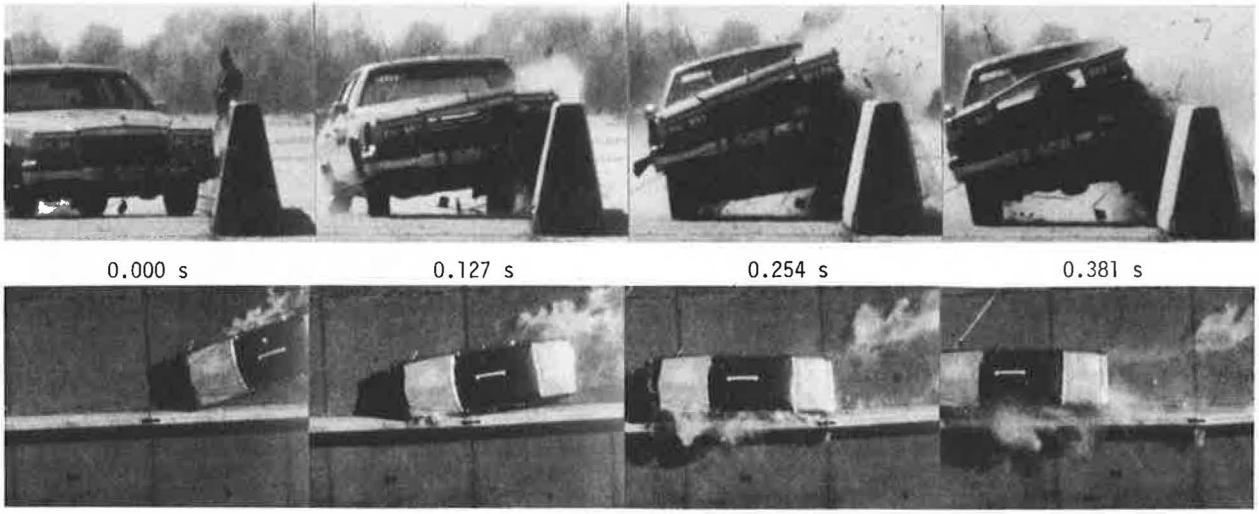

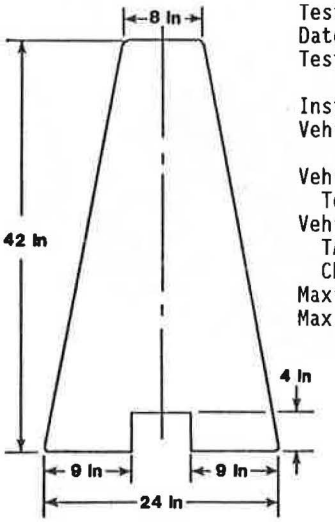

Test No.	9429C-1
Date	11/22/88
Test Installation	Single Slope Concrete Barrier
Installation Length.	120 ft (36.6 m)
Vehicle	1980 Cadillac Sedan DeVille
Vehicle Weight	
Test Inertia	4,500 lb (2,043 kg)
Vehicle Damage Classification	
TAD	11LFQ4
CDC	11FLEK2 & 11LFEW3
Maximum Vehicle Crush.	12.0 in (30.5 cm)
Max. Barrier Movement.	7.0 in (17.8 cm)

Impact Speed.	60.3 mi/h (97.0 km/h)
Impact Angle.	15.2 deg
Exit Speed.	51.3 (82.5 km/h)
Exit Trajectory	0.5 deg
Vehicle Accelerations	
(Max. 0.050-sec Avg)	
Longitudinal.	-3.3 g
Lateral	-6.8 g
Occupant Impact Velocity	
Longitudinal.	14.4 ft/s (4.4 m/s)
Lateral	17.6 ft/s (5.4 m/s)
Occupant Ridedown Accelerations	
Longitudinal.	-2.5 g
Lateral	-7.7 g

FIGURE 7 Summary of results for Test 1.

that four barrier segments would adequately represent a continuous barrier installation.

The four barrier segments were aligned on the subbase so that the impact surface of the barrier was set back approximately 1 ft (.3 m) from the front of the subbase. The reinforcing bar grids were then placed into the slots at the ends of the barrier segments. Another 1 in. (2.54 cm) of hot-mix asphalt was added to the subbase in front and behind the barrier. This final application of asphalt resulted in a 1-ft (0.3-m) wide addition of asphalt on the impact side of the barrier and a 5-ft (1.5-m) wide addition of asphalt on the opposite side of the barrier. Finally, the barrier slots, the gap between the barrier segment ends, and the angle-splice insets on the ends of the barrier were all grouted. The grout was applied so that the 120-ft (36.4-m) barrier had the appearance of a continuous barrier.

A 1980 Honda Civic was directed into the single-slope CMB. The test inertia mass of the vehicle was 1,800 lb (817 kg). The speed of the vehicle at impact was 60.7 mph (97.7 km/hr) and the angle of impact was 19.9 degrees. The vehicle struck approximately 55 ft (16.7 m) from the upstream end of the barrier. The maximum roll angle of the vehicle was about 6.3 degrees. The barrier received minimal cosmetic damage, as shown in Figure 8. There was no discernible movement of the barrier. The vehicle sustained moderate damage to the left side, as shown in Figure 9.

National Cooperative Highway Research Program Report 230 (1) contains occupant impact velocity and occupant ridedown acceleration performance limits for tests involving 1,800-lb (817-kg) vehicles striking with angles of 15 degrees and velocities of 60 mph (96 km/hr). These limits do not apply to the current test; the values are presented for information only. The longitudinal and lateral occupant impact velocities were determined to be 15.7 ft/s (4.8 m/s) and 27.7 ft/s (8.4 m/s), respectively. The highest 0.010-sec occupant ridedown accelerations were determined to be −2.3 g (longitudinal) and −9.2 g (lateral). A detailed summary of these and other pertinent crash test data is presented in Figure 10.

Test 3

Test 3 involved testing the single-slope CMB deployed in a permanent configuration. The same installation used in Test 2 already described was used in this test. The only repair

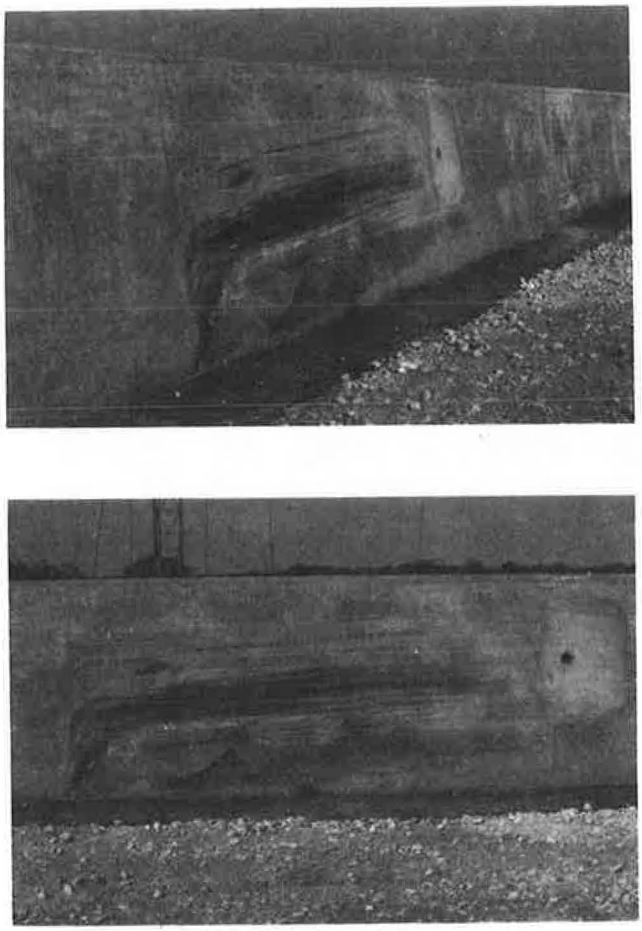

FIGURE 8 Single-slope barrier after Test 2.

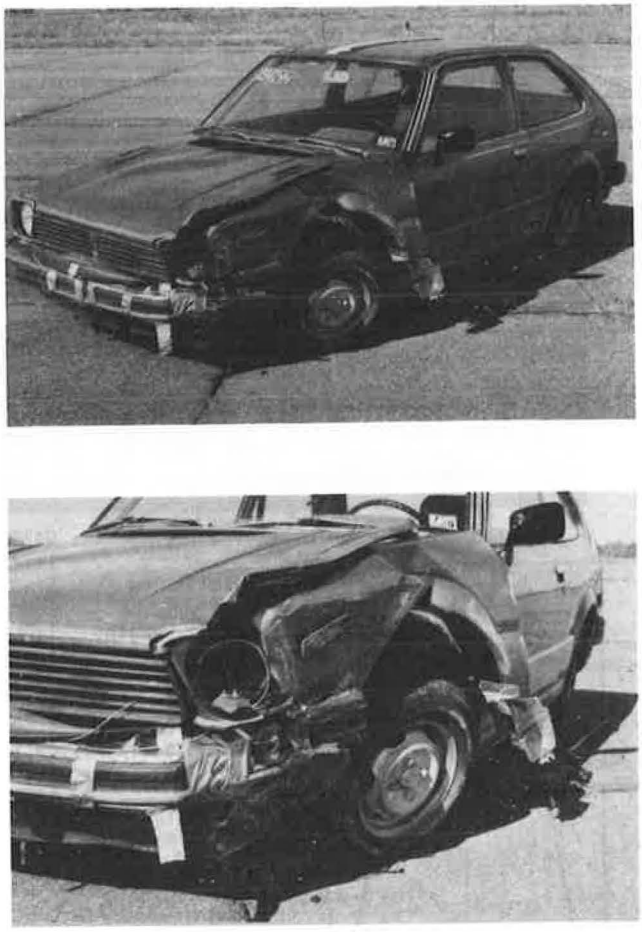

FIGURE 9 Vehicle after Test 2.

involved the application of paint to hide the vehicle and tire marks accrued during Test 2.

Test 3 involved the impact of a 1979 Cadillac Sedan DeVille. The vehicle struck approximately 54 ft (16.5 m) from the upstream end of the barrier. The speed of the vehicle at impact was 63.1 mph (101.5 km/hr) and the angle of impact was 26.5 degrees. There was no discernible movement of the barrier and it received only minimal cosmetic damage, as shown in Figure 11. Examination of the high-speed movies and direct measurements of the markings on the barrier showed that the center of the wheel hub rose to a height of 26 to 30 in. (66 to 76 cm) before losing contact with the barrier. This was the highest vehicle elevation achieved in the set of four crash tests. The maximum vehicle roll angle was about 32 degrees. The vehicle sustained severe damage to the left side, as shown in Figure 12.

National Cooperative Highway Research Program Report 230 (*1*) contains occupant impact velocity and occupant ridedown acceleration performance limits for tests involving 1,800-lb (817-kg) vehicles striking with angles of 15 degrees and velocities of 60 mph (96 km/hr). These limits do not apply to the current test; the values are presented for information only. The longitudinal and lateral occupant impact velocities were determined to be 22.1 ft/s (6.7 m/s) and 28.9 ft/s (8.8 m/s), respectively. The highest 0.010-sec occupant ridedown accelerations were determined to be −4.2 g (longitudinal) and −10.7 g (lateral). A detailed summary of these and other pertinent crash test data is presented in Figure 13.

It should be noted in evaluating the results of this test that both the velocity and the impact angle were higher than specified in *National Cooperative Highway Research Program Report 230* (*1*). The following formula presented in that report allows the impact severity, *IS*, to be quantified in terms of the impact velocity, *V*, vehicle mass, *m*, and impact angle, O.

$$IS = 1/2\ m\ v^2\ (\sin O)^2 \quad (1)$$

The impact severity calculated for the actual test conditions is approximately 25 percent greater than the intended impact severity. This deviation resulted in a much more severe impact than was required in *National Cooperative Highway Research Program Report 230* (*1*). Results from HVOSM suggests that this deviation increased the roll angle by about 31 percent and the occupant impact velocities by about 5 percent. Despite the increased severity of this impact, the vehicle was smoothly redirected and remained upright throughout the test.

Test 4

Test 4 involved testing the single-slope CMB deployed in an alternate temporary configuration. In this test, the barrier

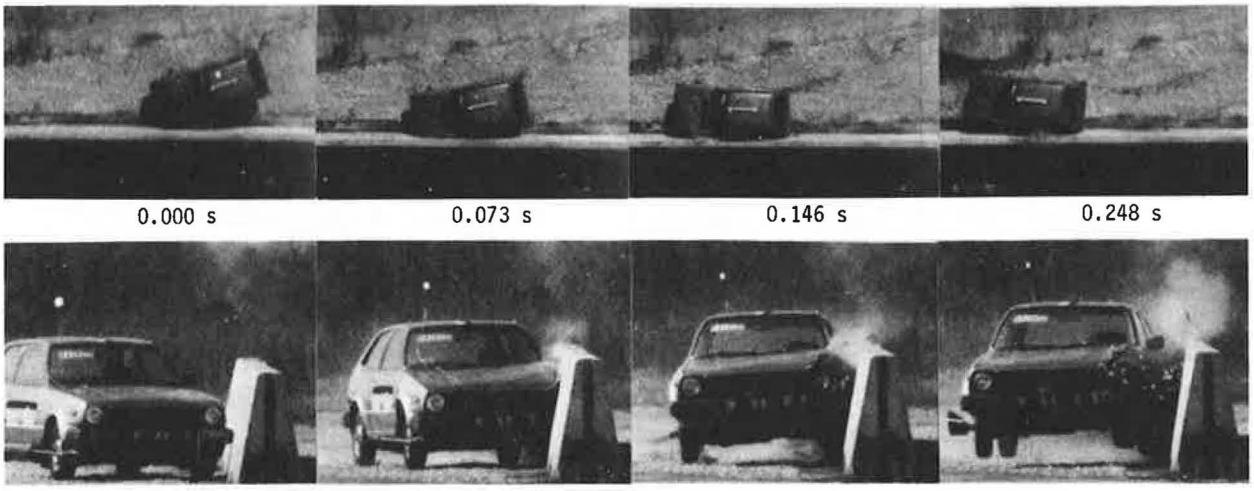

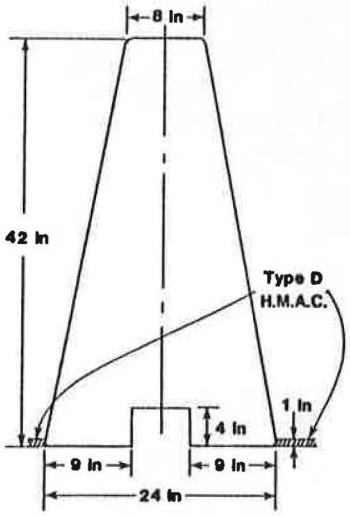

Test No. 9429C-2
Date 12/05/88
Test Installation . . Single Slope Concrete Barrier
Installation Length. . 120 ft (36.6 m)
Vehicle . . . . . 1980 Honda Civic
Vehicle Weight
  Test Inertia . . . . 1,800 lb (817 kg)
Vehicle Damage Classification
  TAD 11LFQ5
  CDC 11LFEW3
Maximum Vehicle Crush. 7.0 in (17.8 cm)

Impact Speed. . . 60.7 mi/h (97.7 km/h)
Impact Angle. . . 19.9 deg
Exit Speed. . . . 52.1 (83.8 km/h)
Exit Trajectory . 4.3 deg
Vehicle Accelerations
  (Max. 0.050-sec Avg)
  Longitudinal. . -6.5 g
  Lateral . . . . -15.3 g
Occupant Impact Velocity
  Longitudinal. . 15.7 ft/s (4.8 m/s)
  Lateral . . . . 27.7 ft/s (8.4 m/s)
Occupant Ridedown Accelerations
  Longitudinal. . -2.3 g
  Lateral . . . . -9.2 g

FIGURE 10 Summary of results for Test 2.

segments were joined together with the ungrouted reinforcing bar grid connection. Because this connection has no moment capacity, it was decided to use all six of the available barrier segments to represent a continuous barrier installation. However, it is believed that the two additional barrier segments had no effect on the outcome of the test. Four of the segments used in this test were the same barrier segments used in the permanent barrier configuration of Tests 2 and 3. The reinforcing bar grids that were grouted into the barriers in the permanent configuration were removed by drilling and chipping. The barrier segments were positioned on an existing concrete surface at the TTI test track, new rebar grids were slipped into place, and no grout was applied. There was no positive attachment to the roadway surface.

A 1981 Pontiac Bonneville was directed into the single-slope CMB. The test inertia mass of the vehicle was 4,500 lb (2,043 kg). The speed of the vehicle at impact was 62.0 mph (99.8 km/hr) and the angle of impact was 15.1 degrees. The vehicle struck approximately 85 ft (26.0 m) from the upstream end of the barrier. The maximum vehicle roll angle was about 17 degrees. The barrier received only minimal cosmetic damage, as shown in Figure 14. The maximum lateral displacement of the barrier was 6.0 in. (15.2 cm). The vehicle received moderate damage to the left side, as shown in Figure 15.

National Cooperative Highway Research Program Report 230 (*1*)contains occupant impact velocity and occupant ridedown acceleration performance limits for tests involving 1,800-lb (817-kg) vehicles striking with angles of 15 degrees and velocities of 60 mph (96 km/hr). These limits do not apply to the current test; the values are presented for information only. The longitudinal and lateral occupant impact velocities were determined to be 16.3 ft/s (5.0 m/s) and 18.4 ft/s (5.6 m/s), respectively. The highest 0.010-sec occupant ridedown accelerations were determined to be −3.2 g (longitudinal) and −6.2 g (lateral). A detailed summary of these and other pertinent crash test results is shown in Figure 16.

When the results of this test are compared with the results of Test 1, it can be observed that the permanent lateral displacements of the barriers are essentially the same. Computer simulations confirm that this observation is to be expected. However, the vehicle in Test 4 rolled almost 50 percent more than the vehicle in Test 1. The reason for the additional roll angle is that the ungrouted grid slot connection allows more torsional rotation of the barrier than the more rigid angle-

FIGURE 11 Single-slope barrier after Test 3.

FIGURE 12 Vehicle after Test 3.

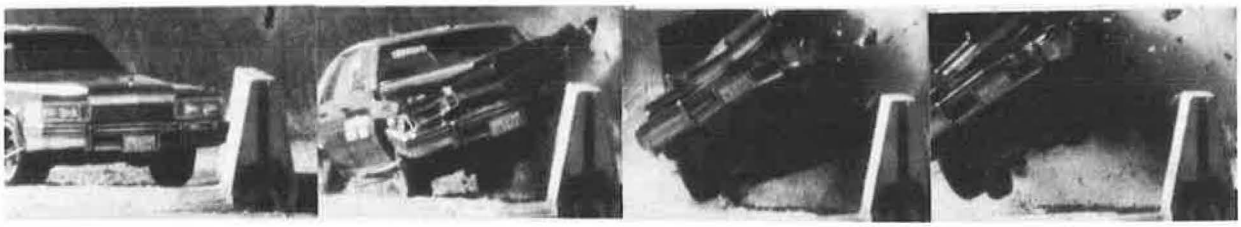

0.000 s 0.120 s 0.240 s 0.363 s

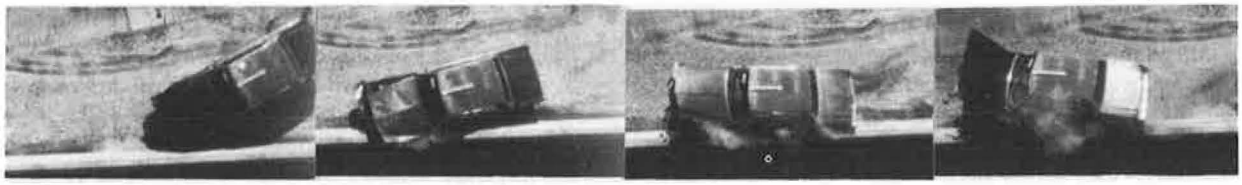

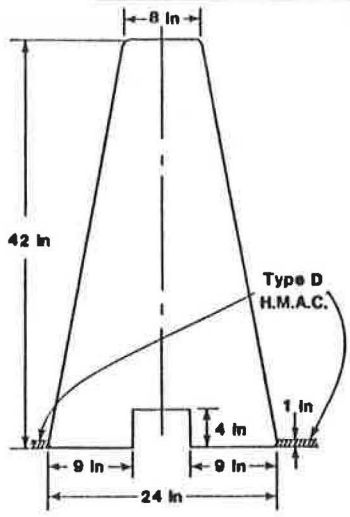

Test No.	9429C-3
Date	12/12/88
Test Installation	Single Slope Concrete Barrier
Installation Length.	120 ft (36.6 m)
Vehicle	1979 Cadillac Sedan deVille
Vehicle Weight	
Test Inertia	4,500 lb (2,043 kg)
Vehicle Damage Classification	
TAD	11LFQ5
CDC	11LFAW3
Maximum Vehicle Crush.	12.0 in (30.5 cm)
Impact Speed.	63.1 mi/h (101.5 km/h)
Impact Angle.	26.5 deg
Exit Speed.	51.8 (83.3 km/h)
Exit Trajectory	8.5 deg
Vehicle Accelerations (Max. 0.050-sec Avg)	
Longitudinal.	-6.4 g
Lateral	-13.1 g
Occupant Impact Velocity	
Longitudinal.	22.1 ft/s (6.7 m/s)
Lateral	28.9 ft/s (8.8 m/s)
Occupant Ridedown Accelerations	
Longitudinal.	-4.2 g
Lateral	-10.7 g

FIGURE 13 Summary of results for Test 3.

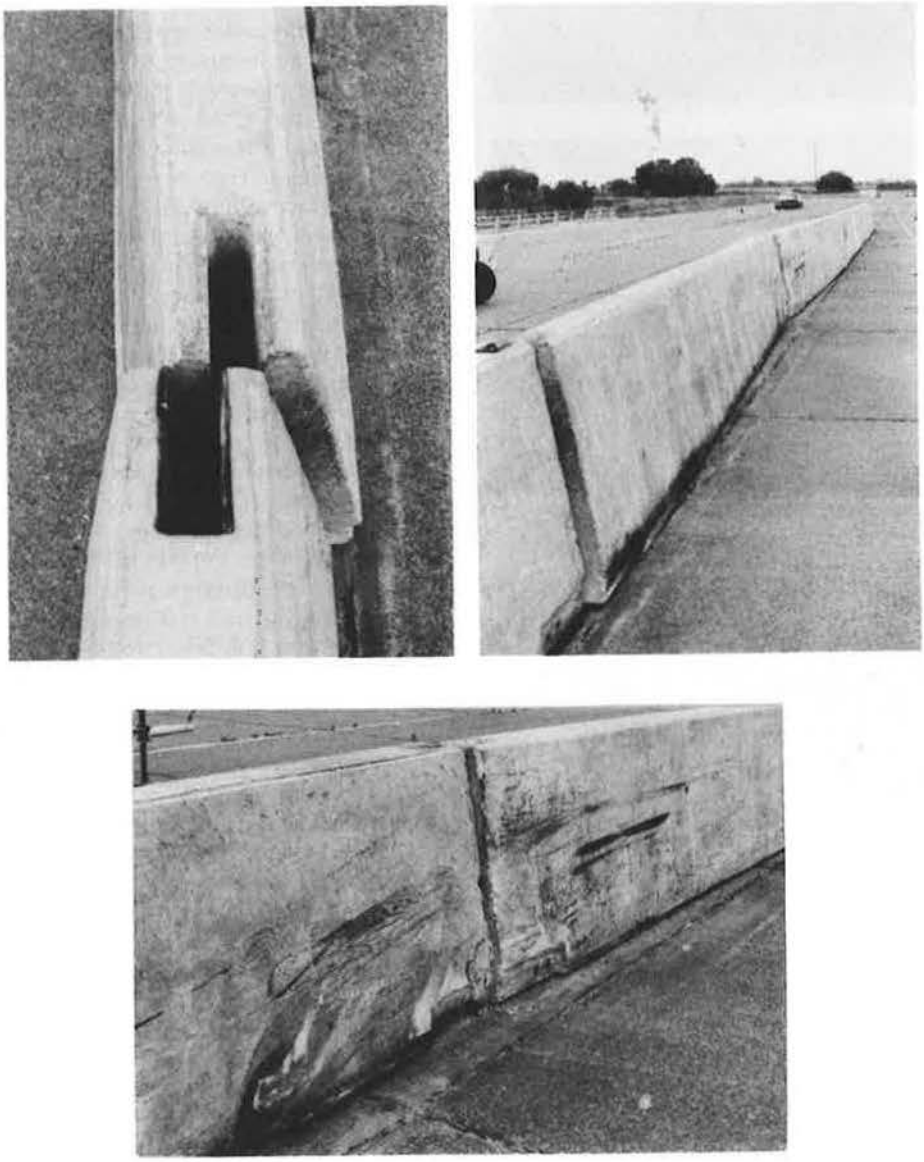

FIGURE 14 Single-slope barrier after Test 4.

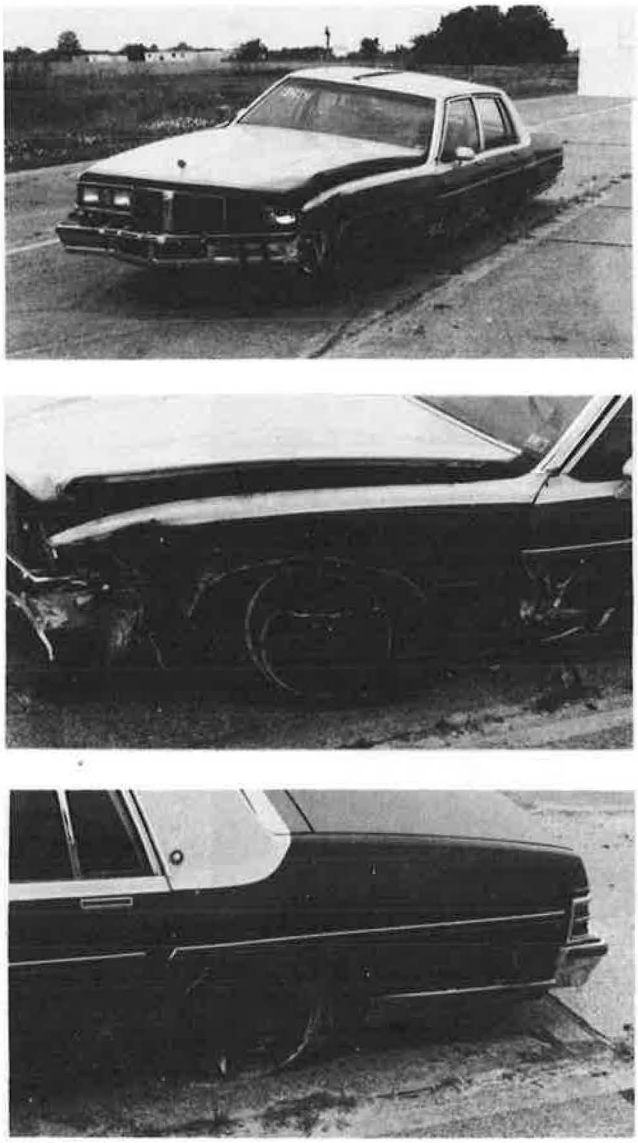

FIGURE 15 Vehicle after Test 4.

splice connection. The added rotation of the barrier about its longitudinal axis increases the angle of the barrier face during the impact, resulting in increased vehicle roll.

The temporary connection used in Test 4 is considerably easier to deploy than the connection used in Test 1. In addition, both connections lead to a barrier installation that is capable of redirecting vehicles based on temporary design considerations.

CONCLUSIONS

A new single-slope CMB has been developed that can be used in both temporary and permanent applications. It was designed to redirect a 4,500-lb (2043-kg) automobile traveling at 60 mph (96.6 km/hr) with an impact angle of 25 degrees allowing only cosmetic damage when deployed in the permanent configuration. Further, it was designed to redirect a 4,500-lb (2043-kg) automobile traveling at 60 mph (96.6 km/hr) with an impact angle of 15 degrees when deployed in either of two different temporary configurations. It is highly probable that the new single-slope CMB will be able to successfully redirect more severe impacts involving heavier vehicles with higher centers of gravity.

The primary advantage of the new single-slope CMB is that it will not be necessary to reset the barrier each time the surrounding pavement is overlaid, as may be required with the New Jersey CMB. As stated in the previous section, the center of the wheel hub of the vehicle in the third test rose to a maximum height of no more than 30 in. (76 cm) before losing contact with the barrier. Experience suggests that the barrier would continue to redirect the vehicle as long as the contact height of the center of the wheel hub does not exceed the height of the barrier. Therefore, it is believed that the overall height of the barrier can be reduced to at least 30 in. (76 cm) by adjacent pavement overlays without significantly affecting the performance of the barrier for the test conditions presented in this paper. It is possible that the barrier would continue to perform satisfactorily at lower heights; however, it is not recommended for use at heights below 30 in. (76 cm) unless further tests are conducted.

Another advantage of the single-slope CMB is that the redirection of the 1,800-lb (817-kg) vehicle was very stable. Although further study is required to make a definitive statement on this matter, it is believed that the new single-slope CMB will result in fewer roll-over crashes than occur with the New Jersey CMB. This is particularly true with nontracking, high-angle, low-velocity impacts of small vehicles (*8,9*).

A total of four full-scale tests were conducted on the new single-slope CMB. The first test involved a 4,500-lb (2043-kg) automobile striking the new barrier in a temporary configuration. The second and third tests involved an 1,800-lb (817-kg) automobile and a 4,500-lb (2043-kg) automobile striking the single-slope CMB in a permanent configuration. The fourth test involved a 4,500-lb (2043-kg) automobile striking the single-slope CMB in an alternate temporary configuration. In all cases, the vehicles were smoothly redirected with no snagging. Results from these tests were within acceptable performance limits described in *National Cooperative Highway Research Program Report 230* (*1*), as applicable. As such, the new single-slope CMB is recommended for immediate use.

ACKNOWLEDGMENTS

This research study was conducted under the sponsorship of the Texas State Department of Highways and Public Transportation. Mark Marek, Harold Cooner, and Gary Humes, of the SDHPT, worked closely with the researchers. Their comments, suggestions, and cooperative spirit were appreciated.

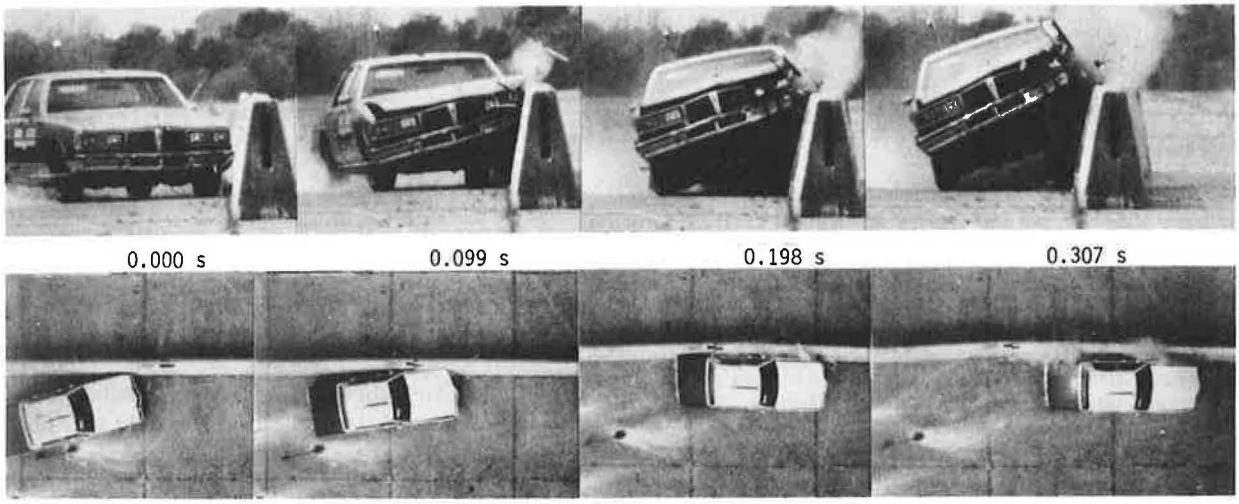

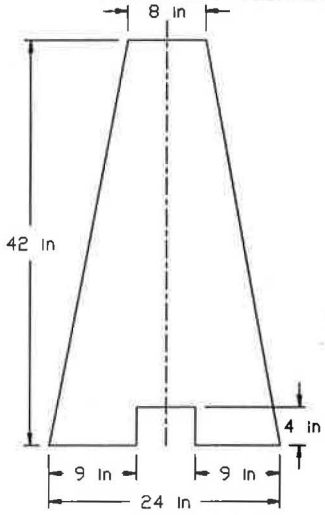

Test No. 9429K-1
Date 04/27/89
Test Installation . . Single Slope Concrete Median Barrier
Installation Length . 180 ft (54.9 m)
Vehicle . . . . . 1981 Pontiac Bonneville
Vehicle Weight
Test Inertia . . . 4,500 lb (2,043 kg)
Vehicle Damage Classification
TAD 11FLQ4
CDC . . . . . 11FLEK2 & 11LFEW1
Maximum Vehicle Crush 8.0 in (20.3 cm)
Maximum Barrier
Movement . . . . . 6.0 in (15.2 cm)

Impact Speed . . . . 62.0 mi/h (99.8 km/h)
Impact Angle . . . . 15.1 degrees
Speed at Parallel. . 57.3 mi/h (92.2 km/h)
Exit Speed . . . . . 57.0 mi/h (91.7 km/h)
Exit Trajectory . . 3.5 degrees
Vehicle Accelerations
(Max. 0.050-sec Avg)
Longitudinal . . . -5.3 g
Lateral . . . . . -7.3 g
Occupant Impact Velocity
Longitudinal . . . 16.3 ft/s (5.0 m/s)
Lateral . . . . . 18.4 ft/s (5.6 m/s)
Occupant Ridedown Accelerations
Longitudinal . . . -3.2 g
Lateral . . . . . -6.2 g

FIGURE 16 Summary of results for Test 4.

REFERENCES

1. J. D. Michie. Recommended Practices for the Safety Performance Evaluation of Highway Appurtenances. *National Cooperative Highway Research Program Report 230*, TRB, National Research Council, Washington, D.C., March 1981.
2. W. L. Beason, H. E. Ross, H. S. Perera, W. L. Campise, and D. L. Bullard. *Development of a Single-Slope Concrete Median Barrier*. Report 9429CDK-1, Texas State Department of Highways and Public Transportation, Texas Transportation Institute, College Station, Tex., June 1989.
3. C. E. Buth et al. *Safer Bridge Railings*. Final Report FHWA/RD-82/074.2, U.S. Department of Transportation, Federal Highway Administration, June 1984.
4. W. L. Beason and T. J. Hirsch. *Measurement of Heavy Vehicle Impact Forces and Inertia Properties*. Final Report FHWA-RD-89-120, U.S. Department of Transportation, Federal Highway Administration, May 1989.
5. D. J. Segal. *Highway-Vehicle-Object-Simulation-Model-1976*. Reports FHWA-RD-75-162-165, 4 Vol., U.S. Department of Transportation, Federal Highway Administration, 1976.
6. H. S. Perera. *Simulation of Vehicular Impacts with Safety-Shaped Barrier*. Ph.D. dissertation, Department of Civil Engineering, Texas A&M University, College Station, Tex., 1987.
7. H. E. Ross, H. S. Perera, D. L. Sicking, and R. P. Bligh. Roadside Safety Design for Small Vehicles. *NCHRP Report 318*, TRB, National Research Council, Washington, D.C., May 1989.
8. K. L. Hancock, M. E. Bronstad, and C. F. McDevitt. *Crash Test Evaluation of Selected Bridge Rails*. Preprint of paper presented at 66th Annual Meeting of the Transportation Research Board, National Research Council, Washington, D.C., Jan. 1987.
9. H. S. Perera and H. E. Ross. Prediction of Rollovers Caused by Concrete Safety-Shape Barriers. In *Transportation Research Record 1233*, TRB, National Research Council, Washington, D.C., 1989.

Publication of this paper sponsored by Committee on Roadside Safety Features.

Guidelines for Installation of Guardrail

JERRY G. PIGMAN AND KENNETH R. AGENT

Kentucky, along with most other states, has in the past relied on the American Association of State Highway and Transportation Officials' (AASHTO) *Guide for Selecting, Locating, and Designing Traffic Barriers* for guidance in the installation of guardrail. Additional information related to barrier selection and installation was recently published in AASHTO's *Roadside Design Guide*. However, considerable judgment is required for application of this information, and it was determined that significant benefit could be derived from development of guidelines representative of conditions in Kentucky. Listed as follows are significant results from this study: (a) results from a previous survey of guardrail standards and guidelines were summarized and it was found that only a few states suggested use of reduced guardrail standards that did not conform to AASHTO's barrier guide; (b) warranting guidelines for clear zones and embankments based on Kentucky accident severities and costs were developed from a computer program included as part of the *Roadside Design Guide*; and (c) a procedure was developed to identify and rank in priority order highway sections in need of guardrail [details to support the identification and ranking of the procedure were included in the full research report prepared for the Kentucky Transportation Cabinet in cooperation with the Federal Highway Administration (FHWA)]. This procedure was based on determination of locations with critical numbers and rates of run-off-road accidents, conduction of a field survey to tabulate hazard-index points, determination of improvement costs and benefits, and performance of a cost-effectiveness analysis.

Kentucky, along with most other states, has in the past relied on the American Association of State Highway and Transportation Officials' (AASHTO) publication, *Guide for Selecting, Locating, and Designing Traffic Barriers* (*1*), for guidance in the installation of guardrail. However, there are geometric constraints on existing roads that do not permit use of the AASHTO guidelines in many cases. In addition, there are other issues to be addressed when outdated guardrail sections or end treatments are damaged and in need of repair. Frequently it is impractical to install guardrail to meet current standards without major reconstruction. Benefits associated with removal of roadside hazards have been well documented and most highway agencies have made significant accomplishments in that area. However, some roadside hazards cannot be eliminated or the cost of removal is prohibitive. An alternative to removal of hazards is to shield those hazards so that the probability of a vehicle striking them is reduced. Longitudinal barriers such as guardrail, median barriers, and bridge rails are used to shield vehicles from hazards. Installation of barriers is usually based on the relative hazard of the barrier versus the unshielded hazard. The AASHTO barrier guide (*1*) has been used by many states to assist in the determination of guardrail need and type. Generally, roadside barriers such as guardrail are used to shield vehicles from embankments or roadside obstacles. Warrants presented in the AASHTO publication are useful; however, considerable judgment is required to apply the generalized cases to specific problems in Kentucky. It appears that benefits could be derived from the development of standards and guidelines for the installation of guardrail, with special consideration given to traffic volumes, geometrics, and terrain representative of Kentucky. Priority ranking of safety features for roadways has been accomplished when sufficient information was available to document costs and benefits. The cost-effective selection procedure for guardrail presented in the AASHTO barrier guide is a method to be considered; however, input data necessary for the procedure may limit its application. With the goal to set up an inventory and rank locations in need of guardrail or other barriers on all state-maintained roads, there is a need for a simplified procedure.

Kentucky Transportation Center, College of Engineering, University of Kentucky, 108 Transportation Research Building, 533 South Limestone Street, Lexington, Ky. 40506-0043.

STANDARDS FOR INSTALLATION AND REPAIR OF GUARDRAIL

AASHTO *Roadside Design Guide*

The AASHTO *Roadside Design Guide* (*2*) was developed as an update of the 1977 AASHTO barrier guide (*1*). The *Roadside Design Guide* was intended to be an updated, consolidated, and expanded source of information containing existing publications and policy statements that pertain to safer roadside design. The publication contains information and guidance on many aspects of safer roadside design for public streets and highways. Information has been extracted from several other AASHTO publications in order to compile in one source the most up-to-date guidelines relating to roadside safety. As with most other AASHTO publications, the *Roadside Design Guide* is not intended to be a standard or policy document, but instead a guide to practices that may be adopted by highway agencies responsible for roadside design, construction, and maintenance. Information contained in the *Roadside Design Guide* that was of particular use to this study was contained in the sections dealing with clear zones, embankments, and the cost-effectiveness analysis. The cost-effectiveness procedure in the 1977 barrier guide (*1*) allowed a designer to examine alternate safety treatments at specific locations to determine which one was more appropriate. In addition, the procedure was used by several highway agencies to analyze site-specific alternatives and to develop warrants in chart and tabular form using local data. Revisions to the cost-effectiveness procedure and adaption to a microcomputer format has made the new procedure included in the *Roadside*

Design Guide more attractive to the user because of increase in speed and flexibility. In general, the cost-effectiveness procedure permits a designer to predict total costs of various alternatives under consideration. Total costs include initial construction, anticipated repair and maintenance, salvage value of the improvement, and user costs. User costs were based on the expected number and severity of accidents associated with each alternative. The number of accidents is directly related to the number of predicted encroachments and the probability of the encroachments resulting in an impact with a roadside hazard. Modifications to the procedure that are incorporated into the microcomputer program include the following:

1. An encroachment rate model,
2. A model relating lateral extent of encroachment and accident severity to design speed, and
3. A traffic growth-rate model.

The clear roadside concept was promoted in the second edition of the AASHTO "Yellow Book" (*3*). It was recommended that an unencumbered roadside recovery area as wide as practical would be desirable. As a result, most highway agencies began to attempt to provide a traversable and unobstructed roadside area of 30 ft or more from the edge of the driving lane. It was noted in the "Yellow Book" that previous studies had shown that 80 percent of the vehicles leaving the roadway out of control were able to recover within a width of 30 ft. The 1977 AASHTO barrier guide (*1*) in its Figure III-A-3 modified the 30-ft clear zone concept by including variable clear zone distances based on speeds and roadside geometry. This same set of curves for clear zone distances was modified further in the *Roadside Design Guide* in its Figure 3.1 to include traffic volume along with speed and roadside geometry. It was noted that the curves shown in the *Roadside Design Guide* were based on empirical data that were extrapolated to provide information on a wide range of conditions. It was also cautioned that site-specific conditions must be kept in mind when attempting to use the curves. Adjustment factors were developed for horizontal curvature with increasing clear zone requirements for increasing curvature. Embankments on fill slopes are generally categorized as recoverable, nonrecoverable, traversable, or critical. Recoverable slopes are embankment slopes 4:1 or flatter. Vehicles on recoverable slopes can usually be stopped or steered back to the roadway. A nonrecoverable slope is defined as one that is traversable, but such that a vehicle cannot be stopped or returned to the roadway easily. Embankments between 3:1 and 4:1 generally fall into this category. Slopes steeper than 3:1 are critical and are usually defined as a slope on which a vehicle is likely to overturn.

Kentucky Guardrail Policy

Kentucky's Department of Highways' *Maintenance Guidance Manual* (*4*) provides guidance for new guardrail installations and upgrading existing ones. It is noted that all projects for guardrail installation and upgrading should meet the warrants of Part I-III-A of the 1977 AASHTO barrier guide (*1*). Each highway district is required to maintain a current inventory of all substandard and obsolete guardrail and all unshielded locations that are known to meet the warrants of Part I-III-A of the barrier guide. In addition, it is required that a cost-effectiveness ranking be defined for each location based on a statewide inventory. An additional requirement is that the Kentucky Department of Highways' Division of Maintenance prepares and administers an annual Guardrail Improvement Program. Funds budgeted for this program are to be allocated to those locations having the highest ranking factor and those that can be constructed without major reconstruction of the roadway. Alternatives to guardrail, such as hazard removal or relocation, flattening slopes, and pipe extensions are to be considered and may be included in the program. The issue of when to upgrade guardrail and when to repair or maintain with equivalent materials is a continuing problem. It is desirable that guidelines exist for details to be included in standards for repair and maintenance of guardrail on existing roadways that have not been designed and built to current standards. The general policy at the present time is that obsolete or substandard guardrail may be repaired or maintained with equivalent materials in stock or with available guardrail elements.

GUIDELINES FOR RECOMMENDED GUARDRAIL NEEDS

The *Roadside Design Guide* (*2*) contains figures and tables giving warrants for guardrail based on embankments and roadside obstacles. When considering the need for guardrail relative to embankments, the embankment height and side slope are the factors used to make the decision. The relative severity of encroachments on the embankment must be compared to impact with the guardrail. A figure using fill section height and slope was included in both the AASHTO barrier guide (Figure III-A-1) (*1*) and the *Roadside Design Guide* (*2*). Modified warrant charts were included in the *Roadside Design Guide* that consider the decreased probability of encroachments on lower-volume roads. The need for guardrail relative to roadside obstacles considers the necessary clear zone for the given roadway and the relative severity of hitting the obstacle versus hitting the guardrail. The necessary clear zone as a function of design speed, traffic volume, and fill or cut slope were given in Table 3.1 and Figure 3.1 in the *Roadside Design Guide* (*2*). Although warrants were presented for the need for guardrail based on embankment and roadside obstacle criteria in the *Roadside Design Guide*, the recommendation was made that highway agencies develop specific guidelines for their agency based on their cost-effectiveness evaluations. A cost-effectiveness selection procedure was given in Appendix A of the publication. This procedure was used to develop guidelines for the need of guardrail based on Kentucky data. A computer program (ROADSIDE) was obtained to conduct the cost-effectiveness analysis. Certain parameters, given as part of the program, had to be used, and values are specified unless changed. The accident cost figures and encroachment model were changed from those given as part of the computer program. The accident cost figures were based on the recommendations given in the FHWA's Technical Advisory T7570.1 (*5*). The encroachment model, which was obtained from TRB *Special Report 214* (*6*), is the exponential

encroachment model documented in Appendix *F*. The decision to use this model was made after analyzing the output from the program using alternate encroachment models. The model presented in TRB *Special Report 214* considered curvature and grade, whereas the model presented in ROADSIDE (2) required the curvature and grade to be input each time. For the type of analysis performed in this study, it was believed that the model in TRB *Special Report 214* would result in a more useful methodology. In general, it was believed that the use of the encroachment model from TRB *Special Report 214* produced results that were more logical for the objectives being addressed in this study.

Two separate types of analyses were conducted that were related to clear zone and embankment criteria. The computer program required various types of input, and the output was the total cost (including accident, installation, repair and maintenance costs, and salvage value). The total cost was then compared with and without a guardrail using the appropriate set of assumptions. These were the only two alternatives considered. When the total cost with a guardrail present became less than that with no guardrail, it was assumed that a guardrail was warranted. The variables analyzed varied, and included the traffic volume, design speed, lateral placement, longitudinal length, width of obstacle, severity index, and cost of installation. In the clear zone analysis, the total costs of striking a guardrail or fixed object at an isolated point with a longitudinal length of 1 ft and a width of 1 ft were compared. If guardrail was warranted for a single object, then it was assumed that a barrier to shield multiple objects would also be warranted. The lateral offset of the fixed object was varied with a 2-ft offset of the fixed object behind the guardrail and a maximum lateral offset of 10 ft for the guardrail. Severity indices were calculated using Kentucky accident data. Severity index is calculated by dividing the number of equivalent property-damage-only accidents by the total number of accidents. Equivalent property-damage-only accidents are equal to 9.5 times the number of fatal or incapacitating accidents, plus 3.5 times the number of nonincapacitating or possible injury accidents, plus the number of no-injury accidents. The severity of accidents involving a collision with a guardrail or a tree as the first event were compared as a function of speed limit. The severity indices used for guardrail were 2.2 for 40 mph, 2.5 for 50 mph, and 2.8 for 60 mph. These indices were developed from a wide range of accidents involving guardrail impacts. Similarly, for impacts at the end of a guardrail, there were several types of end treatments involved. The severity indices used for fixed objects were 3.1 for 40 mph, 3.4 for 50 mph, and 3.7 for 60 mph. The program limited the speeds to 40, 50, or 60 mph. A minimum length of 200 ft and an installation cost of $2,000 was used for the guardrail.

Numerous series of computer runs were conducted with the traffic volume and speed held constant and the lateral offset varied. For a specific volume and speed, two sets of computer runs were made. One used the data assuming no guardrail and the second assumed the appropriate data for guardrail. When the total cost at the lateral offset of the guardrail became less than that for a corresponding offset for the fixed object, the guardrail was determined to be warranted. The results of these analyses are given in Table 1. The traffic volume categories varied from 250 to "over 5,000" with speed categories of 40, 50, and 60 mph. For the 50-mph speed category, the minimum clear zone distance needed without the installation of guardrail varied from 3 ft for average daily traffic (ADT) of 250 to 20 ft for ADT of more than 5,000. A similar type of procedure was used in the embankment analysis. A limiting factor in this analysis was the lack of data related to the severity of accidents as a function of embankment height and slope. The only accident data noted that yielded accident severity versus embankment height and slope were single vehicle embankment accidents in California in 1963 (*7*). It should be noted that the data base representing California embankment accidents in 1963 consisted of a greater proportion of larger cars than are currently in the vehicle fleet. Larger cars are less likely to overturn than smaller cars because their wider track width makes them more stable. Severity indices compatible with indices for accidents involving guardrail in Kentucky were calculated using these data and a severity index formula used in Kentucky (*8*) (Table 2). It was not possible to calculate the severity index as a function of speed. The overall severity index of all accidents involving guardrail in Kentucky was calculated as 2.67. This severity index was compared with those calculated using the California data. It can be seen that the severity of hitting a guardrail (severity index of 2.67) was greater than that for driving over an embankment when the slope was 3:1 or flatter. There was a range of severity indices from 2.47 for embankment height of 3 ft to 2.63 for an embankment height of 25 ft. Therefore, no guardrail could be warranted for a slope of 3:1 or flatter.

TABLE 1 CLEAR ZONE DISTANCES*

	CLEAR ZONE DISTANCE		
	TRAFFIC SPEED		
TRAFFIC VOLUME (ADT)	40 MPH	50 MPH	60 MPH
250	**	3	12
500	**	9	16
1,000	5	13	19
2,000	9	16	21
3,000	11	18	22
4,000	13	18	22
5,000	14	19	23
Over 5,000	15	20	23

* The minimum clear zone distance needed without the installation of guardrail.

** An ADT of 700 was needed before the minimum two-foot clear zone would be required.

TABLE 2 SEVERITY INDEX VERSUS EMBANKMENT HEIGHT AND SLOPE*

	SLOPE			
EMBANKMENT HEIGHT	3:1	2:1	1:1	1:1
3	2.47	2.71	2.96	3.44
8	2.51	2.75	2.99	3.47
15	2.56	2.80	3.04	3.52
25	2.63	2.87	3.11	3.59
35	**	2.94	3.18	3.66
45	**	3.01	3.25	3.74
60	**	3.12	3.36	3.84

* Severity Index (SI) is: SI = (9.5(K+A) + 3.5(B+C) + PDO)/T
where K = fatal accident,
A = incapacitating injury accident,
B = nonincapacitating injury accident,
C = "possible" injury accident, and
T = total accidents.

** No data.

It should be noted that the severity of an accident involving an embankment relates to the vehicle overturning or striking fixed object hazards either on the slope or at its base. Therefore, these severity indices must be used with caution for slopes that are nontraversable or include fixed objects. A speed of 50 mph was used in the embankment analysis. The severity indices were not classified by speed so one representative speed had to be selected. It was believed that the 50 mph speed would be most representative of the roads for which this analysis would be used. For the guardrail installation, a lateral placement of 5 ft was assumed with a longitudinal length of 200 ft and a width of 1 ft. When the embankment was considered, a lateral placement of 7 ft was assumed, with a longitudinal length of 200 ft and a width of the embankment height times the slope (for example, the width would be 20 ft for an embankment height of 10 ft and a slope of 2:1). For a given traffic volume, the total cost of the guardrail was compared with various embankment heights. When the cost associated with the embankment exceeded that for the guardrail, a guardrail was warranted. The results of this analysis are presented in Table 3. For a slope of 2:1, the embankment height at which guardrail was warranted varied from 40 ft for ADT of 250 to 15 ft for ADT of more than 5,000. When the slope became steeper than 2:1, a guardrail was warranted in all cases in which the embankment height was above a minimum level. Using *Roadside Design Guide* Figure 5.1 (*2*) as a reference, this minimum embankment height would be about 5 ft.

PROCEDURE TO IDENTIFY AND RANK LOCATIONS IN NEED OF GUARDRAIL

Develop Critical Numbers and Rates of Run-off-Road Accidents

A procedure has been in place for several years to develop average and critical accident rates for use by the Kentucky Department of Highways in the identification of high-accident locations (*9*). In general, the critical rate for a type of highway is calculated using statistical tests to determine whether the accident rate for a specific class of highway is abnormally high compared with a predetermined average for highways with similar characteristics. The statistical tests are based on the commonly accepted assumption that accidents approximate the Poisson distribution. Using this procedure, locations have routinely been inspected and accident data have been analyzed to offer recommendations for improvements, when appropriate. Another study resulted in the development of accident reduction-factors for use in the cost-optimization procedure to rank proposed safety improvements (*10*). The general procedure to develop critical accident numbers and rates relies on the historical accident file and a volume file. Accident data are available from the Kentucky Accident Records System. Volume data used for the calculation of accident rates were obtained from the Statewide Mileage File. As previously noted, the general procedure to develop accident rates, including critical accident rates and numbers, has been documented (*9,11*). An annual report is now produced to calculate average and critical rates as a means of analyzing statewide accident statistics (*12*). It was necessary to determine numbers of accidents and to develop average rates and critical rates as input for the high-accident identification program. To permit the use of this procedure to develop average and critical numbers and rates of accidents for use with the guardrail location selection program, the procedure to identify only those accidents associated with vehicles running off the road had to be modified. It was assumed that guardrail installation would be of benefit only in accidents where vehicles ran off the road. Analysis revealed that three types of accidents made up a very high percentage (99 percent) of the total. Those three types of accidents were

1. Single-vehicle collision with a fixed-object at an intersection;
2. Single-vehicle collision with a fixed-object not at an intersection; and
3. Single-vehicle, run-off-road accident, not at an intersection.

It was found that approximately two-thirds of all run-off-road accidents involve collisions with fixed objects. Other run-off-road accidents included noncollisions, possibly involving rollovers. A summary of fixed-object accidents and their overall severity based on a calculated severity index was prepared (*8*). It can be seen by the magnitude of the severity index that the most severe fixed-object accidents are those involving trees (3.52), culverts and headwalls (3.38), earth embankments, rock cut, and ditches (3.14), and bridges (2.95). The most frequently occurring fixed-object accidents are collisions with earth embankment, rock cut, and ditches; and trees, utility poles, and fences. The least severe accidents are those involving buildings and walls (1.56) and fire hydrants (1.70). The severity index for guardrail impacts was 2.67, which was in the mid-range of severity indices.

After identification of those accidents that could be affected by the installation of guardrail, average and critical numbers and rates of run-off-road accidents were summarized for 1-mi sections. The average and critical numbers for 1983–1987 are shown in Table 4 for various highway types. Accident rates by highway types for rural and urban areas are presented in Tables 5 and 6, respectively. Also shown in these tables

TABLE 3 EMBANKMENT GUIDELINES

	EMBANKMENT HEIGHT (FT)*
	SLOPE**
TRAFFIC VOLUME (ADT)	2:1
250	40
500	31
1,000	24
2,000	20
3,000	18
4,000	17
5,000	16
OVER 5,000	15

* The maximum embankment height permitted without guardrail.

** Guardrail not warranted for slope of 3:1 or flatter. Guardrail would be warranted for a slope steeper than 2:1 when the embankment height was above a minimum level of about 5 feet.

Note: Refer to text section titled "Guardrail Need Guidelines" for methodology used in development of table.

TABLE 4 STATEWIDE AVERAGE AND CRITICAL NUMBERS OF RUN-OFF-ROAD ACCIDENTS FOR 0.3- AND 1-MILE SECTIONS BY HIGHWAY TYPE CLASSIFICATION (1983–1987)*

		Accidents Per 0.3-Mile Section		Accidents Per 0.3-Mile Section	
Rural or Urban	Highway Type	Average	Critical Number	Average	Critical Number
Rural	One-Lane	0.20	2	0.67	3
	Two-Lane	0.63	3	2.10	6
	Three-Lane	1.64	5	5.46	12
	Four-Lane Divided (Non-Interstate or Parkway)	1.36	5	4.54	11
	Four-Lane Undivided	2.30	7	7.67	15
	Interstate	2.21	7	7.37	15
	Parkway	0.74	3	2.46	7
	All Rural	0.68	3	2.26	7
Urban	Two-Lane	2.75	8	9.18	17
	Three-Lane	3.00	8	10.00	19
	Four-Lane Divided (Non-Interstate or Parkway)	3.48	9	11.59	21
	Four-Lane Undivided	4.27	10	14.24	24
	Interstate	8.56	17	28.53	43
	Parkway	1.28	5	4.26	10
	All Urban**	3.48	9	11.60	21

* Includes small number of miles of one-, five-, and six-lane highways.

TABLE 5 STATEWIDE RURAL RUN-OFF-ROAD ACCIDENT RATES BY HIGHWAY TYPE CLASSIFICATION (1983–1987)

Highway Type	Total Mileage*	AADT	Run-off-the-Road Accident Rate (Acc/100 MVM)
One-Lane	328	200	183
Two-Lane	21,288	1,200	94
Three-Lane	15	2,280	132
Four-Lane Divided (Non-Interstate or Parkway)	293	7,460	33
Four-Lane Undivided	60	8,460	50
Interstate	576	18,380	22
Parkway	545	4,080	33
All	23,106	1,800	69

* Average for the five years.

are the total mileage and annual average daily traffic (AADT) for each highway type. Using the previously referenced equation, critical accident rates were calculated for each type of rural and urban highway, and cross-tabulated by volume category and section length. Also calculated were critical run-off-road accident rates for spots (defined as highway sections 0.3 mi in length) on rural and urban highways.

List Locations with Critical Rates of Run-off-Road Accidents

An existing computer program to identify high-accident locations was modified to identify run-off-road accident locations. Output from this computer program was a listing of accident locations by decreasing critical rate factor in order of county, route, and mileposts. For this analysis, the critical

TABLE 6 STATEWIDE URBAN RUN-OFF-ROAD ACCIDENT RATES BY HIGHWAY TYPE CLASSIFICATION (1983–1987)

Highway Type	Total Mileage*	AADT	Run-off-the-Road Accident Rate (Acc/100 MVM)
Two-Lane	1,161	6,240	81
Three-Lane	11	9,350	59
Four-Lane Divided (Non-Interstate or Parkway)	258	18,940	34
Four-Lane Undivided	168	18,270	43
Interstate	159	44,530	35
Parkway	40	6,780	34
All	1,807**	12,650	50

* Average for the five years.

** Includes small number of miles of one-, five-, and six-lane highways.

rate factor was defined as the average accident rate for a section divided by the critical rate for that same section. Other information presented in the printout included number of accidents, number of lanes, highway class, rural-urban designation, and AADT. The listing represented all highway sections of 1-mi length with five or more accidents in a 5-year period. It was assumed from the beginning that sections 1 mi in length were the most appropriate for analysis to determine the need for guardrail; however, 0.3-mi sections with three or more accidents in a 5-year period were also analyzed and determined to have advantages as alternate means of identifying locations in need of guardrail. A similar computer summary was prepared for 0.3-mi sections listing accident locations by decreasing critical rate factor in order of county, route, and mileposts. Another form of output from the run-off-road accident identification procedure was a listing of all locations with critical rate factors greater than 1.0. A critical rate factor greater than 1.0 means that the accident rate for a section of highway exceeds the critical rate for that class or type of highway statewide. Included for each accident are milepost location, date of accident, directional analysis, description of accident type, light and road surface conditions, collision type, and number injured or killed.

These listings represent the first step of a method for identification of locations in need of guardrail. With the use of previously discussed computer printouts of locations with critical rates of run-off-road accidents, a listing by county can be prepared for selecting highway sections that should be subjected to the field survey. This procedure would eliminate the need to survey all highway sections, thereby concentrating efforts on sections previously identified as having accident rates exceeding the critical level. Locations with critical rates greater than 1.0 have high accident rates; however, these locations do not necessarily need guardrail because guardrail may already exist or there may be other improvement alternatives. A total of 1,069 1-mi and 2,845 0.3-mi sections were identified throughout the state.

Develop a Hazard-Index Point System

Before conducting a field survey, it was found that there was a need to develop a system for relating the operational and geometric characteristics of highway sections with their accident history to determine which sections exhibited the great-

est need for guardrail. In addition to accident statistics, there are several characteristics that can be associated with the potential for accidents. The following characteristics were selected to represent a hazard-index rating of highway sections.

Characteristics	*Rating Points Possible*
1. Number of run-off-road accidents	15
2. Run-off-road accident rate	15
3. Traffic volume	10
4. Speed limit or prevailing speed	10
5. Lane and shoulder width	10
6. Roadside recovery distance	10
7. Embankment slope	10
8. Embankment height	10
9. Culvert presence	5
10. Subjective roadside hazard rating	5

An attempt was made to include characteristics representative of accidents and accident potential, operations, and cross section. Point-system weightings of each characteristic were determined by subjective evaluation. The result was combining number of accidents and accident rate to make up 30 of a possible 100 points. Traffic volume and speed limit, considered to be operational characteristics, totaled 20 of the possible 100 points. Cross-section characteristics made up an additional 40 points. Because of their frequency of occurrence and the hazard associated with culvert headwalls or openings near the roadway, a special category was created to represent this condition. For a culvert present within 5 ft of the road, 5 points were assigned. Also included was a general category representing a subjective roadside hazard rating with 5 points possible. This rating was based on a visual observation that was compared with photographic documentation of roadway sections depicting various degrees of roadside hazard.

Conduct Field Survey

Another step in the overall process of identifying locations in need of guardrail is a field survey of locations having critical rate factors of 1.00 or greater. General guidance in the selection of variables to consider in the field survey was taken from the earlier work by Zegeer (*13*). Specific cross-section information that will require a field survey includes the following: (a) lane and shoulder width, (b) roadside recovery distance, (c) embankment slope, (d) embankment height, (e) presence of a culvert, and (f) subjective roadside hazard rating. Additional field data collection may be required to obtain prevailing speed if it is less than the speed limit.

In order to implement the field survey process, a form was developed for use by Kentucky Department of Highways' personnel to document roadway cross-section and other conditions determined to be useful. This form includes space for all variables that will require rating points to be assigned, in addition to general location information and accident statistics.

It is recommended that additional information be documented for each highway section to be surveyed. Included will be the following general information: date, county, district, route number, range of mile points, type of area, terrain, AADT, and number of lanes. The result will be a combination of field and other data collection, primarily from files maintained by the Department of Highways. Only 10 variables or characteristics will be assigned hazard-index rating points. Other characteristics for which data are not to be collected will not be assigned rating points but will be available to provide general information to the decision maker. Tests of the survey form were conducted to determine if it was reasonable and understandable for use by field personnel to document operational and cross-section information. It was determined that a listing of accident locations by county having critical rate factors shown would provide sufficient information to select those locations to be surveyed. Listings of accident locations are arranged by increasing route number within a county, and mile points are given to permit location of a specific section on a route. In addition, critical rate factors are tabulated for use in selecting factors greater than 1.0 or some other desirable minimum level. The remaining information necessary to prepare for and complete the field survey process consisted of detailed listings of individual accidents at 0.3-mi and 1-mi sections. The resulting package of information determined to be necessary to efficiently conduct the field survey contained the following:

1. A listing of accident locations by county with critical rate factors tabulated,
2. A county map,
3. A route mile point log by county, and
4. A detailed listing of individual accidents for 0.3-mi and 1-mi sections.

Tabulate Hazard-Index Points

After assignment of hazard-index points to each of the variables or characteristics (from the accident history and the field survey), the next step is to summarize and tabulate hazard-index points for each highway section. It is recommended that lists of locations be prepared with total hazard-index points in decreasing order for all locations statewide and then for several subcategories such as district, county, and highway class (federal-aid or functional class). The purpose for this listing will be to identify a manageable number of locations for which cost-effectiveness analysis can be performed. The result will be a listing of locations with a combination of accident history and cross-section characteristics that could serve as the basis for collection of cost and benefit data.

Determine Improvement Costs

As part of the field survey process, it will be necessary to evaluate each location having a critical rate factor of 1.00 or greater to determine whether improvements should be recommended. Because the run-off-road accident analysis will identify locations based on number and rate of accidents only, it is likely that some locations having existing barriers or other roadside improvements will appear on the list. This will require that each location be assessed to determine whether any improvement should be made. However, it is anticipated that improvement alternatives will be available at the majority of locations and that the type and cost of these improvements will need to be documented.

At the beginning of this study, it was generally assumed that the primary type of improvement would be installation of guardrail. The focus on guardrail was the result of an initial

request to identify locations in need of guardrail so that a listing of priority order could be prepared and made available to the Department of Highways. This listing was to be used to assist in the selection of projects to be funded for installation and enhancement of guardrail. It is obvious that several alternatives usually exist when encountering roadside hazards. Among the most frequently mentioned are removal or relocation of fixed objects and flattening side slopes. Frequently encountered roadside hazards and the cost to remove or reduce the hazard potential were tabulated by Zegeer et al. (*13*). Additional information on improvement costs is available from the Kentucky Department of Highways' unit bid prices, which are tabulated for all projects awarded during each calendar year (*14*). As an example, unit bid prices for W-beam guardrail installation was $8.06/linear ft during a recent year.

Determine Improvement Benefits

The benefits of improvements associated with roadside hazards are primarily the result of reduced accidents. To determine the expected benefits from various types of improvements, it will be necessary to relate accident reduction factors to specific types of improvement alternatives. Previous work by Creasey and Agent (*15*) provides a wide range of accident reduction factors that may be directly applied to improvements recommended as part of this program. Selected accident reduction factors from Creasey and Agent's work that may be related to run-off-road accidents were tabulated. Included are reduction factors for the following major areas of safety improvements:

- Pavement marking,
- Construction-reconstruction,
- Safety barriers,
- Safety poles and posts, and
- Removal or relocation of roadside obstacles.

Detailed accident data for each location will be available from the run-off-road accident summaries prepared as part of the analysis to determine critical rates. The type of information presented, previously noted, included the number of fatalities and injuries and the total number of accidents. These data can be converted to total accident benefits by associating accident severity (types of injuries and property damage) with costs for each type. Costs for each level of accident severity have been developed and recommended by FHWA (*4*). Those accident costs recommended by FHWA and recommended for use in determining improvement benefits areas are as follows:

- Fatality: $1,500,000;
- Injury: $11,000; and
- Property damage only: $2,000.

Therefore, the combination of accident reduction factors, accident severity from the historical data at a specific location, and costs for each accident severity level will result in an accident reduction benefit (cost savings) associated with each improvement alternative.

Analyze Cost-Effectiveness

The final step in the process of evaluating roadside safety needs is to combine cost and benefit data to determine the cost-effectiveness of alternative improvements. A simple listing of improvement alternatives in order of decreasing benefit-cost would provide information to allow selection of locations with the greatest benefit-cost ratio. However, with restricted budget amounts available, it would be appropriate to use a budget optimization procedure to select those alternatives so that maximum benefits could be derived. Documentation of a procedure for budget optimization was prepared by Crabtree and Mayes and adapted for the Highway Safety Improvement Program in Kentucky (*16*). Output from the budget optimization procedure will be a listing of information for each location, consisting of the location name and number, accident history, input for each improvement alternative, and benefit-cost ratio for each alternative. For each budget specified, a listing will be provided showing the selected alternative at each location, alternative costs and benefits, and the benefit-cost ratio. In general, budget optimization will provide a listing of selected projects and selected alternatives for a given budget. If a certain amount of money is designated for roadside safety improvements, this procedure will allow maximum benefits to be achieved.

SUMMARY OF RESULTS

The following is a summary of significant results related to this investigation of standards and guidelines for guardrail installations:

1. From a previous survey of guardrail standards and guidelines, it was determined that only a few states suggested the use of reduced guardrail standards. Georgia, Pennsylvania, and Indiana were exceptions, with lower standards considered only for low-volume, low-speed roads.
2. The AASHTO *Roadside Design Guide* (*2*) offered general guidance related to roadside safety and suggested that states develop their own warranting criteria for clear zones and embankments based on localized cost-effectiveness.
3. Kentucky's guardrail policy requires administration of an annual Guardrail Improvement Program, including a cost-effectiveness ranking for each location based on a statewide inventory.
4. A computer program (ROADSIDE) from the *Roadside Design Guide* was modified and used to develop warranting guidelines for clear zones and embankments based on accident severities and costs representative of Kentucky conditions.
5. A procedure was developed to identify and rank in order of priority locations in need of guardrail based on the following steps:
    a. Development of critical numbers and rates of run-off-road accidents,
    b. Preparation of a list of locations with critical rates of run-off-road accidents,
    c. Development of a hazard-index point system,
    d. Conduction of a field survey,
    e. Tabulation of hazard-index points,
    f. Determination of improvement costs,

g. Determination of improvement benefits, and
h. Analysis of cost-effectiveness.

IMPLEMENTATION

A procedure was developed to identify and rank in order of priority highway sections in need of guardrail. This procedure permits adoption of a systematic process of identifying locations with the greatest need for guardrail. Based on an initial selection of locations with critical numbers and rates of run-off-road accidents, a field survey will be required to catalog operational and cross-section characteristics for input into a hazard-index point system. It is recommended that locations be categorized in decreasing order of hazard-index points statewide and for subcategories such as district, county, or highway class. When only guardrail is considered as an improvement alternative, the need for guardrail can be determined based on a comparison of cross-section characteristics with criteria presented in Table 1 for clear zones and Table 3 for embankments. These criteria or warranting guidelines were developed using the computer program ROADSIDE from the *Roadside Design Guide* (*2*) based on accident severities and costs representative of Kentucky conditions. Whether only guardrail or other alternatives are considered, sufficient information will be available to determine improvement priorities based on cost-effectiveness and budget optimization.

REFERENCES

1. *Guide for Selecting, Locating, and Designing Traffic Barriers*. American Association of State Highway and Transportation Officials, Washington, D.C., 1977.
2. *Roadside Design Guide*. American Association of State Highway and Transportation Officials, Washington, D.C., 1988.
3. *Highway Design and Operational Practices Related to Highway Safety*. American Association of State Highway and Transportation Officials, Washington, D.C., 1974.
4. *Maintenance Guidance Manual*. Department of Highways, Kentucky Transportation Cabinet, Frankfort, 1988.
5. *Motor Vehicle Accident Costs*. Technical Advisory T7570.1, Federal Highway Administration, Washington, D.C., June 1988.
6. *Special Report 214: Designing Safer Roads*. TRB, National Research Council, Washington, D.C., 1987.
7. J. C. Glennon and T. N. Tamburri. Objective Criteria for Guardrail Installation. In *Highway Research Record 174*, HRB, National Research Council, Washington, D.C., 1967.
8. K. R. Agent. *Evaluation of the High-Accident Location Spot-Improvement Program in Kentucky*. Report 357, Division of Research, Kentucky Department of Transportation, Frankfort, 1973.
9. C. V. Zegeer. *Identification of Hazardous Locations of Rural Highways in Kentucky*. Report 392, Division of Research, Kentucky Department of Transportation, Frankfort, 1974.
10. J. G. Pigman et al. *Optimal Highway Safety Improvement Investments by Dynamic Programming*. Report 398, Division of Research, Kentucky Department of Transportation, Frankfort, 1974.
11. C. V. Zegeer. *Identification of Hazardous Locations on City Streets*. Report 436, Division of Research, Kentucky Department of Transportation, Frankfort, 1975.
12. K. R. Agent and J. G. Pigman. *Analysis of Accident Data in Kentucky (1983–1987)*. Report KTC-88-7, Kentucky Transportation Center, University of Kentucky, Lexington, 1988.
13. C. V. Zegeer et al. *Safety Cost-Effectiveness of Incremental Changes in Cross-Section Design—Informational Guide*. Report FHWA/RD-87/-94, Federal Highway Administration, 1987.
14. *Average Unit Bid Prices for All Projects Awarded in 1988*. Department of Highways, Kentucky Transportation Cabinet, Frankfort, 1989.
15. T. Creasey and K. R. Agent. *Development of Accident Reduction Factors*. Report UKTRP-85-6, Kentucky Transportation Research Program, University of Kentucky, Lexington, 1985.
16. J. D. Crabtree and J. G. Mayes. *User's Manual for Dynamic Programming for Highway Safety Improvement Program*. Report UKTRP-83-12, Kentucky Transportation Research Program, University of Kentucky, Lexington, 1983.

This publication sponsored by Committee on Roadside Safety Features.

Side Impact Collisions with Roadside Obstacles

LORI A. TROXEL, MALCOLM H. RAY, AND JOHN F. CARNEY III

Side impacts with fixed roadside objects appear to cost society more than $3 billion each year. Reducing the severity of this type of accident would clearly have a beneficial economic effect. Presented in this paper are the results of an investigation of the 1980–1985 Fatal Accident Reporting System and the 1982–1985 National Accident Sampling System data bases. These data bases are used to extract a variety of characteristics of side-impact accidents with fixed roadside objects. Most side impacts with roadside objects involve tall, narrow objects such as trees, utility poles, and luminaires. Young drivers account for the majority of side-impact accidents with roadside objects and such accidents typically occur late at night or early in the morning. These fixed-object collisions have characteristics that differ from those of vehicle-to-vehicle, side-impact collisions. Development of effective counter-measures for side-impact collisions with fixed objects requires an appreciation of their unique characteristics.

Every year approximately 225,000 people are involved in side-impact collisions with fixed roadside objects. One in 3 is injured and 1 in 100 is killed. This level of injury represents a societal loss of more than $3 billion, as shown in Table 1. (All quantities in figures and tables throughout this paper represent yearly averages.) These figures are based on the 1986 accident costs recommended by the Federal Highway Administration (FHWA) for cost-effectiveness analyses (*1*), so they are probably conservative. As shown in Table 2, approximately 910,000 vehicle occupants are involved in side-impact collisions with fixed objects each year, and almost 9,000 are fatally injured. Collisions with the sides of vehicles account for one quarter of the cases in both the National Accident Sampling System (NASS) and Fatal Accident Reporting System (FARS) data bases.

The 1980–1985 FARS data set was used to study fatal collisions. It is comprehensive in that it contains information about virtually every police-reported motor vehicle fatality in the United States. The weakness of the FARS data set is that it is based on police accident reports that vary in quality from report to report, officer to officer, and region to region. The amount of detailed information available in the FARS is also limited. For example, the first and most harmful events are coded but there is no information on the sequence of events. Side impacts in the FARS data were found using the impact location variable. This variable is coded as a clock direction, with 12 o'clock being the front center of the vehicle. Impacts that occurred primarily between the clock directions 2 and 4 or 8 and 10 were included in this study.

Department of Civil and Environmental Engineering, Vanderbilt University, Nashville, Tennessee 37235.

To investigate injury severity and occupant involvement in side-impact collisions, the 1982–1985 NASS data were used. The NASS coding and sampling techniques have varied from year to year, but were thought to be most stable in the 4 years chosen. As with the FARS, the quality of the data depends on the skill of the data collector and other factors discussed later in this paper. Side impacts were identified using a variable that identifies the location of the most severe impact. When this variable was coded left or right side, that accident was included in the study.

The NASS data set is a sample of all accidents in the United States in a given year. The sampling method involves several steps. First, the entire United States is divided into geographical units. No more than 50 of the more than 1,000 geographical units are chosen for use in the NASS data to represent the accident population in all of the geographical units in a year. The units from which a sample is taken are called primary sampling units (PSUs). The selection of these PSUs is based on characteristics such as geography, urbanization, per capita gas station sales, and per capita road miles. The actual sample, then, was built using less than 5 percent of the possible geographic units. Within each PSU, all of the police agencies were categorized by the type and number of accidents reported to the police. A small number of police agencies were then selected randomly within each category. The accidents that were finally investigated were a small subset of all police-reported accidents within those police agencies. These accidents are not chosen at random because the large number of property-damage-only accidents would limit the number of more interesting injury accidents that could be investigated. The accidents included in the NASS data therefore contain an overrepresentation of injury accidents. To eliminate this bias toward injury accidents, an inflation factor is used so that when the sampled number of each accident type is multiplied by this factor, it will represent the total number of that type of accident occurring within that PSU. In order to obtain national estimates, the PSU estimates are then multiplied by an expansion factor based on the 1977 population of that PSU. All of the NASS data shown in this paper use these national estimates of accidents because they eliminate the bias toward severe injury accidents.

As with any statistical sample, the confidence that can be placed in a particular estimate is a function of the size of the sample in relation to the population. When sample sizes are very small, as is the case with the NASS data, the analyst should realize that the true value may be quite different from the value obtained using the sample. The standard error is a statistical parameter that measures the possible variability of the data. Large standard errors will result in wider confidence intervals.

TABLE 1 ESTIMATED YEARLY SOCIETAL COSTS OF SIDE-IMPACT, FIXED-OBJECT ACCIDENTS (1986 dollars)

Accident Severity	Single-Passenger-Vehicle Side-Impact Fixed-Object Accidents		
	Cost per Person($)	Number of Accidents	Societal Cost (x $1,000,000)
Property Damage Only	2,000	106,716	213.4
Injury	11,000	59,996	660
Fatality	1,500,000	1,647	2,470.5
Total		168,359	3,343.9

TABLE 2 ESTIMATED AVERAGE YEARLY NUMBER OF OCCUPANTS IN FIXED-OBJECT COLLISIONS BY LOCATION OF IMPACT

Impact Location	1980-85 FARS		1982-85 NASS	
	Frequency	Percent	Frequency	Percent
Front	5,701	65	602,650	66
Side	2,241	25	226,470	25
Rear	168	2	27,135	3
Other	685	8	57,925	6
Total	8,795	100	914,180	100

Estimates of the standard errors are provided in National Highway Traffic Safety Administration's (NHTSA's) yearly NASS summary reports (*2*). These references provide the standard errors of estimates and percentages for the NASS data based on sampling variability. The standard errors of percentages are based on the national estimates of the number of accidents in the subgroup being studied. The standard errors of percentages for side-impact, fixed-object accidents were computed based on a national estimate of 673,436 (168,359 $\times$ 4 years) accidents of this type. The 95 percent confidence intervals for percentages are shown in the last column of Table 3. These intervals are quite large. When a smaller subset of accidents, such as passenger compartment collisions, is chosen, the standard errors become even larger. For this reason, no other tables include this confidence interval for percentages. The reader should recognize that the values shown in all the tables are, to a certain degree, speculative in that they are based on extrapolations of very small sample counts. On the other hand, the most probable value to be sampled is the mean, so the data shown represents the best available estimate of the fixed-object, side-impact problem.

Despite the large standard errors associated with small subgroups of the NASS data, this data set was used because of the lack of alternatives. The FARS data base is useful for studying fatal collisions, but does not provide the detailed information needed for this study. There is little to be learned from the FARS data beyond the information shown in Table 3. The NASS data provide the best available evidence for examining the total range of severity of accidents and for studying accident characteristics in depth, although it cannot be used with the same degree of statistical confidence as the FARS data. There were three choices open to the authors in performing this study:

1. Completely ignore the NASS data,
2. Use the biased, uninflated counts, or
3. Use the unbiased, inflated estimates.

The first alternative was rejected because nothing is gained by completely ignoring the data. The second alternative was also rejected because uninflated counts (i.e., not using the national estimates) would be seriously biased toward severe accidents and would not take advantage of any of the techniques employed by NHTSA to minimize sampling error and bias. The second alternative would have resulted in an interesting anecdotal set of data that could not be used to hypothesize about the national side-impact problem. The third alternative was chosen because it represents the best available estimate of the side-impact problem.

The number of cases excluded from the FARS and NASS data in assembling the study sample are shown in Table 4. After excluding accidents in which rollover was the most harmful event, the initial sample consisted of 914,180 occupants involved in fixed-object collisions, and 8,795 fatal fixed-object collisions. The occupants in nonside, multiple-vehicle, and nonpassenger car collisions were then eliminated. The final study sample consisted of occupants in single-passenger-car, side-impact collisions with fixed roadside objects.

THE FIXED OBJECT

Listed in Table 3 are the number of occupants involved in (i.e., the NASS data) and the number of occupants fatally injured in (i.e., the FARS data) side-impact collisions along with the types of objects that were most often struck. Occupants were most likely to be involved in collisions with narrow objects. There were three times as many occupants in collisions with narrow objects as there were with broad objects. Occupants who were exposed to fixed-object collisions hit narrow objects nearly 59 percent, broad objects 18 percent, and other objects 23 percent of the time. Trees and utility poles were the objects most often struck, accounting for nearly 50 percent of the occupant involvements in these collisions. Guardrails were hit in 10 percent of the accidents.

Not only were occupants exposed to more narrow-object collisions, they were fatally injured in narrow-object collisions more often than in collisions with broad or other objects. Eighty percent of the fatalities involved impacts with narrow objects, although only 60 percent of the occupant involvements were with narrow objects. In the cases of trees and poles, there are enough accident cases to show that the differences between the NASS and FARS data are statistically significant. For narrow objects as a class, the difference between the FARS and NASS data is also statistically significant. Although between 52 and 66 percent of all side-impact collisions involve narrow objects, 80 percent of the fatalities involve narrow objects. Narrow objects, then, seem to be especially hazardous objects to strike in side-impact collisions.

TABLE 3 ESTIMATED AVERAGE YEARLY NUMBER OF OCCUPANTS BY MOST HARMFUL OBJECTS

Object Struck	1980-85 FARS Frequency	1980-85 FARS Percent	1982-85 NASS Frequency	1982-85 NASS Percent	1982-85 NASS 95% Confidence Range of Percent
NARROW					
Tree	785	48	41,517	25	19-31
Utility Pole	434	26	35,996	22	18-28
Light Support	45	3	5,519	3	1-5
Other Post/Pole	39	2	7,405	4	1-7
Sign Support	11	1	6,958	4	1-7
Mail Box	–[1]	–[1]	2,189	1	0-2
Delineator Post	–[1]	–[1]	413	0	0-1
SUBTOTAL	1314	80	99,997	59	52-66
BROAD					
Guardrail	70	4	15,996	9	4-14
Bridge Pier/Abutment	44	3	1,796	1	0-2
Bridge Parapet	24	1	414	0	0-1
Wall	18	1	2,288	1	0-2
Fence	15	1	4,572	3	1-5
Bridge Rail	11	1	1,921	1	0-2
Concrete Barrier	4	0	1,287	1	0-2
Impact Attenuator	1	0	239	0	0-1
Other Long. Barrier	2	0	1,851	1	0-2
SUBTOTAL	189	11	30,364	18	12-24
OTHER					
Culvert	30	2	970	1	0-2
Other Fixed Object	30	2	6,784	4	1-7
Building	25	2	1,063	1	0-2
Embankment, Unknown	21	1	–[1]	–[1]	–[1]
Embankment, Earth	13	1	6,608	4	1-5
Ditch	15	1	10,042	6	2-10
Embankment, Rock	6	0	1,480	1	0-2
Curb	2	0	11,051	7	3-11
Fire Hydrant	1	0	–[1]	–[1]	–[1]
Shrubbery	1	0	–[1]	–[1]	–[1]
SUBTOTAL	144	9	37,998	24	18-30
TOTALS	1,647	100	168,359	100	–[2]

[1]The object is not in the data set.
[2]Not Applicable.

TABLE 4 CREATING THE STUDY SAMPLE: YEARLY AVERAGES OF OCCUPANTS

Type of Collision	1980-85 FARS	1982-85 NASS
Fixed Object	8,795	914,180
Side Impact, Fixed Object	2,241	226,470
Single Vehicle, Side, Fixed	2,096	212,753
Passenger Vehicle, Single, Side, Fixed	1,647	168,359

Occupants were killed in 1 out of 75 (0.013) of the narrow-object collisions and in 1 out of 160 (0.006) of the broad-object collisions. Narrow-object collisions appear to be twice as likely to result in fatalities as do broad-object collisions. Even these results may understate the harmfulness of narrow-object side impacts because the two most harmful broad objects—guardrails and bridge piers or abutments—would be considered narrow object collisions if they were struck on the end.

Trees were the most numerous harmful objects. They were the objects struck in between 19 and 31 percent of the occupant involvements, but were responsible for 48 percent of the fatalities. Trees are especially dangerous because they are narrow, rigid, and tall. (A tall object in this context simply means one that is capable of striking an occupant's head in a nonrollover side-impact collision.) When the point of impact with the fixed object is adjacent to a vehicle occupant, these three characteristics combine to result in a dangerous accident scenario: during a collision a rigid object does not break, so a tall, rigid object such as a tree or utility pole may come into direct contact with the occupant's head and thorax.

Accidents involving guardrails accounted for 4 percent of fatal fixed-object, side-impact accidents, as shown in Table 3. They appeared to be the third leading cause of fixed-object, side-impact fatalities. The NASS data on guardrail collisions is divided into two categories involving midsections and three categories involving ends and transitions, as shown in Table 5. Guardrail ends are defined in the NASS coding manual (*3*) as sections within 25 ft of the upstream guardrail end—the end upstream from the direction of vehicle travel regardless of which side of the road the guardrail is located.

Codes found in police reports for measuring accident severity in the NASS data are shown in Table 5. All guardrail collisions were considered broad objects in Table 3, when in fact ends and possibly bridge transitions may have been narrow objects. It can be seen from Table 5 that there were more than 14,000 occupant involvements with midsections and fewer than 2,000 with end sections and transitions. Although the NASS data for this sample are not statistically significant, it

TABLE 5 ESTIMATED AVERAGE YEARLY NUMBER OF OCCUPANTS IN GUARDRAIL COLLISIONS BY INJURY SEVERITY (1982–1985 NASS)

Guardrail Type	Police Reported Injury							
	No,Possible, or Minor Injury(0+B+C)		Incapacitating Injury(A)		Killed(K)		Total	
	Freq.	%	Freq.	%	Freq.	%	Freq.	%
Non-Median	11,402	75	374	60	0	0	11,776	74
Median	2,185	14	60	10	0	0	2,245	14
Bridge Transition	352	2	0	0	22	41	374	2
End(Non-Median)	1,309	9	61	10	18	33	1,388	9
End(Median)	14	0	127	20	14	26	155	1
Totals	15,262	100	622	100	54	100	15,938	100
Missing							58	

is interesting to note that not a single fatality was recorded for the estimated 14,000 involvements with midsections of guardrails. These data imply that the most effective countermeasures for guardrail side impacts would involve improving the performance of terminals and transitions. The performance of terminals in frontal collisions has also been an area of active research in recent years. Terminals that are characterized by better frontal performance may also help improve side-impact performance.

All of the fatalities involving guardrails were caused by collisions with end sections and transitions. This would seem to indicate that many, perhaps the majority, of the guardrail accidents in Table 3 could be considered narrow-object collisions. This would create an even wider gap between narrow-object fatalities and narrow-object involvements.

The following example illustrates why blunt-end guardrail accidents are especially dangerous in side impacts. This type of accident usually occurs when a vehicle strikes the end of a guardrail intended for traffic in the opposite direction. An example of this situation is shown in Figures 1 and 2. It is taken from a NASS Longitudinal Barrier Special Studies (LBSS) case. After traveling around the curve at a high speed, the driver lost control of the vehicle. The vehicle crossed over to the other side of the road and then onto the left shoulder. As the driver attempted to bring the vehicle back to the roadway, it struck the blunt end of the guardrail near the driver's side fire wall. The W-beam penetrated the occupant compartment and passed out through the passenger-side door, as shown in Figure 1. The potential for catastrophic injury in this type of accident is apparent from the photographs.

THE VEHICLE

In order to determine whether occupants in lighter vehicles were more at risk than occupants in heavy vehicles, the FARS and NASS data were compared to the Polk registration data. A comparison of the NASS data with registration data shows whether the percentage of occupants involved in collisions in a certain weight of vehicle is greater than the percentage of registered vehicles of that weight. A comparison of the FARS data with registration data shows whether the percentage of fatal collisions in a particular weight range is greater than the percentage of registered vehicles in that weight range. If the NASS data is assumed to be a reasonable representation of the occupants involved in each weight range, then a similar distribution of NASS and FARS would indicate that, given that an occupant is in a fixed-object, side-impact collision, the person is equally likely to be fatally injured in any weight of vehicle. Because the mean vehicle weight has been dropping each year, the FARS and NASS data from 1983 were compared with the 1983 registration data. The cumulative distribution function (CDF) of the weights of vehicles involved in all severities of side-impact collisions (NASS) and in fatal side-impact collisions (FARS), along with the CDF of the weights of registered vehicles, are shown in Figure 3. The FARS curve appears to vary from the registration curve in the 2,800- to 3,200-lb range. The maximum difference between the NASS and registration data sets was 4 percent, and 13 percent between the FARS and the registration data sets. The Kolmogorov-Smirnov and the Chi-squared goodness-of-fit tests were met at the 80 percent confidence level or greater for both the NASS-registration data and the FARS-registration data. This difference between the FARS and registration data may be further reduced by considering the differences in reporting vehicle weight in these two data sets. Partyka and Boehly state that the vehicle weights reported in FARS are generally 100 to 300 lb less than the Polk registration generated weights (*4*). She also notes that accounting for this difference significantly reduces the fatality rate in lighter cars. A correction of the FARS weights in Figure 3 would essentially move the CDF for the FARS data to the right 100 to 300 lb, producing a closer fit of this curve with the registration data CDF.

The issue of other variables, like age, masking the weight effect was not explicitly addressed in this research. Older occupants are more likely to be injured when they are involved in an accident, and they are more likely to drive large cars. These two characteristics combined can make large cars look more hazardous when, in fact, the higher injury rate may reflect the greater susceptibility of older drivers to injury. In this study, 92 percent of the occupants involved in fixed-object, side-impact collisions were under the age of 44 (see Table 6) and 84 percent were under 34 years of age. Because of the absence of elderly drivers, age-masking was not considered a problem.

The labels assigned to locations on the vehicle side indicating the most harmful impact location are shown in Table 7. The "*P*," "*Y*," and "*Z*" locations all involve the passenger compartment. Impacts in these locations account for 51 percent of the severe and fatal (A + K) injuries. Passenger compartment collisions alone account for nearly twice as many A + K injuries as impacts at other side locations. It can be seen in Table 8 that an occupant in this particular data set

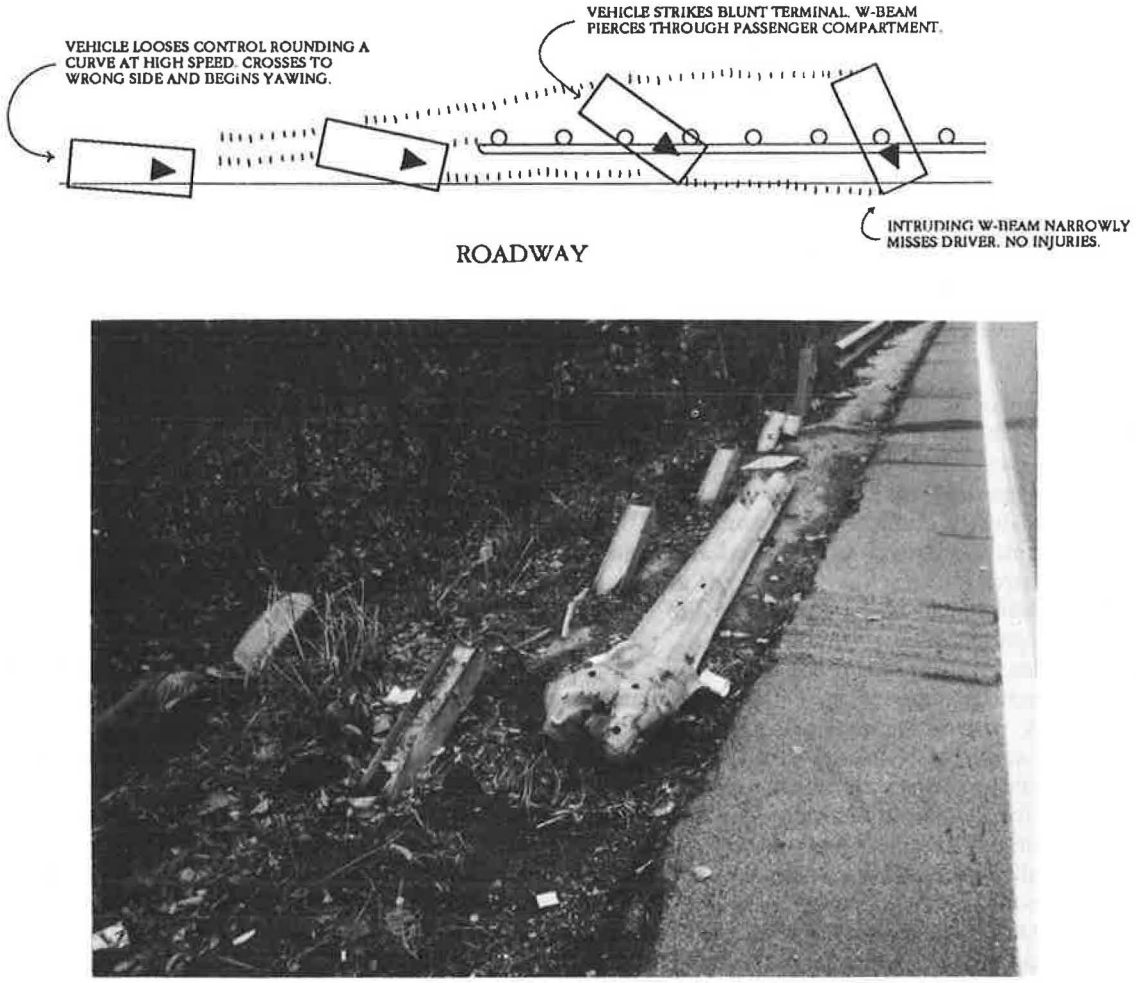

FIGURE 1 Vehicle path and guardrail end in collision: NASS-LBSS Case 83-08-512T.

had a nearly 1 in 100 chance of being fatally injured in a side-impact collision in general, but had more than 1 chance in 40 of being killed when the damage was located at the passenger compartment. A passenger compartment collision appears to be more than twice as likely to result in a fatality as a side-impact collision in general.

The importance of the location of impact was illustrated by the blunt-end guardrail accident in Figure 1. The location of the guardrail intrusion was crucial to the effect it had on the occupant. Another situation in which location of impact is critical is when a vehicle strikes a tall, narrow, rigid object at a point near the occupant. It is then possible for the occupant to directly contact the fixed object through the window.

The specific object in the vehicle that was the most probable injury source is shown in Table 9. To ensure that the injury is correctly attributed to a side impact, only single-event collisions were considered. For example, if a vehicle hit a bridge rail with the front of the vehicle, spun around and collided with a tree on the side, the worst injury may have been caused by either of the collisions. By limiting the study to single event collisions, the injury was correctly attributed to a side-impact collision with a fixed object. This exclusion of certain collisions further reduces the sample size, thus this NASS data sample has an even larger potential variation associated with it than have the previous samples. Those objects that caused injuries of all severities and those that caused injuries with an Abbreviated Injury Score (AIS) greater than three are listed in Table 10. The possible scores range from 1 to 6, with scores over 3 considered life threatening. Unfortunately, the cause of the injuries was unknown in 38 percent of the cases. The leading known cause of injury was a noncontact injury. The two most common known sources of contact injury were the windshield and the instrument panel, both of which are in front rather than on the side of the occupant.

The sources of injury for AIS-greater-than-three injuries differ significantly from those for injuries of all severities. The most frequent known source of injury was from an unknown object in the environment. In fact, all of the injuries caused by an unknown object had an AIS greater than three. These unknown objects may have been exterior objects that intruded into the passenger compartment. The other main sources of serious injury include the side hardware, the A pillar, and the window glass or frame, all objects on the side of the vehicle. Only three of the objects that caused AISs above three were not side hardware. These three—the steering assembly, seat back support, and floor transmission lever—together accounted for only 13 percent of the serious injuries; most side-impact injuries, therefore, appeared to result from

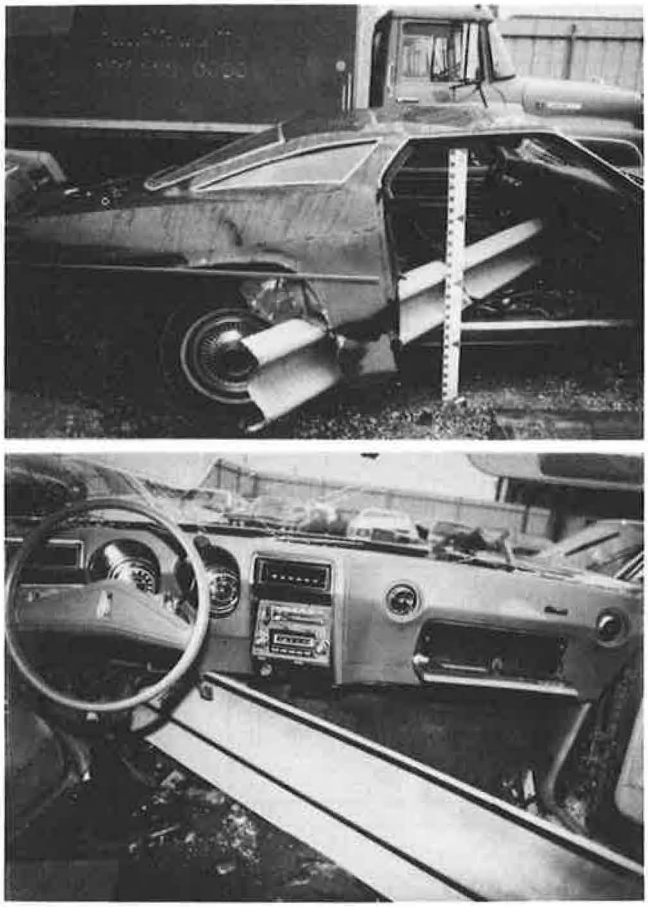

FIGURE 2 Interior views of guardrail end collision: NASS-LBSS Case 83-08-512T.

TABLE 6 ESTIMATED AVERAGE YEARLY NUMBER OF OCCUPANTS BY AGE (1982–1985 NASS)

Age	Freq.	Percent	Cum. Percent
0-15	10,068	6	6
16-19	48,113	30	36
20-24	44,102	27	63
25-34	33,333	21	84
35-44	12,083	8	92
45-54	5,107	3	95
55-64	3,765	2	97
Over 64	5,454	3	100

the body striking an object on or near the doors. Although sampling restrictions preclude firm confidence, it is nonetheless interesting that the injury patterns observed in the data support the results of recent crash testing experiences and intuition. It is intuitively reasonable that the most serious injuries occur when the occupant hits the region of the vehicle experiencing intrusion.

THE OCCUPANT

The NASS data set contains information about which region of an occupant's body was most seriously injured. This sample is also limited to single-event collisions, so the results are also subject to wide variability. Presented in Table 10 is a list of the body regions with the highest AIS for each occupant injured in a single-event, side-impact collision with a fixed object. The first two columns of this table do not indicate severity of injury, rather they show those regions that were most frequently injured. The face, head-skull, and neck-cervical spine were the three areas observed in the data that were the most frequently injured. These three areas account for more than

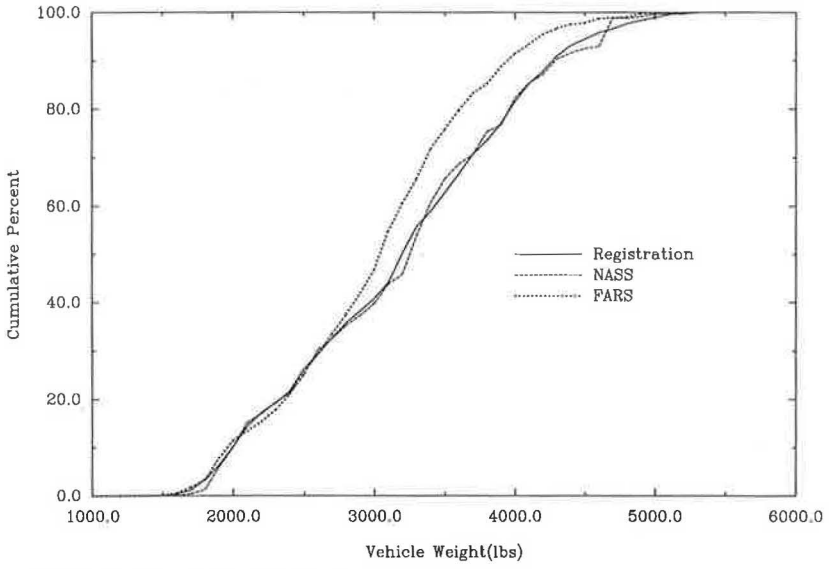

FIGURE 3 Cumulative distribution function for 1983 FARS, NASS, and registration data.

TABLE 7 AVERAGE YEARLY NUMBER OF OCCUPANTS BY LOCATION OF IMPACT (1982–1985 NASS)

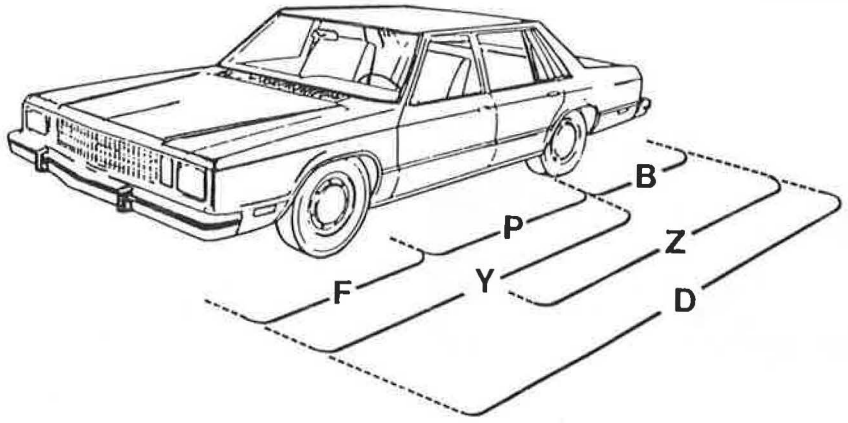

Labels used in Location of Impact (7)

Location of Impact	Nonincap. (0+B+C)		Incap. A+K		Unknown		Total	
	Freq.	Percent	Freq.	Percent	Freq.	Percent	Freq.	Percent
Unknown	43,885	30	3,269	20	112	8	47,266	29
F	28,189	19	1,683	10	200	15	30,072	18
D	20,201	14	1,949	12	407	31	22,557	14
P	15,837	11	4,003	25	152	12	19,992	12
Z	14,972	10	1,744	11	310	24	17,026	10
Y	12,039	8	2,576	16	0	0	14,615	9
B	11,138	8	915	6	131	10	12,184	8
Total	146,261	100	16,139	100	1,312	100	163,712	100
Missing							4,647	

TABLE 8 ESTIMATED AVERAGE YEARLY NUMBER OF OCCUPANTS BY INJURY (1982–1985 NASS)

Type of Injury	All Side Impacts		Passenger Compartment Only	
	Frequency	Percent	Frequency	Percent
No Injury – 0	102,071	62	9,271	46
Possible Injury – C	18,270	11	2,133	11
NonIncapacitating Injury – B	25,919	16	4,433	22
Incapacitating Injury – A	14,585	9	3,521	18
Killed –K	1,555	1	482	2
Unknown	1,312	1	152	1
Total	163,712	100	19,992	100
Missing	4,648			

TABLE 9 ESTIMATED AVERAGE YEARLY NUMBER OF OCCUPANTS BY SOURCE OF INJURY (1982–1985 NASS)

Injury Source	All Injuries		MAIS over3	
	Freq.	Percent	Freq.	Percent
Unknown Source	10,748	38	87	17
Unknown Object in Environment	74	0	74	13
Side Hardware	978	3	72	13
Window Glass/Frame	832	3	69	12
A Pillar	636	2	69	12
Non-Contact Injury	3,556	12	50	9
Steering Assembly	1,490	5	39	7
Side Interior	1,807	6	37	7
Roof Side Rails	321	1	24	4
Floor Trans.Lever	187	1	19	3
Seat Back Supp.	1,004	4	14	3
Windshield	3,082	11	0	0
Instrument Panel	2,004	7	0	0
Mirror	435	2	0	0
Roof/Conv.Top	411	1	0	0
Belt Restraint System	273	1	0	0
Other	752	3	0	0
Total	28,590	100	554	100
Missing	562		0	

TABLE 10 ESTIMATED AVERAGE YEARLY NUMBER OF OCCUPANTS BY BODY REGION INJURED (1982–1985 NASS)

Body Region	All Injuries		AIS Over 3	
	Freq.	Percent	Freq.	Percent
Head-Skull	5,263	18	291	52
Chest	1,949	7	169	31
Whole Body	295	1	50	9
Abdomen	429	1	44	8
Face	6,472	22	0	0
Neck-Cerv.Spine	3,727	13	0	0
Injured, Unknown	1,746	6	0	0
Knee	1,397	5	0	0
Wrist	1,268	4	0	0
Shoulder	1,266	4	0	0
Back-Thorac.Spine	1,203	4	0	0
Ankle-Foot	910	3	0	0
Thigh	708	2	0	0
Unknown	562	2	0	0
Upper Limbs	493	2	0	0
Elbow	461	2	0	0
Pelvic-Hip	371	1	0	0
Upper Arm	279	1	0	0
Lower Leg	298	1	0	o
Forearm	55	1	0	0
Total	29,152	100	554	100

50 percent of the injuries. In the second group of columns in Table 10, the body regions most frequently injured of occupants whose highest AIS scores were greater than three are shown. Most of the serious injuries were to the head (53 percent) and chest (31 percent), presumably because vital organs are located in those regions.

It is not surprising that the areas above the shoulders are the most frequently injured body regions and that the head is the region most seriously injured. Passenger vehicles are not designed to travel sideways, so when they do they begin to roll. The top of the vehicle is usually the first to strike an object in side impacts. This type of accident possibly accounts for the dominance of head, face, and skull injuries in this sample of the NASS data. Other factors also add to this situation to make it more serious:

1. There is little or no lateral restraint for the upper body even when seat belts are used,
2. Side impacts cause the areas above the shoulders to collide with the interior of the vehicle or with exterior objects through the window, and
3. The head is offered little protection from exterior objects that strike the vehicle at the location of the passenger.

Here again, the sample data, even given its sampling restrictions, confirms intuition and crash test experience: namely, that the head and neck are most at risk in fixed-object collisions.

A list of some of the most frequently or most severely injured body regions in the sample and the type of object that caused the injury are presented in Table 11. Guardrail ends and transitions were considered narrow objects in this table. In three of the four body areas that have AIS scores greater than three—head-skull, chest, and abdomen—more than 84 percent of the injuries were caused by narrow objects. The objects most frequently struck for neck-cervical-spine injuries and whole-body injuries were broad objects.

The data suggest that most of the worst accidents could have involved an occupant hitting an exterior object directly. The majority of injuries with an AIS greater than three were to the head, and the type of object most frequently struck was narrow. Most of the narrow objects were tall, as shown in Table 3, and most of the serious injuries occurred at the passenger compartment, as shown in Table 7. These two findings are consistent with the large number of serious head injuries because a side-impact, passenger-compartment collision with a tall, narrow object would most likely cause damage to the head if the object directly contacted the occupant.

Two other notable characteristics of side-impact, fixed-object collisions are the ages of the vehicle occupant and the time of day of the accident. As shown in Table 6, 92 percent of the occupants involved in this type of collision were under the age of 44. The age group most frequently involved was 16- to 19-year-olds. Occupants in this age group, which spans only 4 years, were involved in nearly 30 percent of side-impact, fixed-object collisions. Almost 97 percent of the occupants were under 64 years of age.

Most of the side-impact collisions with fixed objects occur late at night (see Table 12). More than 50 percent of the occupants were involved in accidents that happened between 8 p.m. and 4 a.m.

TABLE 12 ESTIMATED AVERAGE YEARLY NUMBER OF OCCUPANTS BY TIME OF ACCIDENT (1982–1985 NASS)

Time	Frequency	Percent	Cum. Percent
8pm-12am	38,422	23	23
12-4 am	45,913	28	51
4-8 am	16,884	10	61
8am-12pm	14,799	9	70
12-4 pm	19,931	13	83
4-8 pm	28,188	17	100

TABLE 11 ESTIMATED AVERAGE YEARLY NUMBER OF OCCUPANTS BY BODY REGION INJURED AND TYPE OF OBJECT STRUCK: ALL INJURY SEVERITIES (1982–1985 NASS)

Body Region	Type of Object Struck						Total	
	Narrow		Broad		Other			
	Freq.	Percent	Freq.	Percent	Freq.	Percent	Freq.	Percent
Face	4,638	72	862	13	971	15	6,471	100
Head-Skull	4,412	84	331	6	520	10	5,263	100
Neck-Cerv.Spine	1,124	30	2,278	61	325	9	3,727	100
Chest	1,713	88	0	0	237	12	1,950	100
Abdomen	409	95	0	0	19	5	428	100
Whole Body	95	32	124	42	75	26	294	100

FIXED-OBJECT VERSUS VEHICLE-TO-VEHICLE SIDE IMPACTS

Much of the literature about side-impact collisions groups vehicle-to-vehicle collisions with vehicle-to-fixed-object collisions, or neglects fixed-object collisions altogether. Although vehicle-to-vehicle collisions are the most common types of side-impact collisions, fixed-object collisions account for 37 percent of the serious-to-fatal injuries in side-impact collisions (*5*). The differences between these two types of side-impact collisions is discussed in the following section.

The weight of the vehicle appeared to have little, if any, effect on the fatality rate (see Figure 3). Partyka and Boehly (*6*) observe this same phenomenon for all single-vehicle nonrollover accidents. In contrast to this, the fatality rate in multiple-vehicle collisions is sensitive to vehicle weight. A decrease of 0.39 fatalities/100 lb increase in car weight in multiple-vehicle accidents is shown in Figure 4. The rate of decrease in fatalities for single-vehicle collisions, shown in Figure 5, is only 0.02/100 lb increase in vehicle weight—not a statistically significant amount. Although these figures include frontal, rear, and side collisions, they demonstrate the contrast between the effect of weight on multiple-vehicle collisions and the effect of weight on single-vehicle collisions. The weight of the occupant's vehicle is an important factor in multiple-vehicle collisions, but apparently it is not so in single-vehicle collisions, including side impacts with fixed objects.

The location of impact where the most severe injuries occurred in fixed-object collisions appeared to be the passenger compartment (see Table 7). In all types of side-impact accidents combined, however, Huelke (*7*) notes that collisions involving occupants with AISs greater than 3 have the most extensive damage at the "*D*" and "*Y*" locations. A comparison of impact locations by Hartemann et al. (*8*) is shown in Figures 6 and 7. Figure 6 is a distribution of impact points for vehicle-to-vehicle side impacts and Figure 7 is a distribution of vehicle-to-fixed-object side impacts. The distribution of impact points in multiple-vehicle collisions is more spread out. In this study, single-vehicle side impacts with severe injuries were characterized by localized damage to the passenger compartment. Because other vehicles are broader than most fixed roadside objects, the impact area in vehicle-to-vehicle accidents is usually spread out over a larger area. It is important when automobile designers attempt to improve passenger safety in the lateral direction that they realize that there are a significant number of injuries that are caused by impacts with localized damage to the passenger compartment.

Studies by Partyka and Rezabeck (*9*), Frost (*10*), and Dalmotas (*11*) have all concluded that the body regions most likely to be injured in multiple-vehicle side impacts are the chest and abdomen. Lozzi (*12*) noted that car-to-car side impacts resulted in a combination of head, thoracic and abdominal injuries, but that car-to-pole collisions produced mostly head injuries. Head injuries are by far the most common body region severely injured in this examination of NASS single-vehicle, fixed-object collisions, as shown in Table 10. The two types of side-impact collisions have different injury mechanisms that result in different body regions being harmed.

Frost (*10*) concluded that side-impact collisions usually involve older drivers, whereas frontal accidents involve younger drivers. Her data are presented in a graph, shown in Figure 8. Note that the frontal crashes are limited to single vehicles but that the side impacts are not. It is reported in *Fatality Facts*, published by the Insurance Institute for Highway Safety (*13*), that in 1989, occupants under the age of 35 accounted for 68 percent of all roadside-hazard fatalities, whereas occupants over 65 accounted for only 6 percent of these fatal-

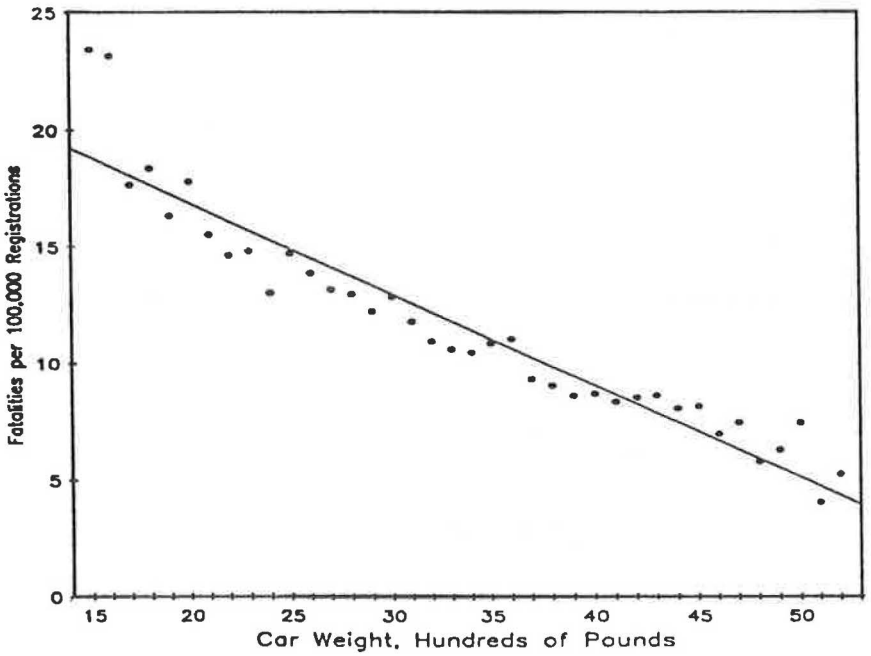

FIGURE 4 Fatalities per 100,000 cars in multiple vehicle accidents (*6*).

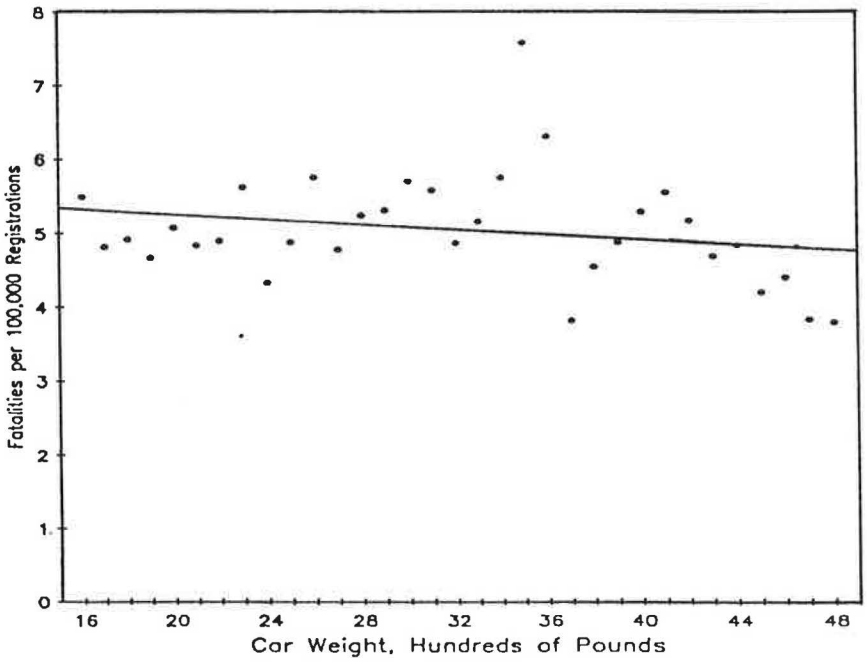

FIGURE 5 Fatalities per 100,000 cars in single vehicle nonrollover accidents (*6*).

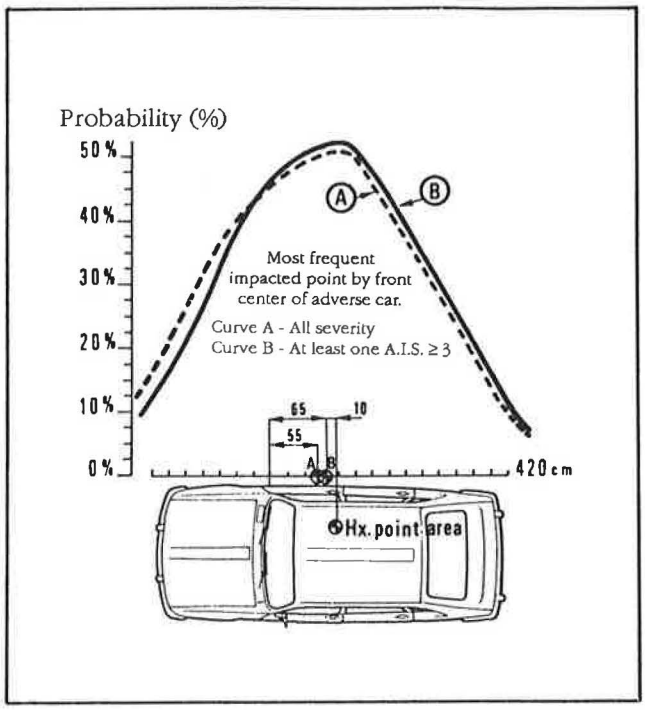

FIGURE 6 Distribution of impact along side of car in vehicle-to-vehicle accidents (*8*).

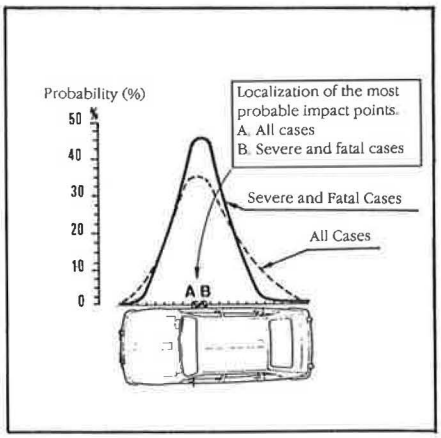

FIGURE 7 Distribution of impact along side of car in fixed-object accidents (*8*).

ities. In contrast, *Fatality Facts* also reports that fatality rates in all types of motor vehicle collisions combined are roughly equivalent for those under 35 and those over 65. These findings indicate that fatally injured occupants in fixed-object collisions are more likely to be young, whereas other types of collisions have a higher percentage of older drivers. The fatality rate per age group appears to be a function of the type of object struck more than a function of the location of impact.

Frost (*10*) also notes that side-impact collisions of all types usually occur during daylight hours. The Insurance Institute (*13*) shows that 42 percent of all roadside hazard fatalities occur between 9 p.m. and 3 a.m. Almost 50 percent of fixed-object, side-impact collisions occur between 10 p.m. and 4 a.m., as shown in Table 12. Fixed object collisions, including side impacts, usually occur at night.

CONCLUSIONS

Side-impact collisions with fixed objects cause a significant loss to society. The 1982–1985 NASS data used in this study

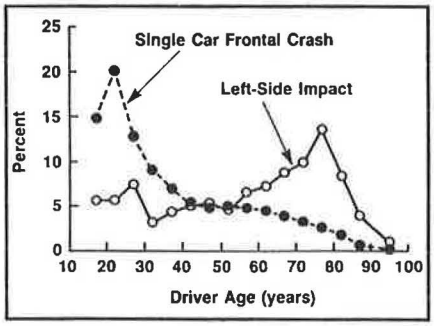

FIGURE 8 Driver age versus percent of occupants involved in single-vehicle frontal crashes and nearside side impacts with moderate damage (*10*).

of side-impact, fixed-object accidents suggested certain characteristics that should be considered when attempting to reduce injury in this type of accident.

Object Characteristics

- The most serious injuries were caused by tall, narrow, rigid objects.
- Guardrail ends caused more serious injuries than midsections.

Vehicle Characteristics

- Heavy vehicles were at no less risk than light vehicles.
- The most harmful injuries occurred in impacts located at the passenger compartment.
- The main injury sources were unknown objects in the environment and side hardware.

Occupant Characteristics

- The majority of serious injuries involved the head-skull area.
- Young drivers at night were involved in the most collisions.

As discussed frequently throughout this paper, these results should be viewed as pointers toward the characteristics of side impacts with fixed objects. The results shown, though not statistically significant, confirm both recent testing experience and intuition about this type of collision.

Side-impact collisions with fixed objects represent one-third of the side-impact problem. The effects of vehicle weight, injury source, injured body region, age of the injured occupants, and time of the accident in fixed-object, side-impact collisions differ significantly from those characteristics in vehicle-to-vehicle, side-impact collisions. For the vehicle design community to improve occupant safety in side impacts, these two types of collision must be approached individually. Improvements in occupant protection in vehicle-to-vehicle collisions may not reduce risks for occupants in fixed-object collisions. The roadside safety community must be aware of these differences also in order to design roadways that are safer for side-impact collisions. Both single-vehicle and multiple-vehicle collisions account for great losses to our society. A clear understanding of the differences between these two important scenarios is necessary if effective countermeasures are to be developed that promote the safety of vehicle occupants.

REFERENCES

1. *Motor Vehicle Accident Costs*. FHWA Technical Advisory T 7570.1, Federal Highway Administration, June 1988.
2. *A Report on Traffic Accidents and Injuries in the United States*. Technical Report, National Highway Traffic Safety Administration, Washington, D.C., 1984 and 1985.
3. *National Accident Sampling System—Coding, Validation, and Editing Manual*. Technical Report, National Highway Traffic Safety Administration, Washington, D.C., 1979–1985 versions.
4. S. C. Partyka and W.A. Boehly. *Effect of Differences in Reported Car Weight on Comparisons of Fatalities per Registered Vehicle*. DOT HS 80744, National Technical Information Service, Springfield, Va. 1989.
5. D. C. Viano, C. C. Culver, L. Evans, M. Frick, and R. Scott. Involvement of Older Drivers in Multivehicle Side-Impact Crashes. *Accident Analysis and Prevention Journal*, 22(2):184, April 1990.
6. S. C. Partyka and W. A. Boehly. *Registration-Based Fatality Rates by Car Size from 1978 Through 1987*. DOT HS 80744, National Technical Information Service, Springfield, Va., 1989.
7. D. F. Huelke. Near Side Passenger Car Impacts—CDC, AIS, and Body Areas Injured (NASS Data). *SAE Technical Paper Series*, (900374), Feb. 1990.
8. F. Hartemann et al. *Occupant Protection in Lateral Impacts*. Technical Report SAE 800098, Society of Automotive Engineers, Warrendale, Pa., 1976.
9. S. C. Partyka and S. E. Rezabeck. Occupant Injury Patterns in Side Impacts—A Coordinated Industry/Government Accident Data Analysis. *SAE Technical Paper Series*, (830459), Feb. 1983.
10. L. L. Frost. Side-Impact Protection: GM Tackles the 'Next Safety Frontier.' *Search*, 24(3), July 1989.
11. D. J. Dalmotas. Injury Mechanisms to Occupants Restrained by Three-Point Seat Belts in Side Impacts. *SAE Technical Paper Series*, (830462), Feb. 1983.
12. A. Lozzi. Motor Car Lateral Impacts and Occupant Injuries. *International Journal of Vehicle Design*, 2(4):470479, 1981.
13. *Facts, 1990 Edition* (A. Fleming, ed.). Insurance Institute for Highway Safety, July 1990.

Publication of this paper sponsored by Committee on Traffic Records and Accident Analysis.

Flexible Post Delineator Mechanical Fatigue Evaluation

HELMUT T. ZWAHLEN, JING YU, MOHAMMAD KHAN, AND RODGER DUNN

The accelerated mechanical fatigue performance for sinusoidal horizontal oscillations (at the natural frequency of the flexible post delineator test specimen, 16-in. free length) was investigated for four types of post delineators. One was an X-shaped post made of a polycarbonate material, two were fiberglass-reinforced thermoplastic posts (T- and C-shapes) and the other was a round polyethylene tube. Three test specimens were tested for the following post conditions: new post, post put into the ground and driven over once with the rear tire of a slow-driving tractor, post driven over twice (in same direction), and post driven over three times (in same direction). The results indicate that the X-shaped polycarbonate material post breaks off after a relatively low number of cycles (fewer than 150,000), whereas the two fiberglass-reinforced posts survive 5 million cycles and show moderate damage (cracks) and do not show an excessive static horizontal deflection when subjected to a 1.5 kg (14.7 Newtons) horizontal pull force. The round polyethylene post also survives 5 million cycles and on some test specimens shows a few cracks on the portion of the tube that is inside the holding fixture. For all four post types tested, there appear to be rather small detrimental effects related to the number of times a post was slowly driven over and its subsequent fatigue performance at 5 million cycles. Based on the test results, it is recommended that 16-in. free length post delineator test specimens (at least 3 specimens per type of post) be tested and that they be subjected to a minimum of 5 million cycles. If all three specimens survive the 5 million cycles (not broken) and their horizontal static deflection (1.5 kg) is less than 2.5 in. (16-in. free length), the post type has passed the accelerated mechanical fatigue evaluation test.

The Ohio Department of Transportation conducts an annual program to install and maintain flexible post delineators along the freeways and expressways in Ohio. It has been claimed that the principal advantage of these flexible post delineators is that they will rebound to their upright position after vehicle impact, resulting in a lower replacement frequency than for conventional metal posts, thus reducing maintenance costs. It has been further claimed that these flexible posts are lighter and less likely to inflict major damage to the vehicles. The Department's specifications for these post delineators contain a number of requirements but do not list any specific values for long-term mechanical fatigue caused by wind load-induced oscillations. Past experience shows that a considerable percentage of these flexible post delineators develop cracks at the base that weaken them and ultimately lead to premature failures. Because the post delineators standing along the highway may bend and oscillate back and forth as a result of either the natural wind force or wind generated by passing vehicles such as large trucks, one reason for the observed failures could be mechanical fatigue. An accelerated test to determine the resistance of post delineators to oscillating mechanical fatigue might be helpful to select superior flexible post delineators for field use.

The Ohio Department of Transportation's Application Standard AS 4C-7 of March 15, 1984, establishes uniform requirements for delineator application, maintenance, and post material on the rural state highway system in Ohio. Application Standard AS 4C-8 (December 1983) provides a summary of flexible post delineator descriptions, and supplements the information found in the *Ohio Manual of Uniform Traffic Control Devices (OMUTCD)* (*1*). Ohio requires field and laboratory tests to pre-qualify. Pre-qualification requires three procedures: a laboratory durability and deflection test, an impact test, and a one-year environmental field test. The department also issued specifications for flexible post delineators in a document dated August 25, 1982; the static deflection test applies to thermosetting reinforced fiberglass posts only. There is also a description of the impact test as well as descriptions of the physical properties, performance, quality assurance tests, and reflectors for flexible post delineators.

Mobility Systems and Equipment Company (MSE) of Los Angeles issued a draft of the final report entitled "Delineator Post Durability Test," on May 31, 1984. This project was supported by the Federal Highway Administration. It required a literature search, the development of a test plan for evaluating samples, and testing of the posts according to the approved test plan. The latter included accelerated ultraviolet and condensation exposure, elevated and reduced temperature tensile strength, flexure, shear, and impact tests. Posts tested were either of a fiber and resin material or a thermoplastic material. The MSE report recommends three tests (shear, vertical extraction, and flexure), all of which are basically static tests. The question about oscillating mechanical fatigue performance has not been discussed and it appears that both test re-test reliability and laboratory versus field validity have not been demonstrated in a statistically satisfactory way.

In research report *Flexible Delineator Posts* (*2*), B. W. Ness of the Michigan Department of Transportation discusses the findings of research project 81 TI-766. The Testing and Research Division was asked to develop procedures for the evaluation of flexible post delineators in the laboratory. The following laboratory tests were devised to compare the various posts: a rigidity test, and impact and deflection resistance tests at high and low temperatures. Again, these tests concentrated on static mechanical capabilities only. The Michigan Depart-

H. T. Zwahlen and J. Yu, Department of Industrial and Systems Engineering, Ohio University, Athens, Ohio 45701-2979. M. Khan and R. Dunn, Bureau of Traffic Ohio Department of Transportation, 25 South Front St., Columbus, Ohio 43216-0899.

ment of Transportation's (DOT) report also discusses the results of controlled field evaluations (pull-out force and impact at 35 and 50 mph) that were carried out by the U.S. Department of Transportation (USDOT) in 1980. The USDOT and the Michigan DOT evaluated several flexible post delineators of the same type. The Michigan DOT's report further looks at economic considerations related to initial post cost and post replacement costs, although the safety aspects and the damages to vehicles striking either metal posts or flexible posts are not taken into account explicitly from a cost point of view. It may be true that the overall system costs for using flexible post delineators compare favorably with using steel posts.

The Safe Hit Corporation also did several tests for its products. These tests include two wind-load tests, reported on October 14, 1983, and March 15, 1984, and *Test of Safe-Hit Driveable Flexible Delineator Post*, reported on June 2, 1986 (*3*). The last test included five different subtests:

1. Laboratory post dimension and reflector check,
2. Laboratory rigidity,
3. Laboratory impact resistance at low temperature,
4. Field impact, and
5. Field environment.

These tests were directed under the test specification of *Driveable Flexible Delineator Post, Prequalification Procedure, Supplement 1020*, Ohio Department of Transportation (*4*).

All of the driveable flexible post delineator tests and test regulations found in the literature are limited to static rigidity and impact tests. Mechanical fatigue caused by dynamic oscillations has not been investigated in any of these tests. It is conceivable that a certain post material could do well under impact and other static tests but might fail mechanically after it has been subjected to a relatively low number of oscillating load cycles. Therefore, an investigation about the oscillating mechanical fatigue resistance for post delineators is important.

Observations on the flexible post delineator test sections in Ohio indicated that many of the flexible post delineators were driven over or bent almost 90 degrees by tractors or wheels, or both, or by decks of mowers cutting the grass along the highway. It was concluded that a lot of the flexible post delineators are damaged at their base because of excessive bending by wheels or other structural mower components at relatively low speeds rather than by high speed (e.g., 55 mph) impacts. Even though this kind of bending caused by being driven over at low speeds does not usually cause damage as severe as the high-speed impacts, it will most likely affect the oscillating mechanical fatigue resistance of the flexible posts. Therefore, the study also investigated the oscillating mechanical resistance of flexible post delineators that have been driven over once, twice, or three times (in the same direction).

The objectives of this study were to

1. Investigate the long-term oscillating mechanical fatigue properties of different new flexible post delineators in the laboratory;
2. Establish minimum specifications for long-term oscillating mechanical fatigue performance for new flexible post delineators and establish an appropriate testing method;
3. Design and build an automatic testing system to test the oscillating mechanical fatigue performance of flexible post delineators; and
4. Investigate the oscillating mechanical fatigue resistance of flexible post delineators that have been driven over slowly once, twice, or three times (in the same direction).

EXPERIMENTAL APPROACH

The experimental approach to test the oscillating mechanical fatigue resistance of post delineators was based on the principle of forced vibration (*5*). The post delineator test specimen was clamped into a holding fixture that was attached to the vertical surface of a mechanical shaker oscillating at the natural frequency of the post test specimen, as shown in Figure 1. Using the natural frequency of the post delineator test specimen, the vibration amplitude or the dynamic deflection on the top of the post reached the maximum. Because the stress on the post delineator test specimen was higher than that on the real post, the testing process was accelerated (*6*). The vibration frequency, the displacement and acceleration of the fixture (base), the amplitude of the post, and the starting and ending times were recorded by a computer-controlled data-recording system. A software package was available to calculate the cumulative oscillating cycles within each running period from the recorded data. Some of the post damage and consequent properties, such as the number and extent of cracks and the static horizontal deflection at the top of the post, were observed and recorded manually by an experimenter.

The developed experimental procedure and the designed and built testing apparatus are capable of testing the fatigue properties of different post delineator designs, different materials, and different production techniques. In this study, the main experiment consisted of four different types of flexible post delineators:

1. "Plastic *X*" post made of extruded polycarbonate with an X-shaped cross section,
2. "Carsonite *T*" (Carsonite Roadmarker) post made of thermo-setting polymers and four types of reinforcing glass fibers with a flat "T" shaped cross section,
3. "Carsonite *C*" (Carsonite Curve-Flex) post made of thermo-setting polymers and four types of reinforcing glass fibers with a slightly curved cross section like a letter *C*, and
4. "Safe Hit" (Safe-Hit cylindrical marker) post made of extruded low-density polyethylene with a circular cross section and an inside tube in the base portion of the post.

The information for these four types of flexible post delineators is listed in Table 1. For each post type there were four test cases:

1. New post,
2. New post driven over once by the rear wheel of a slow-moving tractor,
3. New post driven over twice, and
4. New post driven over three times (driven over in the same direction).

For each case, three samples were tested (four samples were prepared). To identify the post samples for the data collection

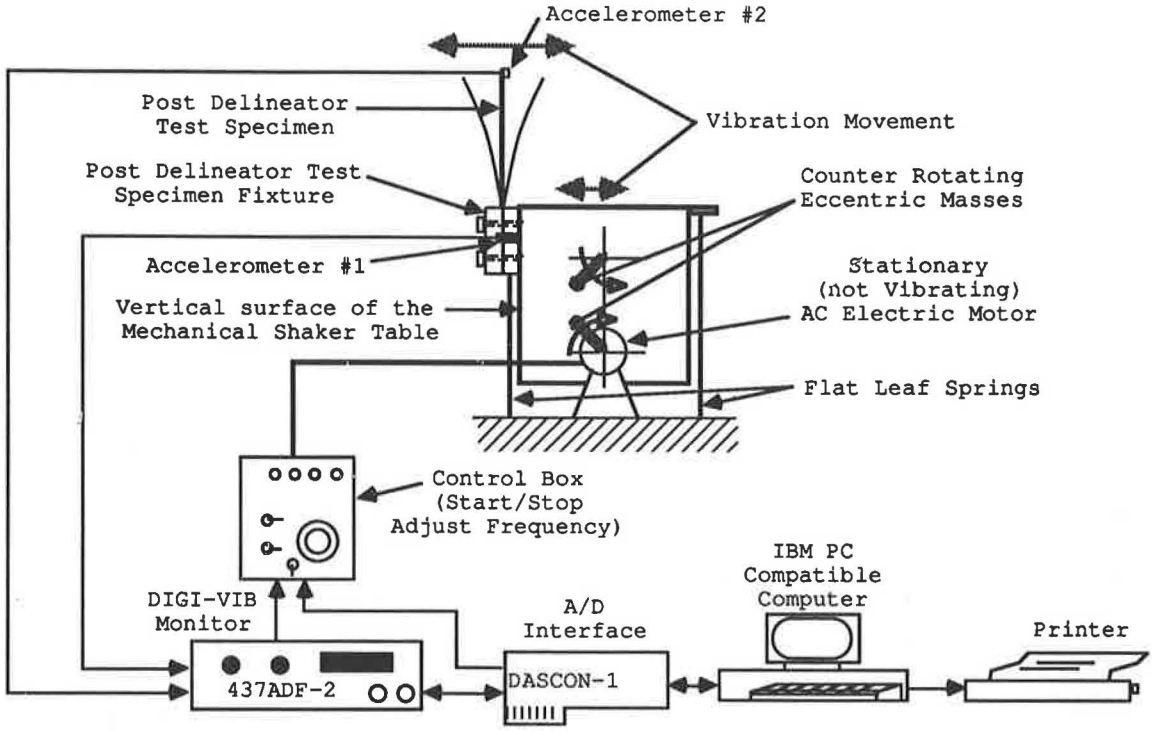

FIGURE 1 Schematic representation of mechanical shaker, post delineator test specimen, and monitoring-control system.

TABLE 1 INFORMATION ON TESTED POST DELINEATOR TYPES IN MAIN EXPERIMENT

Name	Material (Approximate Weight)	Shape and Approximate Dimensions (inches) of Cross Section
Plastic X	Extruded Polycarbonate (0.44 oz/in) (5.31 oz/ft)	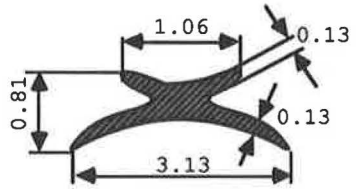
Carsonite C(Curve-flex)	Thermo-setting polymers and four types of reinforcing glass fibers (0.55 oz/in) (6.55 oz/ft)	
Carsonite T(Roadmarker)	Thermo-setting polymers and four types of reinforcing glass fibers (0.69 oz/in) (8.27 oz/ft)	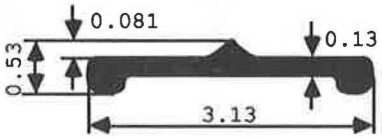
Safe-Hit (Cylindrical Marker)	Extruded low densityPolyethylene (0.40 oz/in) (4.76 oz/ft) (Center Tube: 0.17 oz/in 2.0 oz/ft)	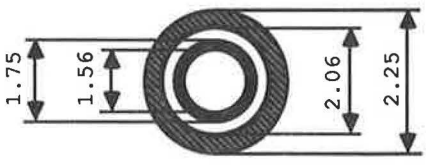

in the main experiment, the different types, cases, and samples were given specific codes. The first one or two letters of the code represent the post type: letters *XX* are used for the posts of Plastic *X*, *C* for the Carsonite *C*, *T* for the Carsonite *T* and *S* for the Safe-Hit. The numbers after the initial letter(s) refer to the different cases or samples. The numbers 20, 21, 22, and 23 indicate new posts. The numbers 1, 2, 3, and 4 refer to posts that have been driven over once, the numbers 5, 6, 7, and 8 refer to posts that have been driven over twice, and the numbers 9, 10, 11, and 12 refer to posts that have been driven over three times. For example, post *T*10 means the Carsonite *T* post that has been driven over three times. All the flexible delineator posts were provided by the manufacturers. For comparison purposes, some additional *X*, *C* and *T* posts that were provided by ODOT were also tested; the results are given in the report by Zwahlen (*7*). Besides the flexible post delineators used in the main experiment, a few posts named *XX*100, *C*100, *T*100 and *S*100 were used for special additional tests and investigations such as determining the relationships of free length versus natural frequency.

The mechanical shaker used in the mechanical fatigue oscillating test was a horizontal mechanical shaker model *T*111-97 manufactured by M/RAD Corporation, Woburn, Massachusetts, according to specifications provided by Ohio University. The available frequency range of the mechanical shaker was 5 to 30 Hz. The capabilities and operating range of the machine are shown in Figure 2.

The fixtures (aluminum) for the post delineator specimens were specially designed and fabricated to fit the contour of the cross section of the posts (see Table 1). Because the clamping surfaces fit the contour of the cross section of the post fairly closely, any additional stress caused by clamping was reduced to a minimum.

The mechanical shaker was monitored by a dual-axis vibration monitor, DIGI-VIB model: 437ADF-2, made by M/RAD Corporation. Two accelerometers were installed, one on the vertical table surface of the mechanical shaker and one near the top of the post delineator specimen respectively (see Figure 1). The accelerometer (Number 1) installed on the table was an ICP (Integrated Circuit Piezoelectric) Accelerometer model 308M159. The accelerometer (Number 2) installed near the top of the post delineator test specimen was a micro-ICP accelerometer model 303A02. Vibration signals were collected by the accelerometers and processed by the monitor. The monitor DIGI-VIB Model 437 provided the means for monitoring quantitative parameters in the measurement of vibration. The DIGI-VIB is capable of measuring and displaying acceleration, displacement, and frequency. It also features a Trip circuit to provide the test specimen and the shaker protection in the event that the testing is carried out beyond the machine's operating range, or in the event of a shaker failure, fixture failure, post delineator specimen break off, or any other failures causing exceedance of the Trip level that has been set. The monitor can display the data on a three-digit light-emitting diode and can also output the data to other devices, such as a tape recorder or a computer.

An IBM PC-compatible microcomputer was connected to the monitor through an I/O board model DASCON-1 made by the MetraByte Corporation. It was designed to allow the use of the IBM PCs or compatibles in low-speed, high-precision data acquisition and control. The board has four analog input channels that were used for frequency, displacement and acceleration of the table, and displacement of the top of the post (displacement amplitude). The full-scale input of each channel was ± 2.0475 volts with a resolution of 0.0005 volts. The speed of throughput was 30 channels/sec. The ad-

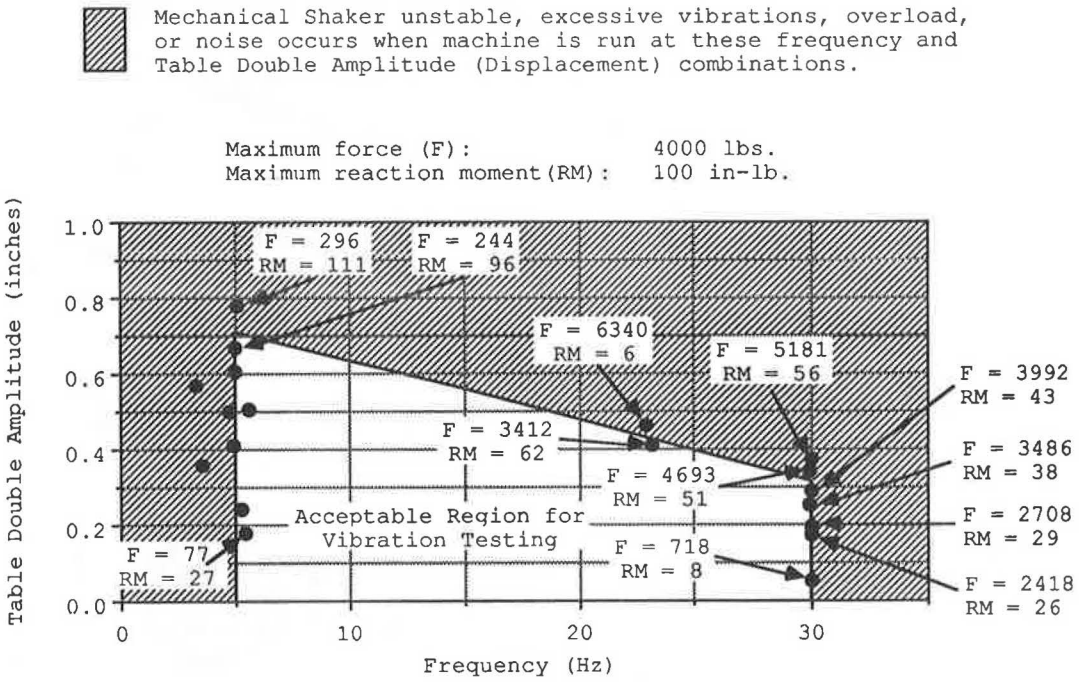

FIGURE 2 Table double amplitude versus frequency operating range of mechanical shaker.

ditional amplification and attenuation circuits were built to convert the DC output of the DIGI-VIB into the input range of 0 to ± 2 volts. Digital input-output (I/O) is available on the board and each port may be independently programmed as an input or an output and is TTL/CMOS-compatible. One digital I/O port was used to provide the experimenter with an option of starting and shutting down the mechanical shaker. To do this, relay and digital circuitry were added between the I/O board and the shaker power control system. The control of the whole mechanical fatigue testing system is shown in Figure 1.

A user-friendly computer program has been especially developed. The main purpose of the program is to collect data and to create new data files or append the data at the end of an existing file on the computer for later analysis. The program also enables the experimenter to edit, list (on the screen), print the data with the calculation of cumulative number of cycles, or plot the collected data. Experimenters have the option either to read from the displays, measure and observe the data and input all the data by the keyboard, or let the computer collect the data. Besides the data collection, the software can list, print, and edit old data files. The software is menu based and does not require any computer programming knowledge from the user. The software can communicate with the analog-digital board installed in the computer. The software also enables the experimenter to start and stop the mechanical shaker through the computer.

The items of data to be collected at each data-collecting interval are the date, the start time (of the interval), the frequency, the displacement of the vibration table, the acceleration of the vibration table, the deflection (double) amplitude on the top of the post, the end time (of the interval), the static horizontal deflection, the free length of the post delineator test specimen, and the damage code. Among these items, the date, the start time, the frequency, the displacement of the machine table, the acceleration of the machine table, the deflection amplitude of the post, and the end time can be collected by the computer automatically. The static horizontal deflection, the length of the post, and the damage code have to be recorded manually and input through the keyboard into the computer. The data collection therefore cannot be a fully automatic process.

The post delineator fatigue testing system is a type of vibration system having a distributed mass and elasticity. Theoretically, the natural frequency of the system is given by the following equation:

$$f_n = (C_n/l_2)\,(EIg/rS)^{1/2} \tag{1}$$

where

f_n = is the natural frequency for mode n (1/rad or Hz),
l = is the length of the post (in.),
E = is the Young's modulus (lb/in^2),
I = is the area moment of inertia of the post cross section (in.4),
g = is the acceleration of gravity (in./sec^2),
r = is the weight density (lb/in.),
S = is the area of the post cross section (in.^{2}), and
C_n = is a constant for the vibration mode n.

Considering that for each type of post the values E, I, S, and r are constants, Equation 1 can be simplified to

$$F = C/L^2 \tag{2}$$

where

F = is the natural frequency (Hz),
C = is a constant (Hz-in.^{2}), and
L = is the free length of the post (in.).

The constant can be easily obtained from a series of tests. The natural frequency versus the length for the Industrial Plastic *X*, Carsonite *T*, and Carsonite *C* post delineators by tests is shown in Figure 3. The natural frequencies were measured by the free vibrations of each post for different free lengths. The constant C in Equation 2 for each type of post was calculated by the least square method. The Safe Hit post is made of a type of soft plastic material with a high damping property and its damping coefficient is too high for free vibration to exist to observe and count. The natural frequency of the Safe Hit post could therefore not be observed and determined under the free vibration condition.

According to the *Ohio Manual of Uniform Traffic Control Devices (OMUTCD)* (*1*), the length of a flexible delineator post above the edge of the pavement should be about 48 in. With a free length of 48 in., the natural frequencies of these three posts (Carsonite *T*, Carsonite *C* and Industrial Plastics *X*) shown in Figure 3 will be lower than 5 Hz, which is the lower limit of the mechanical shaker's frequency capability. If the posts are cracking during the experiment, the system stiffness would be weakened and therefore the natural frequency would be even lower than before. Further, the total number of cycles of the vibration is the product of time and frequency and usually reaches several millions. If the frequency is too low, the experiment would take too much time. In order to maximize the testing efficiency, the frequency of the experiment should be as near to the upper limit of the mechanical shaker's capability as possible. Looking at Figure 3, it can be seen that if the length of the Carsonite *T* and Industrial plastics *X* post is 15 in., the natural frequency will be slightly below 30 Hz, which is the upper limit of the mechanical shaker's capability. Considering the variability in the properties of the materials, 16 in. was selected as an initial testing length for the Carsonite *T* and the Industrial Plastic *X* posts.

The Carsonite *C* post appears to have a nonlinear vibration property when the deflection amplitude is large. If the amplitude of the vibration at the top of the post is very small, say 1/64 in., deflection amplitude for a 16-in.-long post specimen, the post vibrates like a linear system, but if the deflection amplitude at the top of the post is made larger, say 3 in., deflection for a 16-in. long post specimen, the post will bend significantly and the system will appear to act like a kind of softening restoring force vibration system. The natural frequency of the large deflection softening restoring force vibration system is lower than the natural frequency measured when the system works as a linear vibration system. In the experiment, when the free length of the *C* post was cut to 16 in., the natural frequency for small amplitude vibration was higher than 30 Hz, but the frequency of the new *C* post for the larger amplitudes (usually larger than 3 in. for a 16-in.-long free post specimen) was about 28 to 30 Hz. Based on

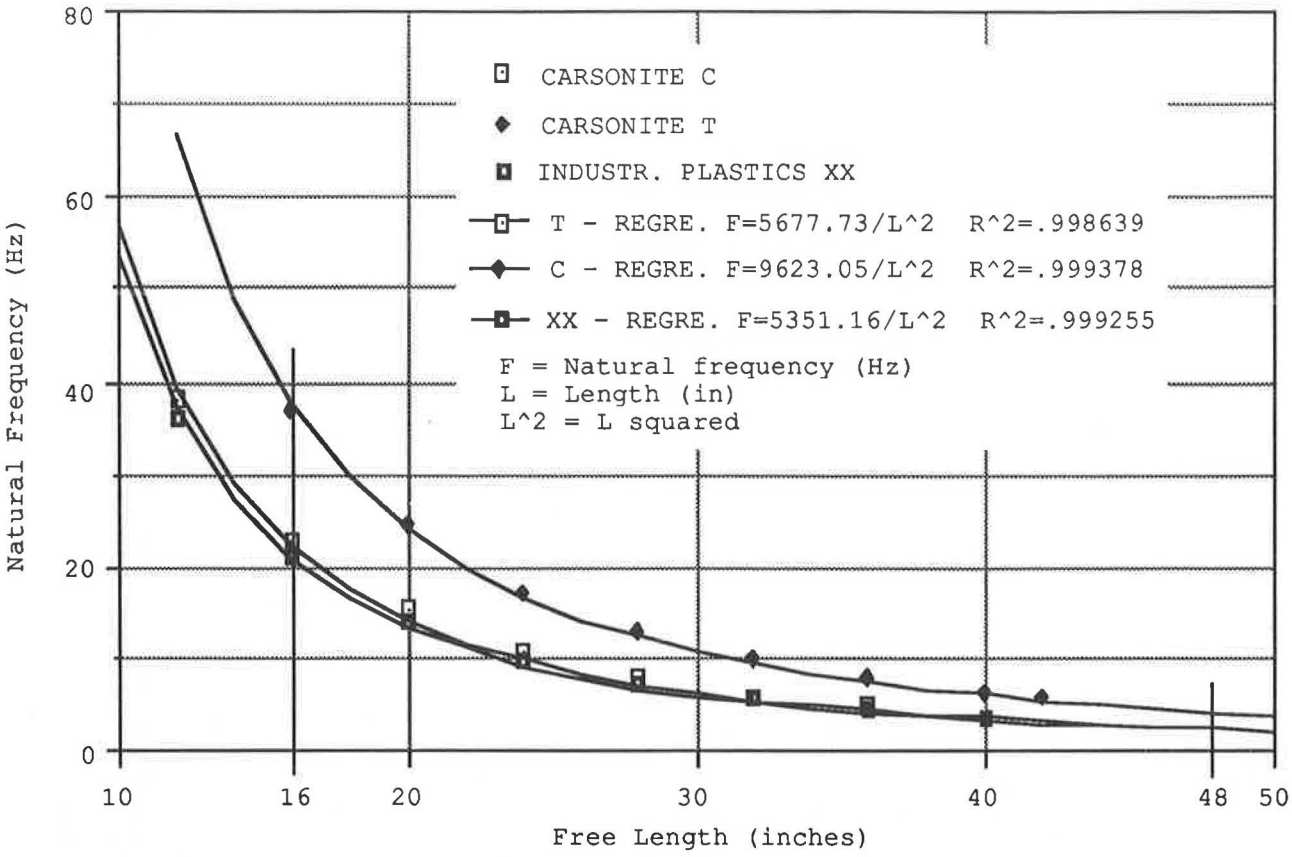

FIGURE 3 Relationship between natural frequency and free length of posts.

this nonlinear characteristic, the length of the Carsonite *C* post delineator for the experiment was also set to 16 in.

The Safe Hit post material is composed of a relatively soft plastic with a circular cross section (outer and inner tube). The Safe Hit posts have an inner liner tube, the bottom of which can absorb a lot of energy during the vibration. This soft plastic material has a very high damping characteristic. If the length of the post is 16 in., the largest amplitude is obtained between 20 and 30 Hz. No significant resonance was observed in this test. Therefore, the length of Safe Hit post delineator test specimens was cut to 16 in.

In general, the cracks emerging on any of the posts tested reduce the natural frequency. Therefore, during testing the frequency of the mechanical shaker should be checked every 2 or 3 hr, sometimes every 20 min, depending on the observed decrease in the natural frequency. The mechanical shaker's frequency has to be adjusted so that the post deflection amplitude is kept at a maximum. The example shown in Figure 4 illustrates that the frequency decreases when the cumulative number of vibrating cycles increases. With some posts like the Carsonite *T*, after some period of testing, the natural frequency would decrease too much and reach a rather low frequency. If a large number of vibration cycles are required, the testing would last for a long time. To accelerate the testing further, a rule was implemented that stated that when the natural frequency decreased to about one-third or one-half of the initial natural testing frequency (close to 30 Hz), the length of the post is cut (4 in. off at the top; e.g., a 16-in. free post is cut to 12 in.). The length of the Carsonite *T* post (post *T*100) was cut from 16 to 12 in. after 217,500 cycles, and the length of the Carsonite *C* post (post *C*100) was cut from 16 to 12 in. after 465,930 cycles. As expected, the natural frequencies of these two posts moved up again at these two points. The amplitude at the top of the delineator post test specimen would then be a little bit smaller if the length of the post was cut from 16 to 12 in.

Another value that should be measured periodically during the testing is the horizontal static deflection. A horizontal force is put at the top of the vertical clamped post delineator test specimen, and the horizontal deflection at the top of the post is measured. Because cracks decrease the stiffness of the post, more cracks mean more horizontal static deflection of the post. Cracks also affect the natural frequency of the posts. The more a post is damaged by the cracks, the lower the natural frequency will be. There exists a relationship between the natural frequency of the post and the horizontal static deflection (see Figure 5). The post delineators containing reinforced glass fibers, even after they were heavily damaged by cracks, were still held together by some of the intact glass fibers, and it appeared to be difficult to achieve the total break off of these posts using the shaker. In practice, the failure of a post may be defined either by the natural frequency, which would be lower than a threshold value, or by the horizontal static deflection (larger than some critical value). The natural frequency can be easily measured with good accuracy (errors could be less than 1 percent) in the laboratory but cannot be easily measured in the field. The static horizontal deflection at the top of the post can be measured fairly easily in the real

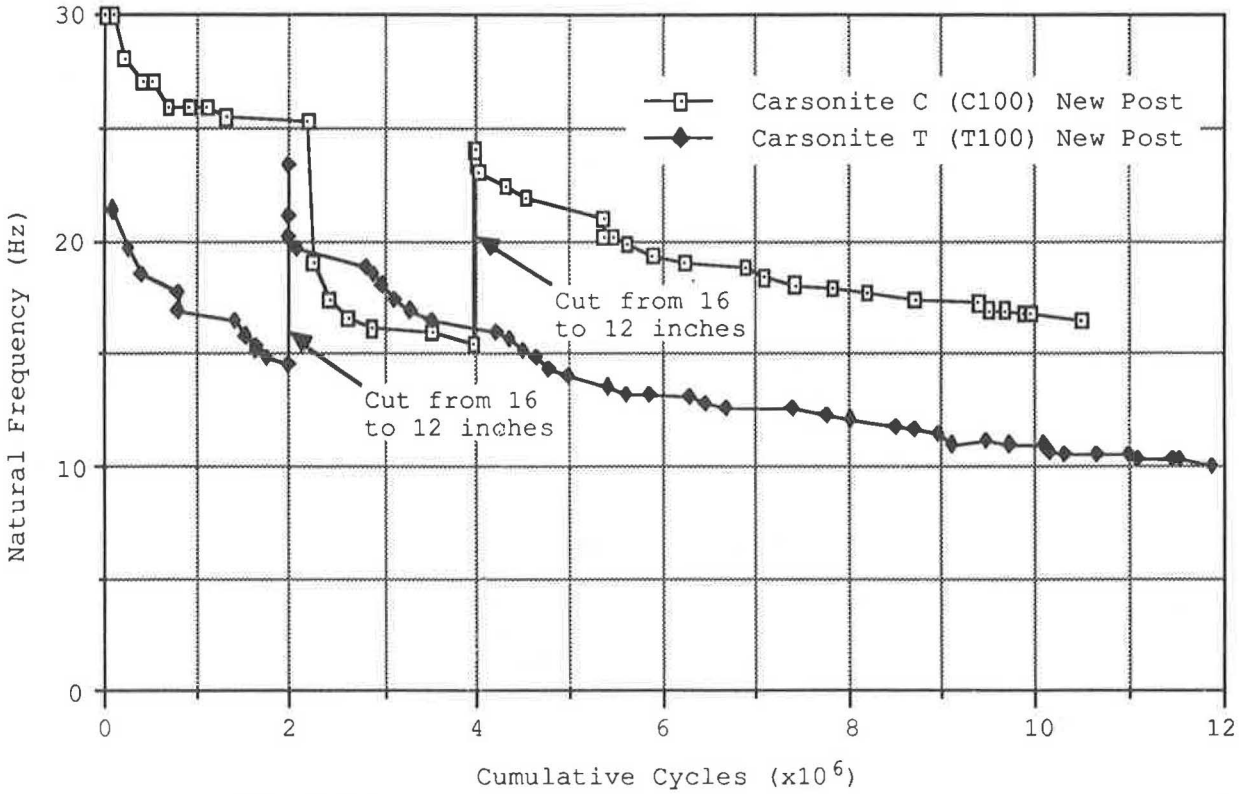

FIGURE 4 Typical relationship between natural frequency versuscumulative number of vibrating cycles for new Carsonite *C* and *T* posts.

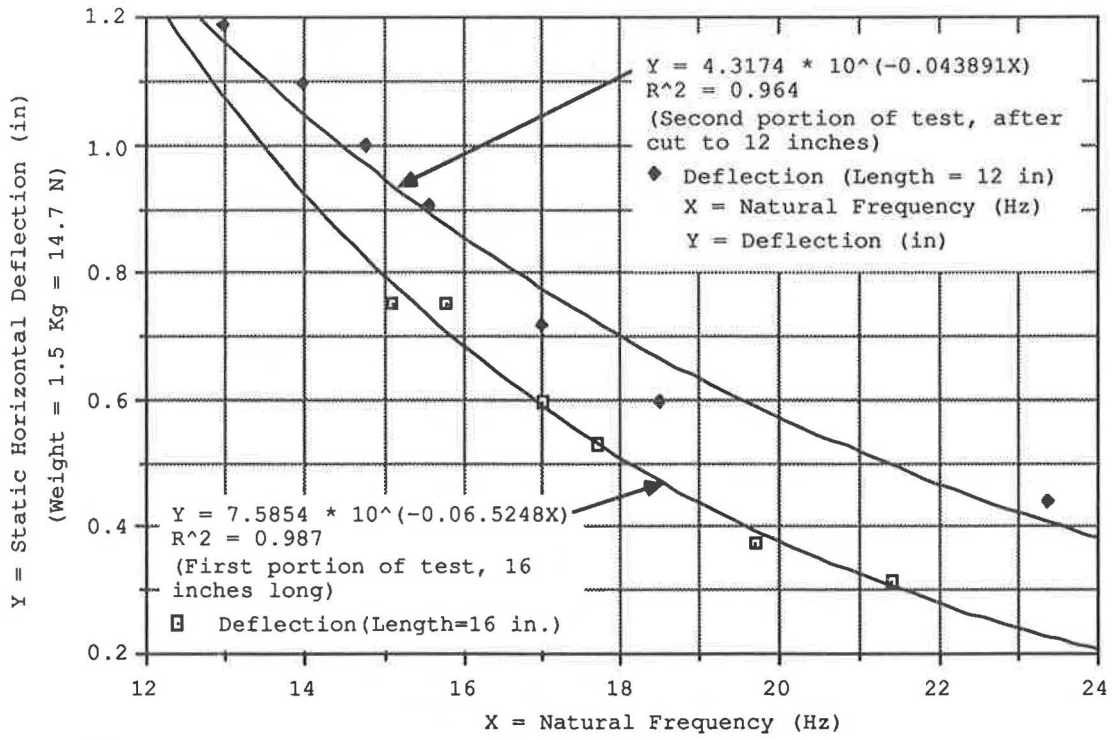

FIGURE 5 Typical relationship between static horizontal deflection as a function of natural frequency for Carsonite *T* (*T*-100-1) flexible delineator post.

environment (e.g., along the highway), but it is not easy to obtain an accurate deflection value in the laboratory. In this study, the damages were assessed primarily as a function of the natural frequency.

To investigate the influence of the low-speed bending (close to 90 degrees) caused by the mechanical structures, elements, or tires of mowers, or tires or elements of other low-speed vehicles, the mechanical fatigue testing program was expanded to include not only new undamaged flexible post delineator samples but also new flexible post delineator samples that had been driven over by a typical mowing tractor (rear tire) once, twice, or three times. The driven-over bending can be considered as an experimental factor that has four levels (new post, driven over once, twice, or three times). For each of the four levels, three post delineator test specimens were tested. The total number of tested samples in the main experiment was 48 (i.e., 4 types × 4 levels × 3 test specimens each = 48 tested samples).

During the experiment, cracks of the posts would develop at any time causing the natural frequency to decrease. However, because the experiment took place continuously during several days and nights, the experimenter could neither collect the data nor adjust the frequency of the mechanical shaker every second or in a continuous way. The computer was able to collect data every second and create a huge data file for a 5 million-cycle test. However, it is hard to analyze and store such a large amount of data. Further, the recording of cracks, crack propagation, and horizontal deflection still needs to be done manually. From past experience, in most cases it was found that the natural frequency usually did not significantly change within 2 hr for the Carsonite *T* and Carsonite *C* posts. The frequency of the Safe Hit post did not change much even over a period of several days or several million cycles. Therefore, it seemed reasonable that the data of the Carsonite *C*, Carsonite *T*, and Safe Hit posts were collected every 2 hr, and the frequency was adjusted at the time of data collection. For the Plastic *X* post, as a result of its relatively short fatigue lifetime, the data were collected using a time period in the range of 1 to 10 min, depending on the rate of decrease in the natural frequency. The testing of posts like the *XX* posts should be monitored continuously by an experimenter.

RESULTS

The damage summary for the main experiment for a total of 48 post delineator test specimens is shown in Table 2. Except for the Plastic *XX* post, all the tested post delineators were not totally broken after 5 million oscillating cycles; some posts were tested for more than 10 million cycles and did still not

TABLE 2 DAMAGE SUMMARY FOR MAIN EXPERIMENT

TYPE OF DEL. POST		XX	C	T	S
NEW POST	Test Specimen No.	20	20	20	20
	Cyc. First Crack app.	38016	211488	203502	NO
	Test Cyc. Damage *	65550			
	Test Specimen No.	21	21	21	21
	Cyc. First Crack app.	1650	390708	557538	NO
	Test Cyc. Damage *	29850			
	Test Specimen No.	22	22	22	22
	Cyc. First Crack app.	9936	3831918	838170	NO
	Test Cyc. Damage *	49134			
DRIVEN OVER ONCE	Test Specimen No.	1	1	1	1
	Cyc. First Crack app.	55164	1608	Already	NO
	Test Cyc. Damage *	95076			
	Test Specimen No.	3	3	3	3
	Cyc. First Crack app.	74767	495600	Already	In Fixture
	Test Cyc. Damage *	94907			
	Test Specimen No.	4	4	4	4
	Cyc. First Crack app.	66552	3313104	Already	In Fixture
	Test Cyc. Damage *	131526			
DRIVEN OVER TWICE	Test Specimen No.	5	5	6	6
	Cyc. First Crack app.	40338	Already	Already	NO
	Test Cyc. Damage *	83999			
	Test Specimen No.	6	6	7	7
	Cyc. First Crack app.	46752	Already	Already	NO
	Test Cyc. Damage *	88727			
	Test Specimen No.	8	7	8	8
	Cyc. First Crack app.	33564	Already	Already	NO
	Test Cyc. Damage *	51798			
DRIVEN OVER THREE TIMES	Test Specimen No.	9	9	9	9
	Cyc. First Crack app.	9036	Already	Already	In Fixture
	Test Cyc. Damage *	51084			
	Test Specimen No.	10	10	11	10
	Cyc. First Crack app.	65808	Already	Already	NO
	Test Cyc. Damage *	140772			
	Test Specimen No.	12	12	12	11
	Cyc. First Crack app.	20130	Already	Already	In Fixture
	Test Cyc. Damage *	48510			

Completely broken | Severly Damaged | Visible Surface Cracks | No Visible Damage

* Damage Estimate Made at Approximately 5 Million Cycles.

Already means that cracks were visible after the post were slowly diven over

break. With the Carsonite *C*, Carsonite *T* and Safe Hit post delineator specimens using a minimum free length of 12 in., it would take too long to keep the experiment going until the posts broke off. It was observed that the natural frequency of the post changed fairly fast when the first cracks appeared or at the beginning of the test. When the test went on to about 5 million oscillating cycles, the natural frequencies of most *C*, *T* or *S* posts changed very slowly. Therefore, the results of the experiment for the Carsonite *C* and *T* and Safe-Hit posts do not provide the number of oscillating cycles at which these posts totally broke off, but do provide information about the damage and how the natural frequency changed over the period from the beginning to about 5 million oscillating cycles. The *XX* post was the only type that broke off totally after a relatively small number of oscillating cycles. The first column shown in Table 2 presents the results for the *XX* posts (oscillating cycles at which the first cracks appeared and when the posts broke). Two analyses of variance (ANOVA) tests using a 0.05 significance level for the number of the cumulative cycles when the first crack appeared and for the complete breaking of the *XX* posts (the new post, the posts driven over once, twice, and three times) showed no significant differences (probabilities are 0.0663 for the appearance of the first crack and 0.227 for the complete breaking of the post). These results imply that when *XX* posts are driven over slowly a few times (in this experiment it was at most three times) it appears not to significantly influence the lifetime of these posts; the major reason for the recorded damages might be mechanical fatigue.

The typical damage and crack development for the Carsonite *C* posts is that they first appeared either on the left or right side of the post near the fixture, and then the cracks continued to develop on either the left or right side until they nearly covered one-half of the post width in irregular directions and usually extended through the whole thickness of the post (see Figure 6). The damage of the Carsonite *C* post is hard to quantify or classify. The damage levels listed in Table 2 could not be defined with a high degree of accuracy.

The typical damage and crack development for the Carsonite *T* posts was different from that of the Carsonite *C* posts. The cracks for the *T* post first appeared at the three ribs and then developed and extended across the post, but seldom appeared to go clear through the thickness of the post as was the case with the *C* posts (see Figure 7). The glass fibers near the surface along the cracks were frayed, but the inner intact glass fibers still held the post up. The *T* post damage is also hard to classify.

The Safe Hit posts appeared to have a very good mechanical fatigue resistance property. There were no cracks observed outside the fixture after 5 million testing cycles. Among the

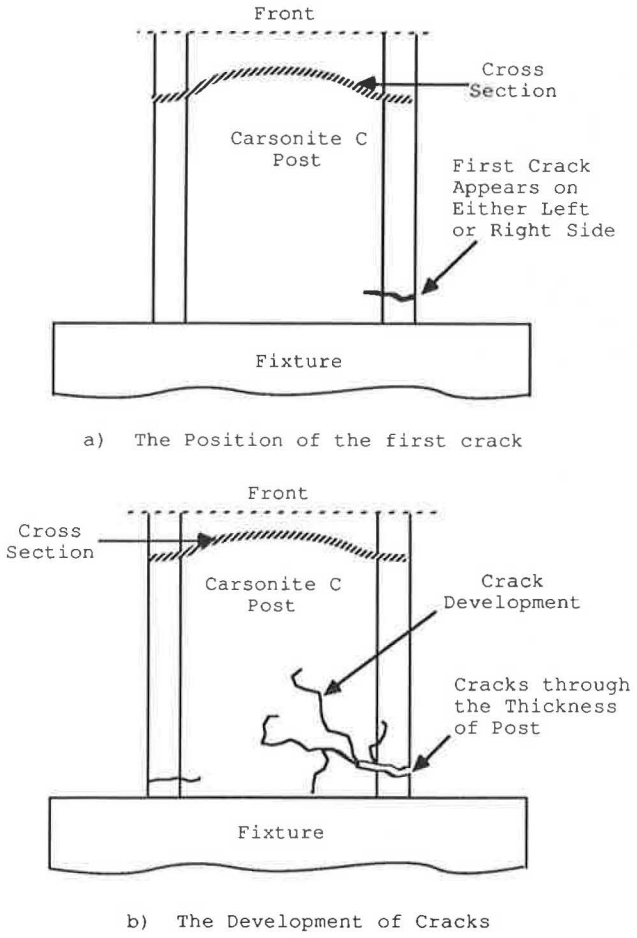

FIGURE 6 Typical damage and crack development on a Carsonite *C* post.

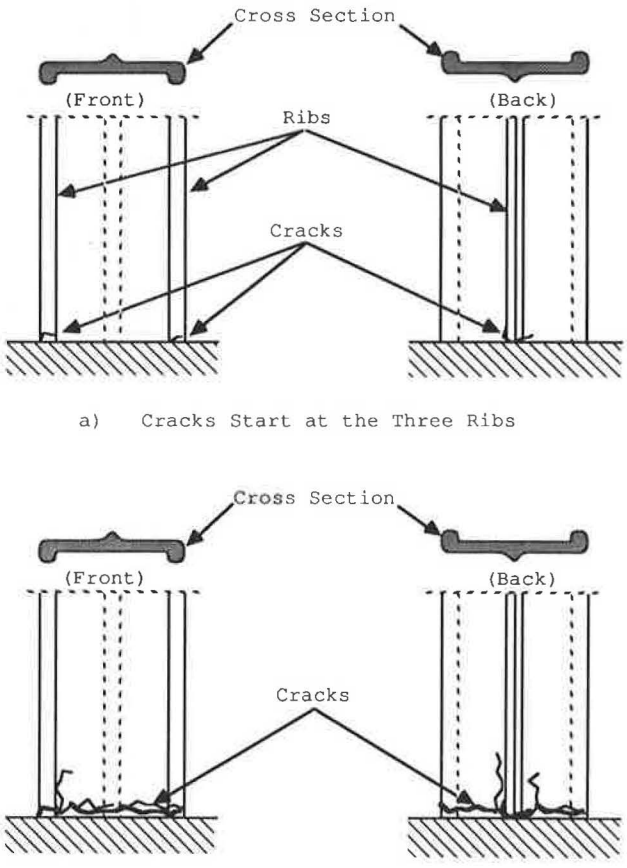

FIGURE 7 Typical damage and crack development on a Carsonite *T* post.

12 specimens, 4 posts had some minor cracks inside the fixture (see Figure 8). All the Safe Hit post specimens with cracks inside the fixture were driven over at least once.

For the *C*, *T* and *S* posts, it would have taken too long or it might not have been possible to continue the experimental runs until the post specimen were totally broken. Therefore, the natural frequency and dynamic deflection behavior become important factors relating the observed post damage and the post mechanical fatigue performance. A summary of the starting natural frequencies and the natural frequencies at the end of 5 million cycles for the posts tested in the main experiment is shown in Table 3.

More detailed results concerning the frequency and deflection performance of the post delineators (such as the natural frequency and dynamic deflection at the top of the post delineator test specimen as a function of the cumulative number of cycles), the horizontal deflection at the top of the post delineator test specimen as a function of the natural frequency, and the cumulative number of cycles, are given in Zwahlen (*7*).

The natural frequency can be used to quantify the post damage. The more severe the damage to the post, the lower the post frequency, but as was mentioned in the testing approach section, when the natural frequency decreases the free length of the post should be shortened by cutting 4 in. at the top. It is not unusual that the length of the different specimens in the same group is different. For the same type of post specimen with the same level of damages, different lengths would be expected to result in different natural frequencies, so that the natural frequency results with different free lengths cannot be used in the analysis directly. In order to compare the natural frequency results for post specimens with different lengths on a one-to-one basis, the factor of length should be removed from the frequency or equivalent factors. In Zwahlen (*7*), an equivalent factor for the comparison of the post damage for the posts with different free lengths was derived. Using the equivalent values derived by Zwahlen (*7*), the cracks or post damage presented by the frequency for different free lengths can be analyzed on a one-to-one basis. Two ANOVA tests using a 0.05 significance level showed that at the end of 5 million cycles the influence of driving slowly over a post a few times for both the Carsonite *C* post (probability equals to 0.59) and the Carsonite *T* post (probability equals to 0.0618) are statistically not significant. The ANOVA results suggest that for the Carsonite *C* and the Carsonite *T* posts under accumulated mechanical fatigue testing, the effect of almost 90 degrees of slow bending cannot be considered as a significant factor for the damage of the post delineator test spec-

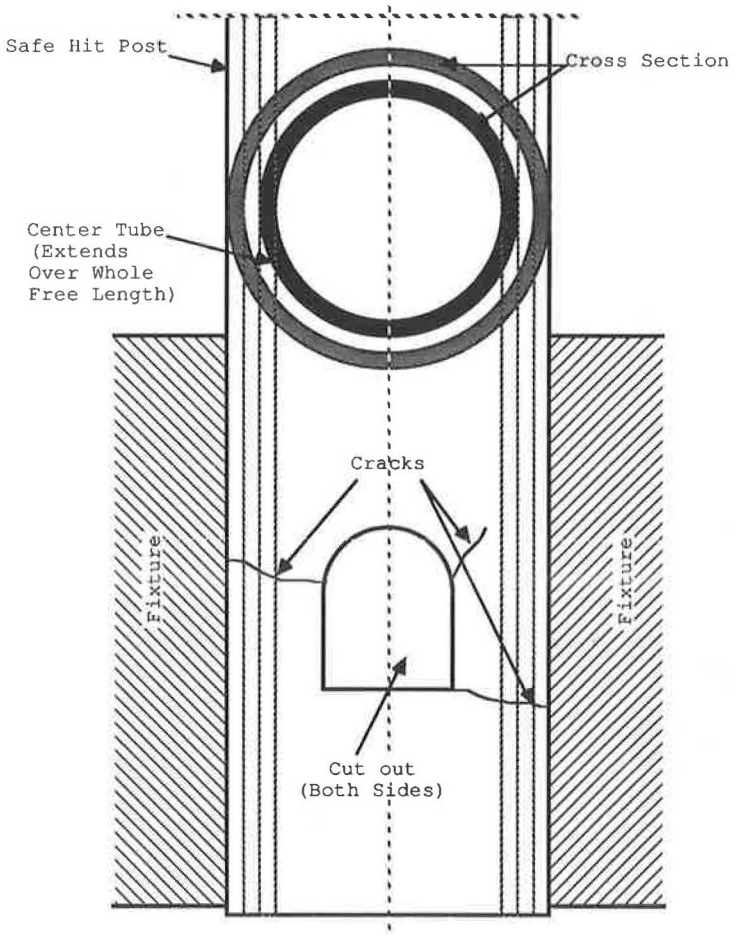

FIGURE 8 Typical damage and crack development on a Safe Hit post.

TABLE 3 SUMMARY OF NATURAL FREQUENCIES (STARTING AT END OF 5 MILLION CYCLES) FOR FLEXIBLE DELINEATOR POSTS TESTED IN MAIN EXPERIMENT

Unit: Hz

TYPE OF DEL.POST		XX	C	T	S
NEW POST	Del. Post No.	**20**	**20**	**20**	**20**
	Starting Freq.	28.8	31.6***	28.0**	29.1
	5M.Cycle Freq.	Broken	12.99***	10.94**	28.2
	Del. Post No.	**21**	**21**	**21**	**21**
	Starting Freq.	27.5	32.0	19.9	31.5
	5M.Cycle Freq.	Broken	12.08	16.10	27.2
	Del. Post No.	**22**	**22**	**22**	**22**
	Starting Freq.	20.7	29.9	20.6	29.8
	5M.Cycle Freq.	Broken	27.19	18.0	27.9
DRIVEN OVER ONCE	Del. Post No.	**1**	**1**	**1**	**1**
	Starting Freq.	18.4	26.8	12.8*	21
	5M.Cycle Freq.	Broken	13.0*	10.71*	24.3
	Del. Post No.	**3**	**3**	**3**	**3**
	Starting Freq.	18.9	29.5	14.5*	20.7
	5M.Cycle Freq.	Broken	15.75	11.2*	21.2
	Del. Post No.	**4**	**4**	**4**	**4**
	Starting Freq.	18.8	31.7	13.4*	21.3
	5M.Cycle Freq.	Broken	26.74	11.00*	17.3
DRIVEN OVER TWICE	Del. Post No.	**5**	**5**	**6**	**6**
	Starting Freq.	18.3	29.9	8.5	16.7
	5M.Cycle Freq.	Broken	15.99	11.2*	18.4
	Del. Post No.	**6**	**6**	**7**	**7**
	Starting Freq.	18.7	28.9	12.7*	20.5
	5M.Cycle Freq.	Broken	10.51	10.2*	17.0
	Del. Post No.	**8**	**7**	**8**	**8**
	Starting Freq.	18.6	31.8	12.6*	19.9
	5M.Cycle Freq.	Broken	14.82*	10.69*	17.9
DRIVEN OVER THREE TIMES	Del Post No.	**9**	**9**	**9**	**9**
	Starting Freq.	17.4	26.7	8.8	29.9
	5M.Cycle Freq.	Broken	10.89	11.9*	23.8
	Del. Post No.	**10**	**10**	**11**	**10**
	Starting Freq.	18.4	29.1	12.4*	27.5
	5M.Cycle Freq.	Broken	16.74	11.0*	27.7
	Del. Post No.	**12**	**12**	**12**	**11**
	Starting Freq.	18.6	31.5**	8.5	19.5
	5M.Cycle Freq.	Broken	11.28**	10.78*	17.1

Reg. Length = 16 in.
* Length = 12 in. ** Length = 14 in. *** Length = 17 in.

imens at about 5 million vibrating cycles. In addition, the major reason for the damage appears to be mechanical fatigue.

In the real field measurement, the natural frequency of the post delineators cannot be measured easily; the post damage might therefore be more readily estimated by the static horizontal deflection at the top of the post delineators. Based on the static horizontal deflections measured from the post delineator test specimens in the laboratory (12 or 16 in. long) using a 1.5 kg (14.7 Newtons) horizontal force, the static horizontal deflection at the top of the post with 48 in. free length using a 0.5 kg (4.9 Newtons) horizontal force could be estimated by extrapolation. For such an extrapolation to work, some static horizontal deflection values for a new 48-in. post have to be measured before dynamic testing. This can be done by putting a 0.5 kg (4.9 Newtons) horizontal force at the top of a clamped 48-in.-long post. Let D_x denote the deflection (in.) measured at a position x in. from the fixture, and D denote the deflection (in.) at the top of the post. After the dynamic testing, the static horizontal deflection of the post delineator test specimen is measured and denoted by D_0 (in). If the free length of the test specimen is x inches, the static horizontal deflection using 0.5 kg (4.9 Newtons) force for the post with the length of 48 in. at the same damage level $D(48)$ in inches could be estimated by the relation

$$D(48) = D + (D_0 - Dx * x/16) * 768 /(x^2) \quad (3)$$

The extrapolated average values for the static horizontal deflections at the top of the 48-in. free-length post delineators based on the post specimens used in the main experiment are indicated in Table 4.

CONCLUSIONS AND TESTING RECOMMENDATIONS

A post delineator mechanical fatigue testing system for accelerated testing has been designed and built for laboratory

TABLE 4 SUMMARY TABLE SHOWING ESTIMATED (EXTRAPOLATION) DEFLECTION VALUES FOR 48-IN. FREE-LENGTH POSTS

TYPE OF POST		X	C	T	S***
New Post (0 Cycl) (in)	D	4.79	1.38	3.21	3.88
	D16	0.83	0.25	0.56	0.50
	D12	0.5	0.13	0.31	0.31
Measure after Approx. 5 Million Cycles Post Del. Test Specimen	Post No.	20	20*	20**	20
	Deflec.(in)	Broken	1.31	0.56	0.69
	Cumul.Cycl.	65,550	6,417,551	6,240,341	12,288,320
	Post No.	21	21	21	21
	Deflec.(in)	Broken	1.06	0.94	0.81
	Cumul.Cycl.	29,850	7,470,923	11,158,570	33,301,260
	Post No.	22	22	22	22
	Deflec.(in)	Broken	0.375	0.63	0.69
	Cumul.Cycl.	49,134	6,153,984	8,215,080	6,475,722
Estimated Deflection**** (in)	Post No.	20	20	20	20
	Deflec.	Not Avail.	4.11	3.76	4.44
	Post No.	21	21	21	21
	Deflec.	Not Avail.	3.81	4.34	4.81
	Post No.	22	22	22	22
	Deflec.	Not Avail.	1.75	3.4	4.44
	Average	Not Avail.	3.23	3.83	4.56

Length of posts = 16 inches:
* Length of C20 post = 17 inches
** Length of T20 post = 14 inches
*** Measured one minute after the hori. force put on the top of posts
**** Free post delineator length = 48 inches

experimentation. This system works well, collects the test data partly automatically, and is capable of testing the mechanical fatigue performance of post delineator specimens. However, considering the millions of cycles required for testing post delineator test specimens with a free length of usually 16 in., this type of testing may easily take 70 hr/test specimen (5 million cycles, average frequency 20 Hz). Using the recommended minimum of three test specimens results in a testing time of 210 hr, or more than 4 weeks (40 hours a week), during which the natural frequency of the test specimen has to be adjusted and test data have to be collected at least every 2 hr. A laboratory procedure for accelerated testing using the mechanical fatigue testing system and test criteria has been developed and recommendations have been established to evaluate the fatigue performance of flexible post delineators. Based on observations and measurements in the field and in the laboratory, a static horizontal deflection caused by a 1.5 kg (14.7 Newtons) force must be equal to or less than 2.5 in., after 5 million cycles for each of a minimum of three post delineator test specimens with a free length of 16 in., to pass the mechanical fatigue test. Based on the test results and using the test criteria (cumulative cycles and static horizontal deflection), we may conclude that the Safe Hit post shows the best overall mechanical fatigue performance (some damage to some driven-over specimens inside the fixture), followed by the Carsonite *C* and *T* posts, which, in spite of moderate damage (cracks at the base) at 5 million cycles, also pass the proposed test criteria and retain a fair amount of the initial stiffness and initial mechanical fatigue performance. The Industrial Plastics *X* posts break off fairly quickly at a number of cycles—usually fewer than 150,000 cycles—and do not pass the proposed test criteria. Somewhat surprisingly, the mechanical performance of the post delineators that have been driven over slowly once, twice, or three times (in the same direction) is not very different from the fatigue performance of the new undamaged posts (at 5 million cycles). Static horizontal deflection at the top of a post delineator caused by a 0.5 kg (4.9 Newtons) force in the field appears to be a promising measure to estimate the equivalent number of cumulative cycles a 16-in. free-length test specimen would have been subjected to in a horizontal sinusoidal force field at the natural frequency in the laboratory. The scope of this labo-

ratory study did not include an investigation of how these laboratory mechanical fatigue testing results relate to the post delineator mechanical fatigue performance and useful life in the field, or real world, or under temperature extremes. One major aim of this laboratory study was to be able to have a testing apparatus, a testing procedure, and testing criteria to screen new post delineator types and new post delineator materials for mechanical fatigue performance before such new post delineators are installed in large numbers in the field.

It is recommended that when testing a new material or a new post type before running the actual mechanical fatigue test, at least one test specimen is needed to determine the best initial length to obtain an initial natural frequency that is in the 30 to 35 Hz range. After the best initial free length has been determined, the test specimens used in the mechanical fatigue test can be prepared. To conduct the mechanical fatigue test, a minimum number of three post delineator specimens is recommended. From a statistical point of view, a number between 7 and 10 would certainly be much more desirable. However, if an average testing frequency of 20 Hz is assumed, the time to test three post specimens up to 5 million cycles each is about 210 hr. Therefore, testing 9 post specimens would take about 630 hr, which may well be beyond the available time resources, especially if there was more than one post type to be tested within a period of 3 months on a 40 hr/week basis. The clamping fixture for the test specimens should be made of aluminium, special two- or multi-piece design, depending on the cross section of the post delineator test specimens. First, it is recommended that a post delineator test specimen should be able to survive and withstand 5 million cycles at a frequency that is always close to its natural frequency at any point in time during the testing period (maximum excitation and stress). Second, after about 5 million cycles, the horizontal static deflection when subjected to a horizontal pulling force of 1.5 kg (14.7 Newtons) should not be more than (a) 2.5 in. for a 16-in. free-length post delineator test specimen, (b) 1.4 in. for a 12-in. free-length test specimen, and (c) 3.9 in. for a 20-in. free-length test specimen (the deflection measurement can be adjusted in a similar way for any other free length between 12 and 20 in.). Adherence to these two proposed test criteria (which will also assure testing frequencies usually not lower than about 8 Hz) will ensure to a relatively high degree that such flexible post delineators should perform acceptably and satisfactorily in the field.

REFERENCES

1. *Ohio Manual of Uniform Traffic Control Devices, (OMUTCD)*. Ohio Department of Transportation, Revision 14, July 1990.
2. B. W. Ness, *Flexible Delineator Posts*. Report R-1247, Research Laboratory Section, Testing and Research Division, Michigan Department of Transportation, Lansing, June 1984.
3. R. Cunningham. *Test of Safe-Hit Driveable Flexible Delineator Post*. Industrial Testing Laboratory Report 92396, Safe Hit Corporation, Hayward. Calif., June 1986.
4. *Driveable Flexible Delineator Post, Prequalification Procedure, Supplement 1020*, Ohio Department of Transportation, Columbus, Jan. 30, 1985, revised Feb. 10, 1986.
5. C. M. Harris and C. E. Crede. *Shock and Vibration Handbook*. Vols. 1, 2, and 3, McGraw-Hill Book Co., Inc., New York, 1961.
6. B. I. Sandor. *Fundamentals of Cyclic Stress and Strain*. University of Wisconsin Press, Madison, Wis., 1972.
7. H. T. Zwahlen. *Post Delineator Mechanical Fatigue Evaluation*. Final Report, FHWA/OH-89/015, Federal Highway Administration, 1989.

Publication of this report sponsored by Committee on Roadside Safety Features.